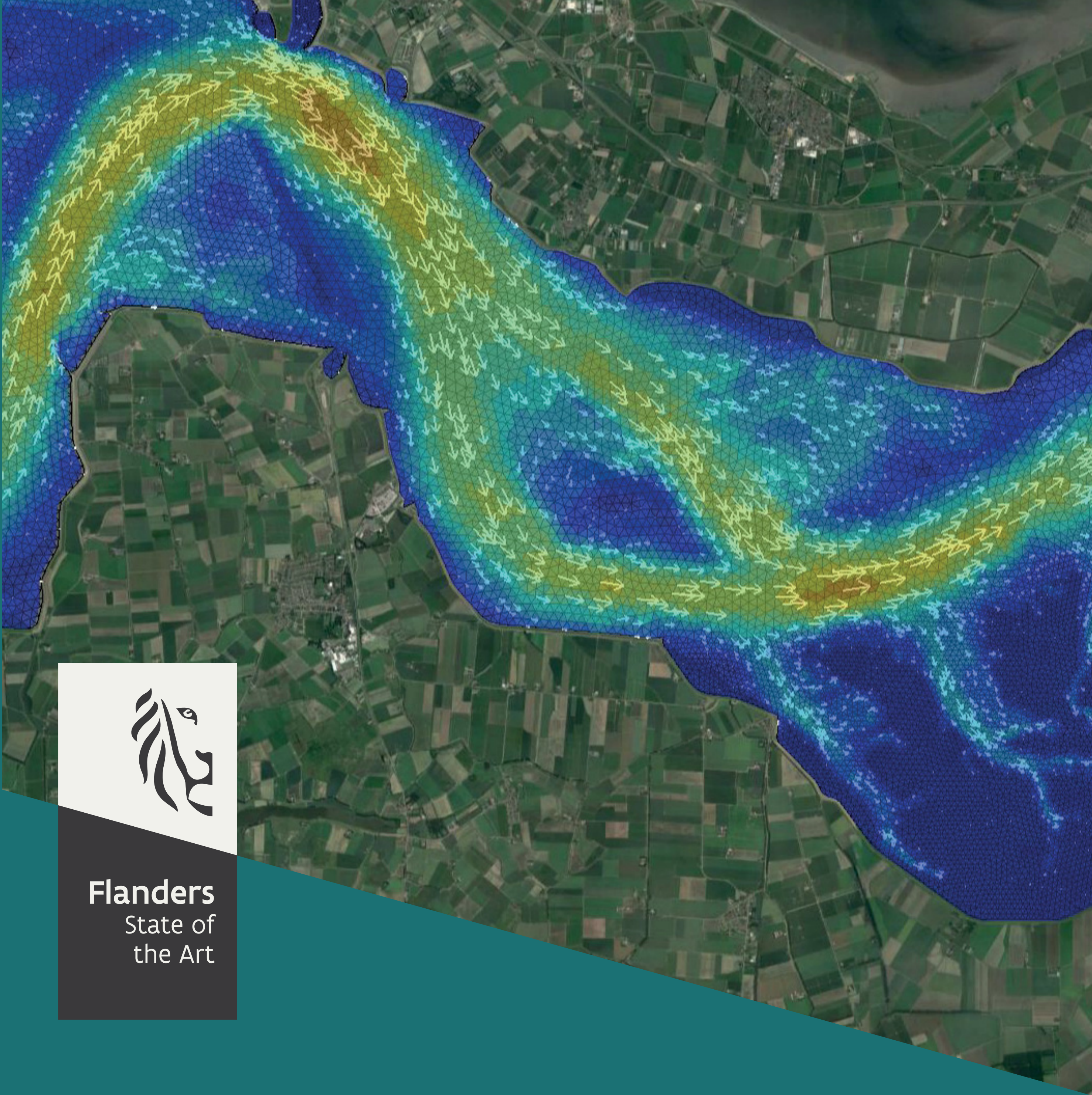

Flanders
State of
the Art

00_081_1
FHR reports

Update snelheidsvelden Zeeschelde en Sluistoegangen

Technical Report

DEPARTMENT
MOBILITY & PUBLIC WORKS

www.flandershydraulicsresearch.be

Update snelheidsvelden Zeeschelde en Sluistoegangen

Technical Report

Chu, K.; Vanlede, J. Decrop, B.; Verwilligen, J.; Mostaert, F.

Legal notice

Flanders Hydraulics Research is of the opinion that the information and positions in this report are substantiated by the available data and knowledge at the time of writing.
The positions taken in this report are those of Flanders Hydraulics Research and do not reflect necessarily the opinion of the Government of Flanders or any of its institutions.
Flanders Hydraulics Research nor any person or company acting on behalf of Flanders Hydraulics Research is responsible for any loss or damage arising from the use of the information in this report.

Copyright and citation

D/2017/3241/286

This publication should be cited as follows:

Chu, K.; Vanlede, J. Decrop, B.; Verwilligen, J.; Mostaert, F. (2017). Update snelheidsvelden Zeeschelde en Sluistoegangen: Technical Report. Version 2.0. FHR Reports, 00_081_1. Flanders Hydraulics Research: Antwerp.

IMDC: I/RA/11502/16.179/KCH/

Document identification

Customer:	Flanders Hydraulics Research	Ref.:	WL2017R00_081_1
Keywords (3-5):	Snelheidsvelden, Hydraulisch model		
Text (p.):	68	Appendices (p.):	6
Confidentiality:	☒ No	☒ Available online	

Author(s):	Chu, K.

Control

	Name	Signature
Reviser(s):	Verwilligen, J. Decrop, B. Vanlede, J.	
Project leader:	Vanlede, Joris	

Approval

Head of Division:	Mostaert, F.	

ISO 9001 CERTIFIED VINÇOTTE

Abstract

The main objective of this study is to update the flow field of the Scheldt, which can be used as an input for the shipping simulator. For this modelling exercise, 8 numerical models in 3 different modelling suites (Simona, Delft3D, TELEMAC) are updated to the year 2015 with the necessary inputs (bathymetry, salinity, boundary conditions, river discharge and wind). Two modelling approaches are compared.

The structured grid approach consists of the combination of the NEVLA 3D model with 4 detailed 2D models (which are nested in the NEVLA model). The unstructured grid approach consists of the 3D SCALDIS model. Model performance is checked by comparing model predicted velocities against 67 different ADCP measurement campaigns.

In general, SCALDIS shows the best performance on velocities throughout the Scheldt. The updated flow fields are therefore extracted from SCALDIS. The velocity data calculated by the SCALDIS model is exported as ASCII files over one tidal cycle during both spring and neap tides.

Contents

List of tables

List of figures

1 Introduction

Project '00_081: Update Snelheidsvelden' aims for an update of the modelled flow velocity fields in the Scheldt.

Two modelling approaches are compared in this study. The **structured grid approach** consists of the combination of the NEVLA 3D model with 4 detailed 2D models (which are nested in the NEVLA model). The **unstructured grid approach** consists of the 3D SCALDIS model.

NEVLA3D is designed in the SIMONA software and includes a large part of the BCS[1], the Scheldt estuary and its tidal tributaries. The NEVLA model is extensively used in research both internally and externally of Flanders Hydraulics Research. Already a large effort has been done improving the performance of the 3D version of the NEVLA model. An extensive calibration and validation exercise is described in (Vanlede et al., 2015). The latest 3D version of the model described in this report (simG162) has been used as a basis for this study.

Four detailed models are nested in the NEVLA model. The combination of the NEVLA model and the four detailed (Delft3D and Telemac) models forms the modelling approach with the structured grid with boundary nesting. The flow pattern is potentially influenced by the orientation, orthogonality and the staircase-pattern of the structured grid. Therefore additionally an unstructured grid approach is added to the comparison. The SCALDIS model has recently been calibrated and validated (Smolders, S. et al. 2016).

The details of the different models, and their latest calibration reports are summarized in Table 1.

The models are not calibrated further, but are updated to the bathymetry and boundary conditions of 2015 and are validated against the measurements taken along the Scheldt. For the modelling approach of 'Structured Grid with Boundary Nesting (SG-BN)', the model results are extracted based on the priority for highest resolution over the entire Scheldt to arrive at flow fields showing the best available accuracy at any given point. The SG-BN is then inter-compared with 'Unstructured Grid (UG)'. The final flow field is selected based on a statistical analysis of the error between modelled and measured flow fields.

For the sake of completeness, two detailed models were not used in this study. Wang et al. (2005) describe the hydrodynamic model used in the design of the Current Deflecting Wall (CDW). The model files of this model however remain intellectual property of WL Delft, and were never delivered to FHR, prohibiting their use in future research. Currently FHR has no code base available that can simulate the effect of a current deflection wall on the flow.

The detailed model "dwarsstromingen Ossenisse-Zuidergat" (Decrop et al., 2009) also wasn't considered, because the grid of this 2Dh model is a mere cut-out of NEVLA (there was no grid refinement) and because the flow pattern around Ossenisse is also well represented in the overall NEVLA model as reported in Vanlede et al. (2008). This was attributed to a better representation of the higher harmonics M4 and M6 in this version of NEVLA, compared to previous versions of NEVLA. Subsequent calibrations of NEVLA (e.g. Vanlede et al., 2015) always paid attention to the model performance in the higher harmonics. Vanlede et al. (2015) also check the model performance of NEVLA for the specific flow pattern at Ossenisse and conclude that the 3D NEVLA model is able to reproduce adequately the circulating cross-currents that have been observed at Ossenisse-Zuidergat, which supports the hypothesis that a model of tidal dynamics of the entire estuary that has sufficient accuracy in representing bathymetry and higher tidal harmonics can successfully reproduce the physics of cross currents at Ossenisse. Therefore, maintaining a separate model for the cross-currents is not deemed necessary, and the model of Decrop et al. (2009) is not included in this project. Both overall models (NEVLA and SCALDIS) have similar model performance for velocities in this

[1] Abbreviations see chapter 2

area in the Western Scheldt (see Table 21 and more specifically the model performance against measurement 20120509_R6_GatVanOssenisse).

Table 1 – Summary of models used for this study

Type	No.	Project area	Modelling platform	Report	Author
Structured Grid with Boundary Nesting (**SG-BN**)	1	NEVLA	SIMONA	Verbetering randvoorwaardenmodel: Subreport 7 - Calibration of NEVLA 3D	Vanlede et al., 2015
	2	Boudewijn – Van Cauwelaert – en Kallosluis	Delft3D	Ontwikkeling detailmodel omgeving Boudewijn - Van Cauwelaert - en Kallosluis	Maximova et al. 2011
	3	Zandvliet – Berendrecht	Delft3D	Stroming aan de toegang tot het Zandvliet-Berendrecht sluizencomplex	Decrop et al. 2010
	4	Wintam	Telemac	Stroomatlas sluis van Wintam	Maximova et al. 2014
	5	Terneuzen	Telemac	Terneuzen model - Deelrapport 1 - Numeriek 2D model	Maximova et al. 2013
Unstructured Grid (**UG**)	6	SCALDIS	Telemac	SCALDIS: a 3D Hydrodynamic Model for the Scheldt Estuary	Smolders et al. 2016

2 Abbreviations and Conventions

2.1 Abbreviations

Table 2 – Used abbreviations

ADCP	Acoustic Doppler Current Profiler
BCS	Belgian Continental Shelf
BeZS	Beneden-Zeeschelde (Lower Sea Scheldt)
BoZS	Boven-Zeeschelde (Upper Sea Scheldt)
CRC	Current – Riemann – Current
CSM	Continental shelf Model of the North Sea
HIC	Hydrological Information Centre
HMCZ	Hydro Meteo Centrum Zeeland
LTV	Lange Termijn Visie Onderzoek en Monitoring
MET	Middle European Time
MVB	Meetnet Vlaamse Banken
NAP	Normaal Amsterdams Peil (Dutch vertical reference level)
NEVLA	Dutch-Flemish hydrodynamic model
RD	Rijksdriehoekscoördinaten
RMAE	Relative Mean Absolute Error. See Annex 1 for mathematical description
RMSE	Root Mean Square Error. See Annex 1 for mathematical description
RWS	Rijkswaterstaat
TAW	Tweede Algemene Waterpassing (Belgian vertical reference level)
WES	Westerschelde (Western Scheldt)
ZUNO	Zuidelijke Noordzee Model (Sourthern North Sea model)

2.2 Conventions

The following conventions are followed by this report:

- Times are represented in MET.
- The coordinate reference system, used by the model and for presentation of the model output is RD Parijs, expressed in meters.
- The vertical reference level used by this project is NAP. NAP is 2.33 m above TAW level.
- Current directions refer to the direction in which the flow is flowing to: e.g. a current direction of 090°N means that the currents are flowing towards the east.
- Wind directions refer to the direction which it is coming from: e.g. a wind direction of 090°N means that the wind is coming from the East.
- SI units are used.

3 Modelling Period

The modelling period is chosen to represent two spring-neap cycles (28 days) and is chosen using a comparable tide analysis. Comparable tide analysis is a method developed in-house to allow comparison of model results to measurements which are outside of the simulation period.

The short term water level that occurred during a 13h measurement campaign (ADCP or Q) is compared with long term water level measurements. Those tidal cycles within the long term water level that have the best match with the tidal cycles in the short term water level are found and ranked. From this analysis, the period that contains the best similar tides to a set of 13h measurements (ADCP or Q) can be determined by calculating the RMSE or RMSE0 of all occurring tides.

For this study the comparable tide analysis searched the most representative period in the entire year 2015. Figure 1 shows the results of this analysis. The computed RMSE gently increases from 8.5 cm (if an entire year would be modelled) to 12.7 cm when the searching period is limited to 28 days. The optimal representative period of 28 days is found from **16-Aug-2015 to 13-Sep-2015.**

Therefore the modelling period for this study is selected from 14-Aug-2015 00:00 to 13-Sep-2015 00:00. The first two days are taken as hydrodynamic spin-up time and will be excluded from the analysis of the results.

Figure 1 – Comparable tide analysis results based on RMSE calculation for the entire year of 2015.

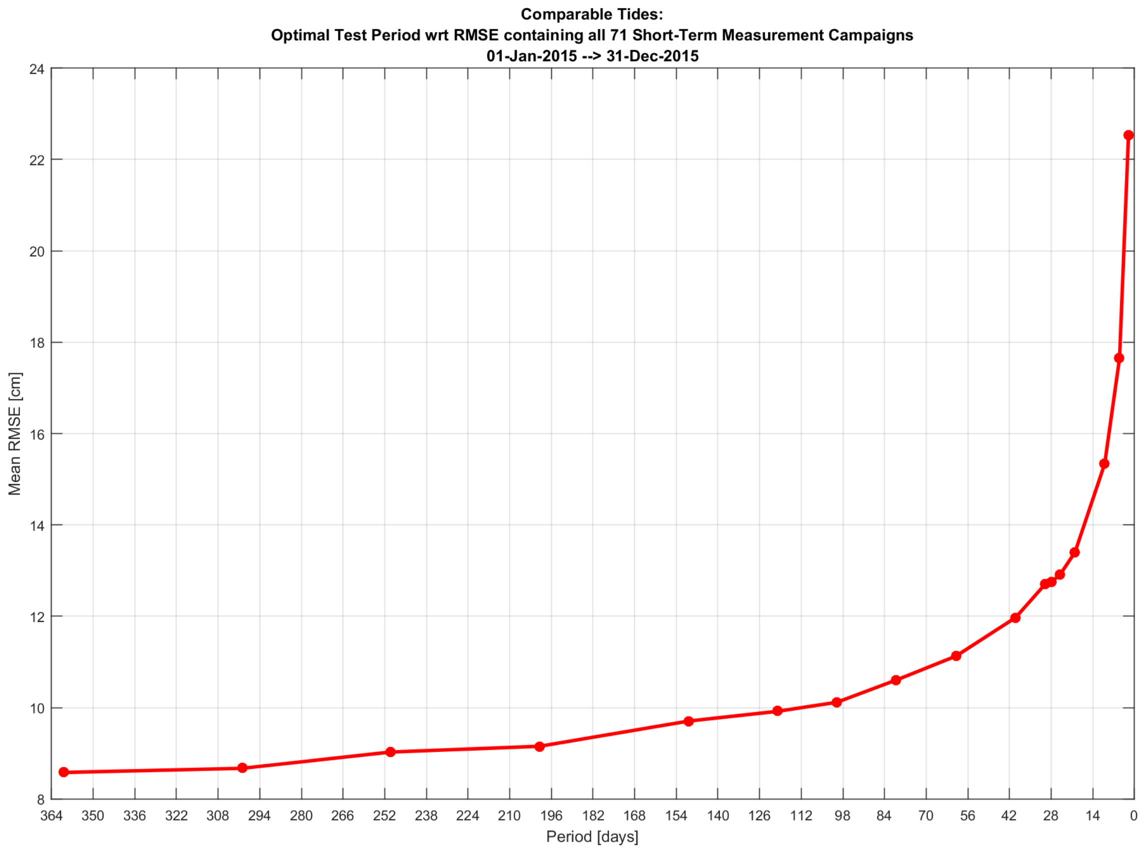

4 Available Data

4.1 Bathymetry

In order to perform model simulations for the year 2015, all the model bathymetries are updated with bathymetric measurements up to the target year. Figure 2 presents the bathymetric measurements merged from 4 different data sources. Table 3 presents the detailed description of the source data.

For the area where the latest bathymetric data are not available in the NEVLA domain (Figure 2), the bathymetry is taken from the final NEVLA3D calibration run simG164 (Vanlede et al., 2015). For the SCALDIS domain, the bathymetry gaps are filled in with bathymetry from the finial calibration run SCALDIS _039_0 (Smolders et al., 2016). The updated bathymetry of each model are presented in §5.3 to §5.9.

Figure 2 – Demonstration of four different sources of bathymetric data (upper panel) and the values of the data (lower panel; positive downwards [m NAP]).

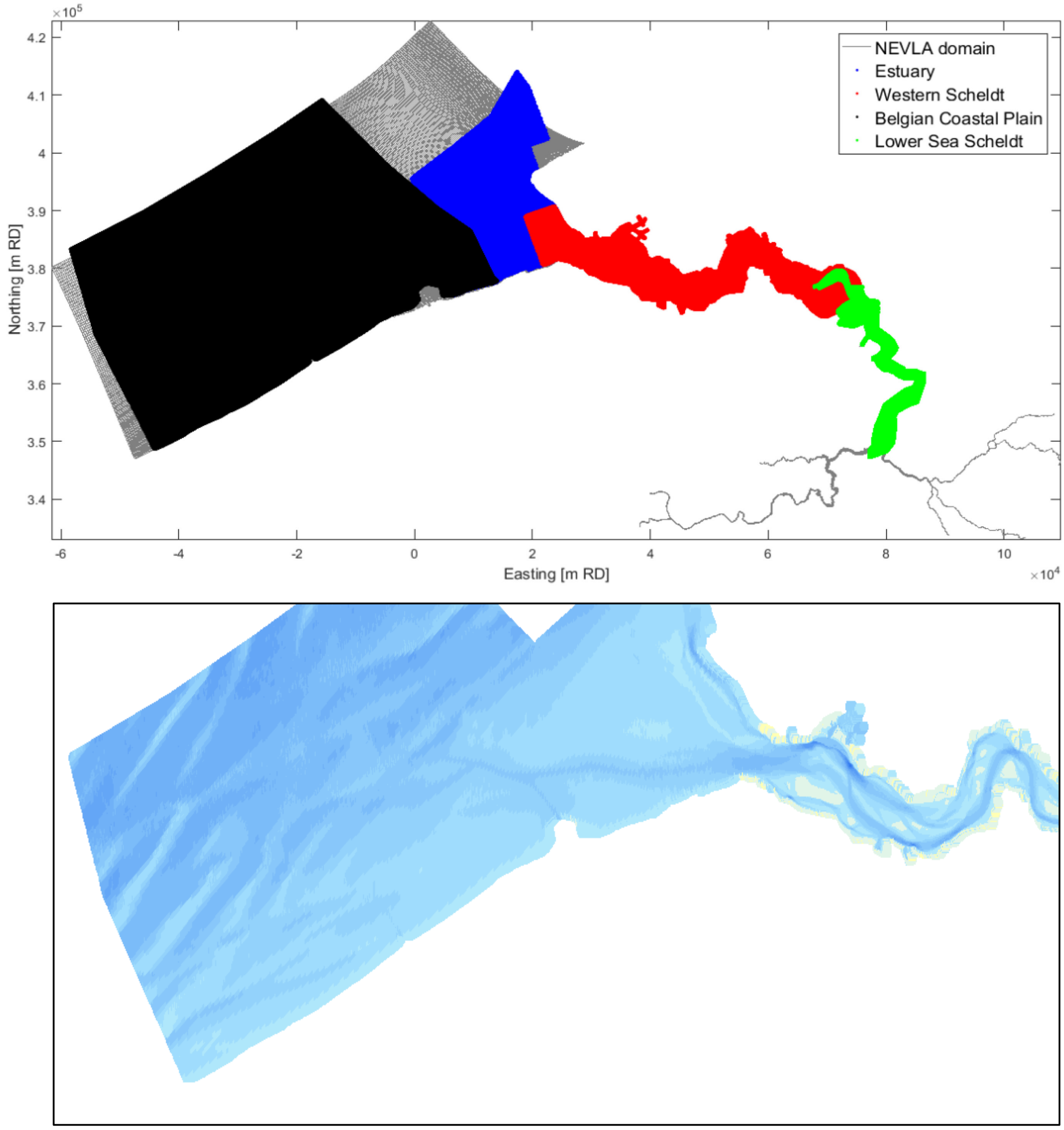

Table 3 – Description of bathymetric sample data.

Zones	Year	Resolution [m]	Source Files
Belgian Coastal Plain	2004-2016	20 x 20	G:\Masterarchief\tob\BCP_bth_2004-2016_VH_utm31etrs89_taw_R_meest-recent-beschikbaar-in-2016\
Estuary	2014	20 x 20	G:\Masterarchief\tob\WES_bth_2014_RWS_rds_NAP_R°_vaklodingen-vak-11-19\export ascii\
Western Sea Scheldt	2015	20 x 20	G:\Masterarchief\tob\WES_tob_2015_RWS_RDS_nap_R°\ga2015_in_m.tif
Lower Sea Scheldt	2015	5 x 5	G:\Masterarchief\tob\BEZ_tob_2014_MT_rds_taw_R

4.2 Water levels

For the year 2015, 42 stations are available with water level measurements every 10 minutes, see Table 4. The stations are also shown in Figure 3.

Table 4 – Available water level measurements for the year 2015.

No.	Station Name	Source	No.	Station Name	Source
1	Duffel_HIC	HIC	22	Dendermonde_HIC	HIC
2	Lier_Molbrug_HIC	HIC	23	Schoonaarde_HIC	HIC
3	Mechelen_benedensluis_HIC	HIC	24	Wetteren_HIC	HIC
4	Mechelen_opw_stuw_HIC	HIC	25	Melle_HIC	HIC
5	Rijmenam_HIC	HIC	26	Baalhoek_HMCZ	HMCZ
6	Tielrode_HIC	HIC	27	Bath_HMCZ	HMCZ
7	Lier_Maasfort_HIC	HIC	28	Borssele_HMCZ	HMCZ
8	Kessel_HIC	HIC	29	Breskens_HMCZ	HMCZ
9	Emblem_HIC	HIC	30	Cadzand_HMCZ	HMCZ
10	Boom_HIC	HIC	31	Hansweert_HMCZ	HMCZ
11	Walem_HIC	HIC	32	Kallo_HMCZ	HMCZ
12	Hombeek_HIC	HIC	33	Liefkenshoek_HMCZ	HMCZ
13	Zemst_HIC	HIC	34	OverloopHansweert_HMCZ	HMCZ
14	Prosperpolder_HIC	HIC	35	Prosperpolder_HMCZ	HMCZ
15	Zandvliet_HIC	HIC	36	Terneuzen_HMCZ	HMCZ
16	Liefkenshoek_HIC	HIC	37	Vvdr_HMCZ	HMCZ
17	Kallo_HIC	HIC	38	Vlissingen_HMCZ	HMCZ
18	Antwerpen_HIC	HIC	39	Walsoorden_HMCZ	HMCZ
19	Hemiksem_HIC	HIC	40	Westkapelle_HMCZ	HMCZ
20	Temse_HIC	HIC	41	Nieuwpoort	Meetnet Vlaamse Banken
21	StAmands_HIC	HIC	42	Oostende	Meetnet Vlaamse Banken

Figure 3 – Measurement locations 2015

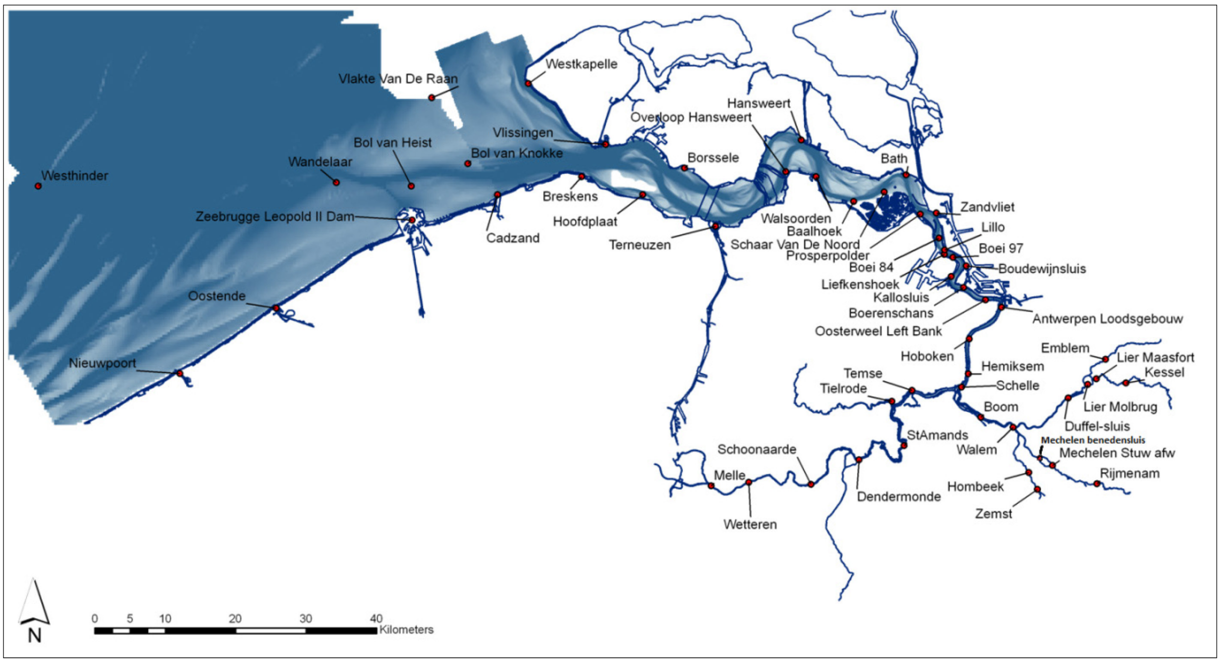

4.3 Velocities

Stationary velocity measurements from year 2015 are available at 3 locations of Boei84, Oosterweel and Driegoten (Vanlierde et al., 2016; see locations in Figure 5 and Figure 6). Table 5 describes the data source and at which elevation the velocities are measured.

Table 5 – Description of stationary velocity measurements.

Location	**Height**	Available from
Buoy 84 top	3.95 m above the bottom	MONEOS
Buoy 84 bottom	1.2 m above the bottom	MONEOS
Oosterweel top	4.7 m above the bottom	MONEOS
Oosterweel bottom	1.2 m above the bottom	MONEOS
Driegoten	3 m above the bottom	MONEOS

67 ADCP transects are available (Figure 4 to Figure 6) for model results comparison (§6). The measured tide during these 67 measurement campaigns are used to determine the modelling period from comparable tide analysis (§3).

Table 6 – Description of ADCP transects from downstream to upstream.
The campaign names contain the information of the date and location of the campaign.

No.	Campaign Names	No.	Campaign Names
1	20110706_R7_Terneuzen	35	20050217_Liefkenshoek
2	20080604_Debietraai_7	36	20060322_Liefkenshoek
3	20110705_R7_Everingen	37	20060927_Liefkenshoek
4	20070321_Terneuzen_haven	38	20080311_Liefkenshoek
5	20120508_R6_Middelgat	39	20090527_Liefkenshoek
6	20120509_R6_GatVanOssenisse	40	20100430_Liefkenshoek
7	20060323_Waarde	41	20130625_Liefkenshoek
8	20060928_Waarde	42	20140514_Liefkenshoek
9	20050217_Zandvliet	43	20050218_Kallo
10	20060912_Doelpolder	44	20090529_Oosterweel
11	20140715_Noordzeeterminal	45	20100429_Oosterweel
12	20100319_dwarsraaiD	46	20130627_Oosterweel
13	20060322_DGD	47	20140516_Oosterweel
14	20060927_DGD	48	20090526_Kruibeke
15	20071024_DGD	49	20100414_Kruibeke
16	20080311_DGD	50	20130530_Kruibeke
17	20080619_DGD	51	20140702_Kruibeke
18	20080626_DGD	52	20130529_Terhagen
19	20080924_DGD	53	20140630_Terhagen
20	20080930_DGD	54	20090623_Driegoten
21	20081001_DGD_X	55	20100415_Driegoten
22	20081001_DGD_Y	56	20130612_Driegoten
23	20081001_DGD_Z	57	20140617_Driegoten
24	20081202_DGD	58	20110218_Kramp_ebb
25	20081210_DGD	59	20110218_Kramp_flood
26	20090306_DGD	60	20140417_Dendermonde
27	20090312_DGD	61	20110801_Appels_downstream
28	20050216_DGD_K	62	20110801_Appels_upstream
29	20050217_DGD_K	63	20090625_Schoonaarde
30	20060322_DGD_K	64	20100414_Schoonaarde
31	20060323_DGD_K	65	20130527_Schoonaarde
32	20060927_DGD_K	66	20140703_Schoonaarde
33	20060928_DGD_K	67	20140415_Schellebelle
34	20080311_DGD_K		

Figure 4 – Available ADCP measurements in the **Western Scheldt**.
Black line represents the land boundary; red lines represent each transect. Note: for the purpose of concision, different ADCP transects (executed on different dates) at the same locations are labelled only once.

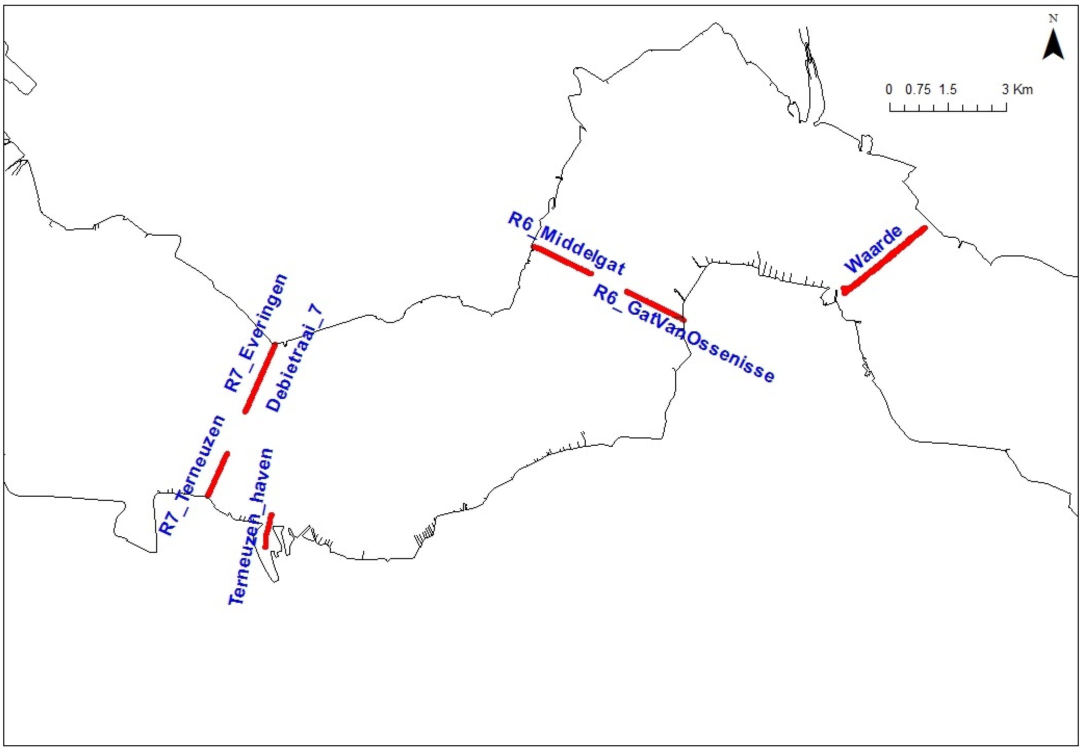

Figure 5 – Available ADCP and stationary measurements in the **Lower Sea Scheldt**.
Black line represents the land boundary; red lines represent each transect; green points represent stationary measurement locations. Note: for the purpose of concision, different ADCP transects (executed on different dates) at the same locations are labelled only once.

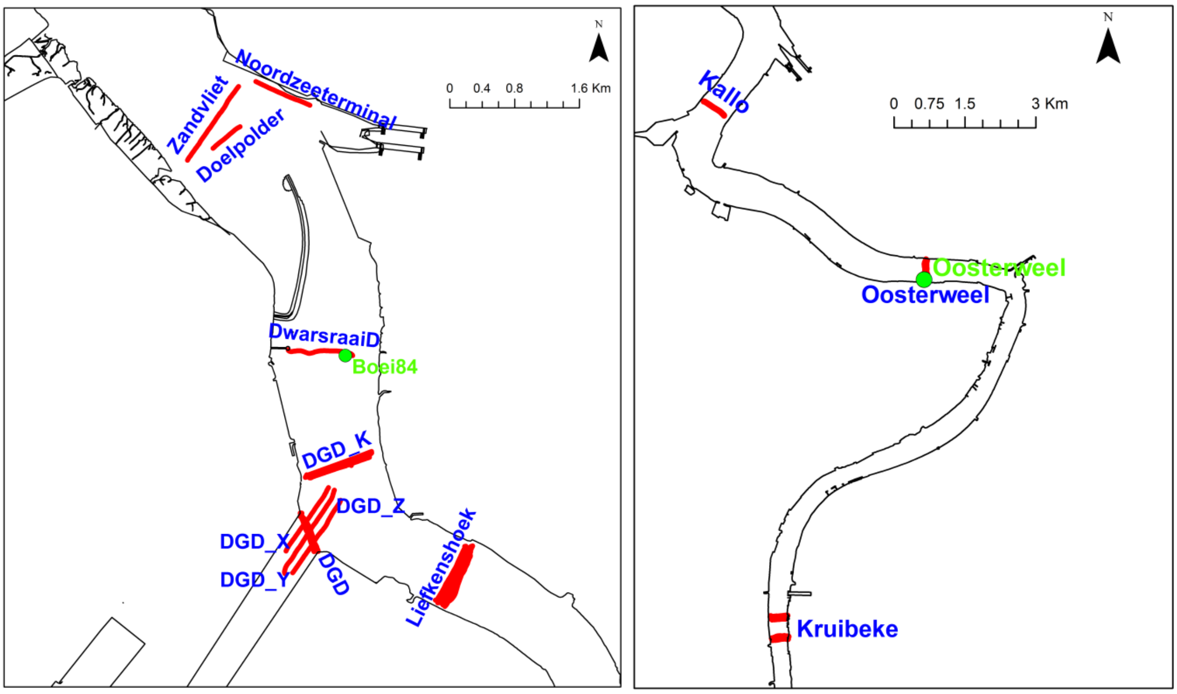

Figure 6 – Available ADCP and stationary measurements in the **Upper Sea Scheldt and Rupel**.
Black line represents the land boundary; red lines represent each transect; green points represent stationary measurement locations. Note: for the purpose of concision, different ADCP transects (executed on different dates) at the same locations are labelled only once.

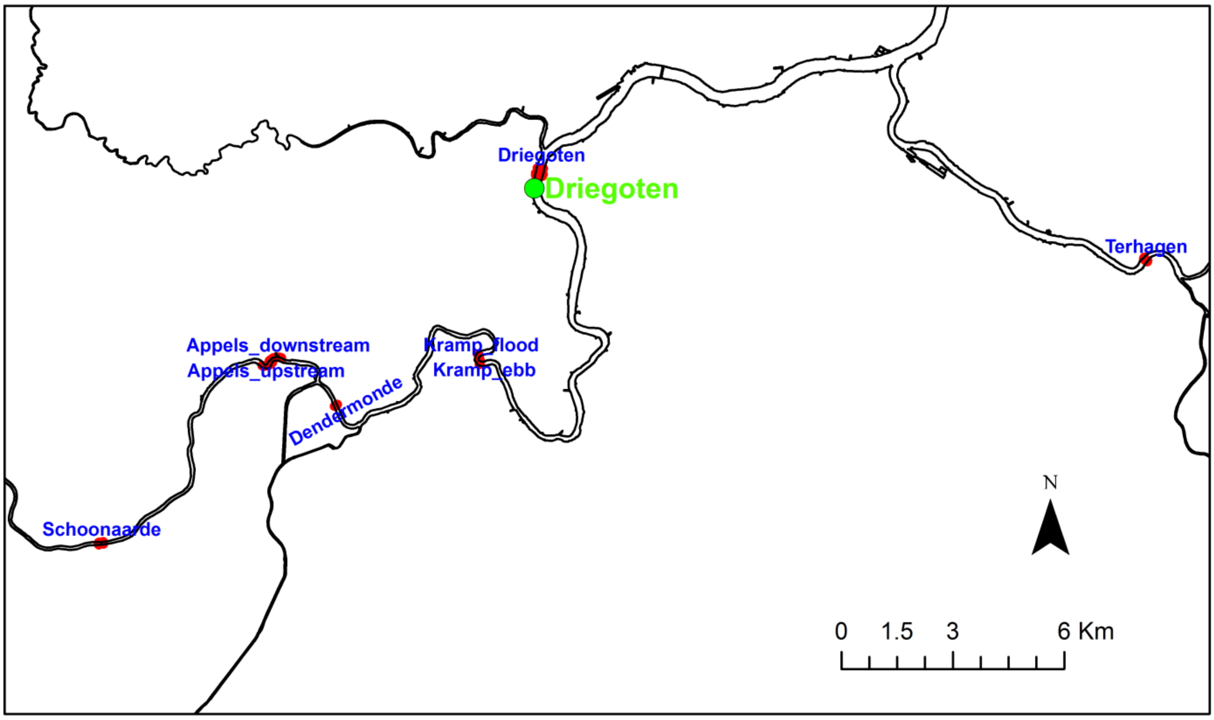

4.4 Salinity

Salinity measurements are available at 8 stations (see locations in Figure 7) and are listed in Table 7. Salinity measurements are used to initialize the NEVLA3D and the SCALDIS model. The initial salinity map is constructed by linear interpolation along the estuary with the salinity measurements of 16-Aug-2015 00:00.

Figure 7 – Initial salinity field for the NEVLA3D model and available stations with salinity measurements.

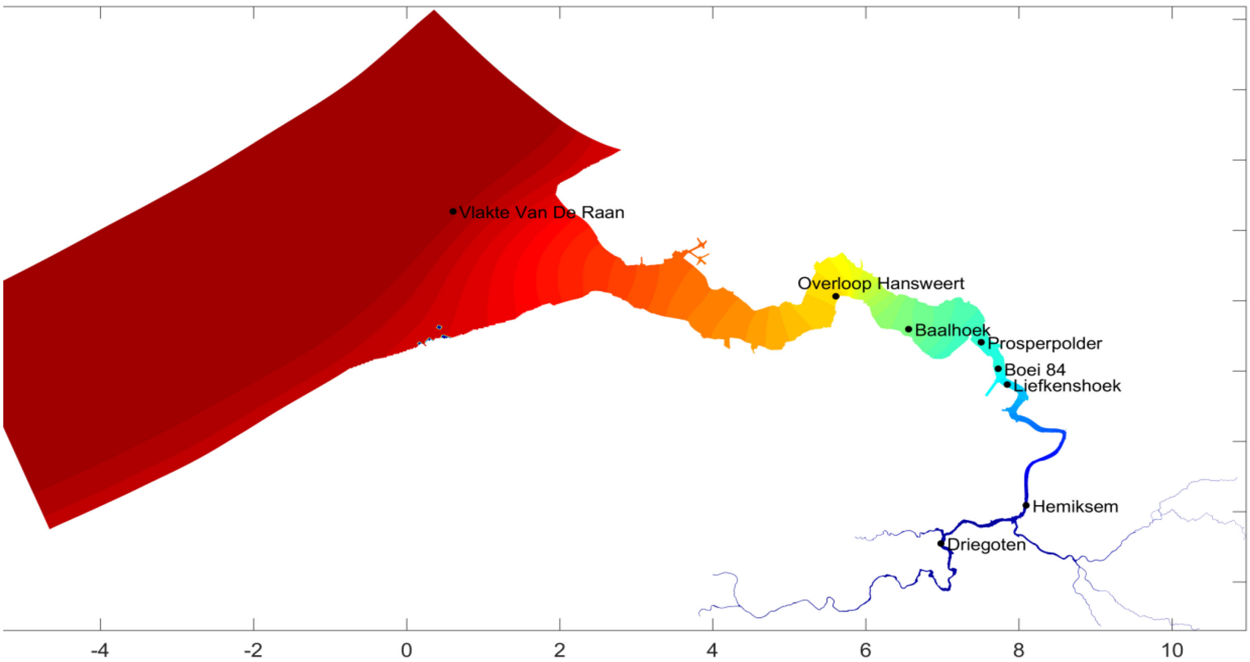

Table 7 – Overview of available stations with salinity measurements.

Nr	Measuring station	Data source	Initial salinity at 16-08-2015 00:00 [ppt]
1	Vlakte Van De Raan	HMCZ	33.5
2	Overloop Hansweert	HMCZ	22.8
3	Baalhoek	HMCZ	17
4	Prosperpolder	HIC	14.2
5	Boei 84	HIC	13.7
6	Liefkenshoek	HIC	12
7	Hemiksem	HIC	1.3
8	Driegoten	HIC	0.66

4.5 Discharges

River discharges are imposed at 8 stations in the NEVLA3D and SCALDIS model (See details in Table 8). Be aware that the river discharge data at Terneuzen is not available for the year 2015. Alternatively an averaged value of discharge over the entire year of 2014 (33.78 m^3/s) is applied there. Note that the discharge at Terneuzen is less substantial, with limited impact on the model results.

The time series of discharge at the other stations over the simulation period are presented in Figure 8. Most of the fresh water is imported from Bath (where every 10 minutes data are available) while river discharges from the other stations are less significant.

Table 8 – Description of river discharge data.

Station Names	Source	Year	Data Type	Temporal Resolution
Kleine Nete	www.waterinfo.be	2015	Measurement	daily
Grote Nete	www.waterinfo.be	2015	Measurement	daily
Dijle	www.waterinfo.be	2015	Measurement	daily
Dender	www.waterinfo.be	2015	Measurement	daily
Melle	www.waterinfo.be	2015	Measurement	daily
Zenne	www.waterinfo.be	2015	Measurement	daily
Bath	RWS	2015	Measurement	10 minutes
Ternuezen	RWS	2014	Calculated	Constant at **33.78** m^3/s

Figure 8 – Time series of river discharge.

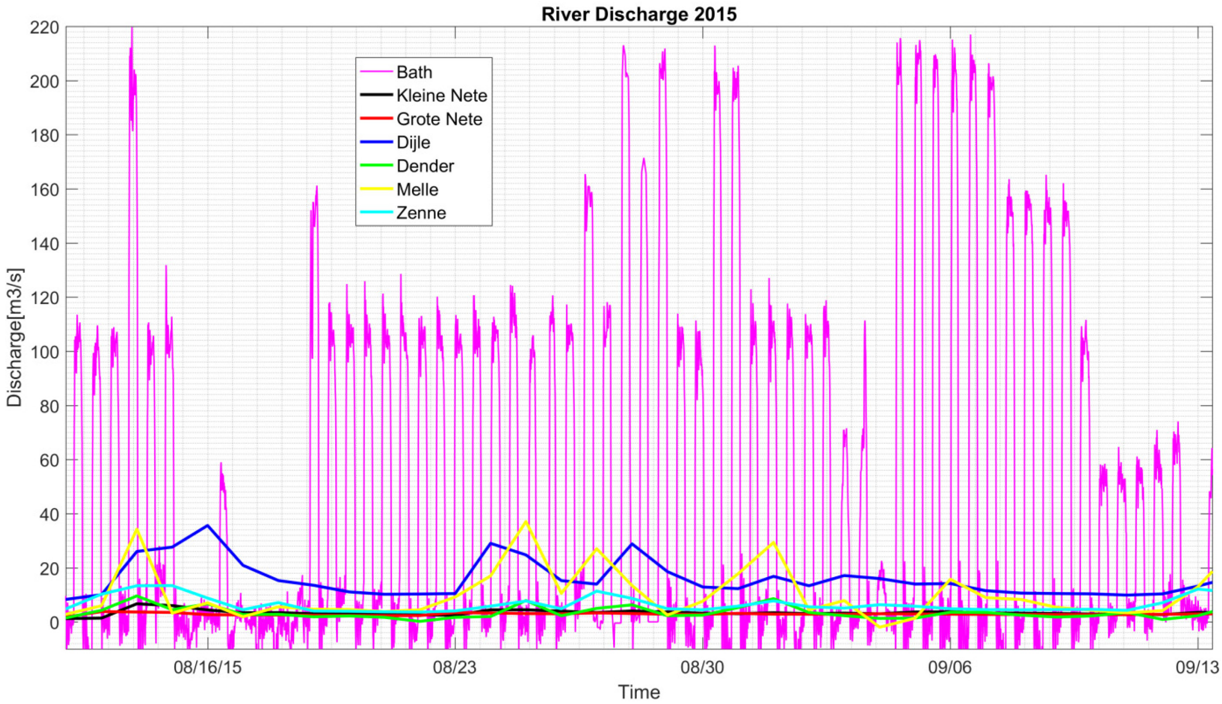

4.6 Wind

4.6.1 Hirlam wind

The wind field data (format: Grib) are received from Hirlam (High Resolution Limited Area Model), which is a Numerical Weather Prediction (NWP) forecast system developed by the international HIRLAM programme. The Grib data are converted into a SDS-file (binary format) by means of Simona script of **waqwnd**. The spatial resolution is 1/12° latitudinal and 1/8° longitudinal, corresponding to the grid resolution of the Continental Shelf Model (CSM). The temporal resolution is 3 hours.

The Hirlam wind field data are utilized to force the CSM and ZUNO model.

4.6.2 Measurement

Wind measurements are available at Hansweert with time interval of 10 minutes (RWS). The wind rose (Figure 9) indicates that winds mostly come from the SW with magnitudes generally smaller than 20 m/s.

The time series of wind measurement at Hansweert of 2015 (Figure 10) are utilized to force the NEVLA3D and SCALDIS model.

Figure 9 – Wind rose at Hansweert from measurements (analysis period: 01-01-2015 to 31-12-2015).

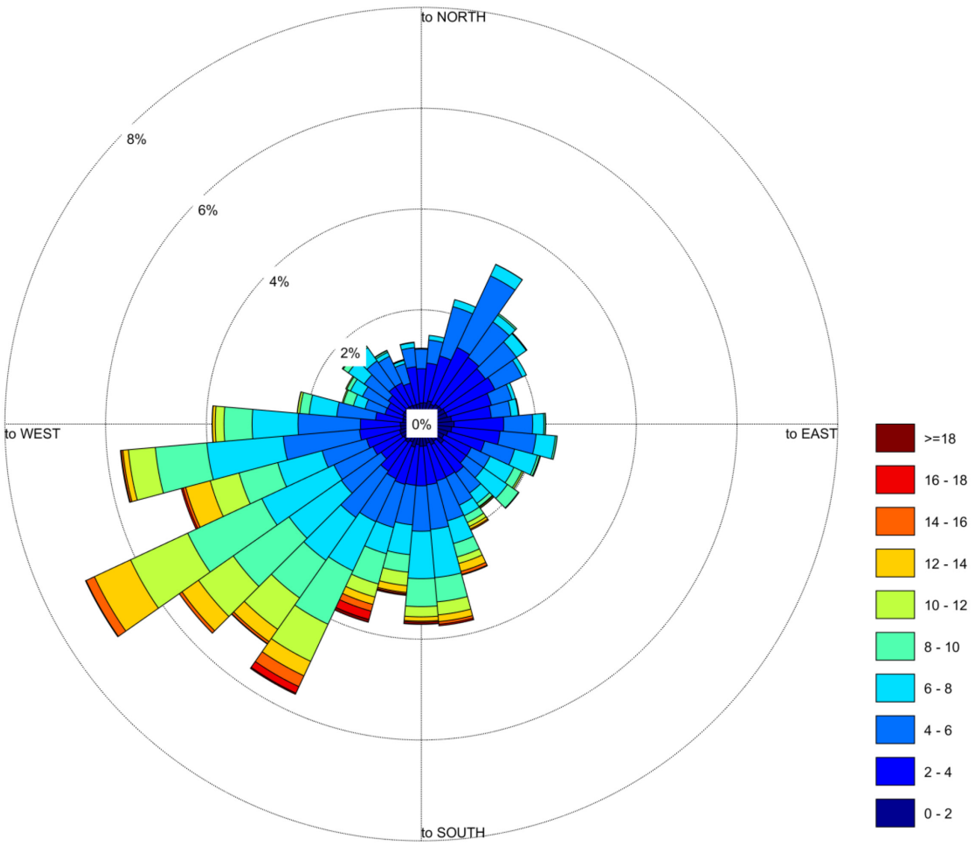

Figure 10 – Time series of measured wind speed and direction in the year 2015 at Hansweert (data source: RWS).

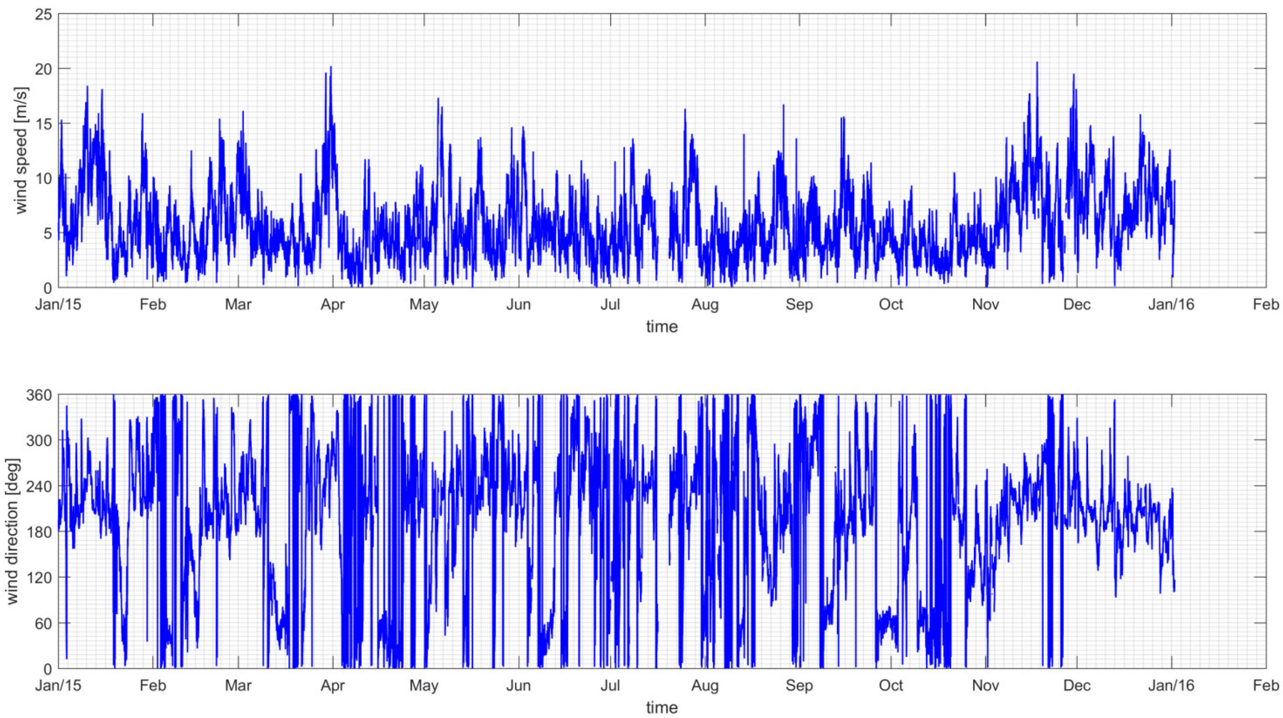

5 Model settings

5.1 Modelling software

The study is carried out using three different modelling suites: SIMONA, Delft3D and TELEMAC. Table 9 shows the domains and the modelling suites in which they were modelled.

SIMONA (Simulatie Modellen Natte waterstaat) is a program developed by Rijkswaterstaat, for 2D (WAQUA module) and 3D (TRIWAQ module) modelling of water movement and consists of a number of programs for preprocessing (preparation of simulations) and post processing (visualisation of the model results). The 2010 version of SIMONA is used in this study.

Delft3D-FLOW is a multi-dimensional (2D or 3D) hydrodynamic (and transport) simulation program developed by Deltares which calculates non-steady flow and transport phenomena that result from tidal and meteorological forcing on a rectilinear or a curvilinear, boundary fitted grid (WL/Delft Hydraulics, 2007). Delft3D allows the use of a domain decomposition technique, which helps to decrease computational time. Domain decomposition is a technique in which a model domain is subdivided into several smaller model sub-domains. Both the models of Boudewijn-Kallo and Zandvliet use this technique to reduce the computational time and increase the resolution in the area of interest.

The TELEMAC software is based on the finite element method. The model domain is discretized into an unstructured grid of triangular elements and can be locally refined in the study area. This way, the complex geometry of the study area can be taken into account. The Blue Kenue software (Canadian Hydraulics Centre, 2011) is used for the grid and bathymetry generation.

In all three cases, parallel computing is used to decrease the computational time.

Table 9 – Overview of use of different modelling suites

No.	Model domains	Modelling suite
1	CSM	SIMONA
2	ZUNO	
3	NEVLA3D	
4	Boudewijn-Kallo	Delft3D
5	Zandvliet	
6	Terneuzen	TELEMAC
7	Wintam	
8	SCALDIS3D	

5.2 CSM and ZUNO

The detailed model settings of CSM and ZUNO are recently reported by Maximova et al (2016) and are not repeated in this report. The model parameters of the CSM and ZUNO are being kept the same, except that the wind forcing has been updated with Hirlam wind filed data of 2015 (§4.6.1).

The hydrodynamic boundary conditions for both of the NEVLA3D and SCALDIS models are nested from the CSM-ZUNO model train. During the boundary nesting, the hydrodynamic and salinity boundary conditions are corrected based on analysis of model output from ZUNO model.

5.2.1 Correction on harmonic components

A correction of the harmonic components is calculated based on the comparison of the harmonic components of the ZUNO results and measurements from 01-08-2015 to 01-10-2015. Average differences in harmonic components (Measurements - ZUNO) are found for stations in the Belgian and Dutch Coastal zone for the M2, M4, S2 phases and Z0 component. The calculation of the corrections are presented in Table 10. The correction terms found here are different from the findings of Maximova et al., 2016 (Table 11), especially in terms of S2 phase and Z0 amplitude. This is justified because the analysis periods are different. It is therefore recommended to always carry out a new correction on the harmonic components for future studies when the simulation periods are subject to change.

Table 10 – Correction of harmonic components (analysis period: 01-08-2015 to 01-10-2015).

	M2 PHASE [deg]					**M4 PHASE [deg]**					**S2 PHASE [deg]**					**Z0 Amp [cm]**		
Stations	Measurement		ZUNO		Measurement-ZUNO	Measurement		ZUNO		Measurement-ZUNO	Measurement		ZUNO		Measurement-ZUNO	Measurement	ZUNO	Measurement-ZUNO
	Value	Error	Value	Error	Value	Value	Error	Value	Error	Value	Value	Error	Value	Error	Value	Value	Value	Value
Cadzand	49	0.2	45	0.2	4	97	2.9	101	4.3	-4	110	0.8	107	0.8	3	1.6	12.2	-10.6
Vlissingen	60	0.2	59	0.2	1	124	2.5	132	4.2	-8	123	0.7	123	0.8	0	3.8	11.8	-8.0
Westkapelle	54	0.2	49	0.3	5	103	2.4	107	3.5	-4	115	0.6	111	0.9	4	2.7	11.4	-8.7
Vlakte van de Raan	47	0.2	41	0.3	6	97	2.5	98	3.5	-1	107	0.7	101	0.8	6	3.7	10.1	-6.4
Oostende	34	0.2	28	0.2	6	39	3.0	50	4.4	-11	94	0.5	88	0.7	6	4.1	9.6	-5.5
Nieuwpoort	31	0.1	24	0.2	7	17	2.5	26	4.2	-9	90	0.6	84	0.7	6	4.3	8.6	-4.3
AVERAGE					**5**					**-6**					**4**			**-7.3**

Table 11 – Correction of harmonic components.

Harmonic component	**Correction (Maximova et al., 2016)**	**Correction (NEVLA2015)**
Phase M2	+4°	+5°
Phase M4	-6°	-6°
Phase S2	+7°	+4°
Z0	-16 cm	-7.3 cm
Analysis Period	**01-01-2013 to 31-12-2013**	**01-08-2015 to 01-10-2015**

The time series of the boundary conditions of the NEVLA3D model are eventually 'harmonically corrected' with the obtained correction terms (as shown in Table 11). This means that the time series at the boundary locations of the NEVLA3D model that are obtained out of ZUNO, are decomposed in harmonic components and a residual term. The harmonic components are corrected, and the signal is re-synthesized. Applying these corrected boundary conditions in the NEVLA3D model makes that the hydrodynamics in the NEVLA3D model does not have the systematic bias in harmonic components that is present in ZUNO.

5.2.2 Correction on Salinity Boundary

Model results for salinity are highly influenced by values imposed at the boundaries. Therefore, it is very important to have accurate salinity boundary conditions.

The modelled (ZUNO) and measured salinity at Vlakte van de Raan are compared in Figure 11. The ZUNO model underestimates the salinity values in the area of interest. Therefore, it is necessary to implement a salinity correction at the boundaries.

The correction is calculated based on the comparison of the calculated and measured salinity time series at Vlakte van de Raan (this salinity measurement point is the closest to the boundaries). The signal of the daily average difference is added to all the salinity boundaries.

Figure 11 – Comparison of salinity at Vlakte van de Raan between measurement and ZUNO predictions.

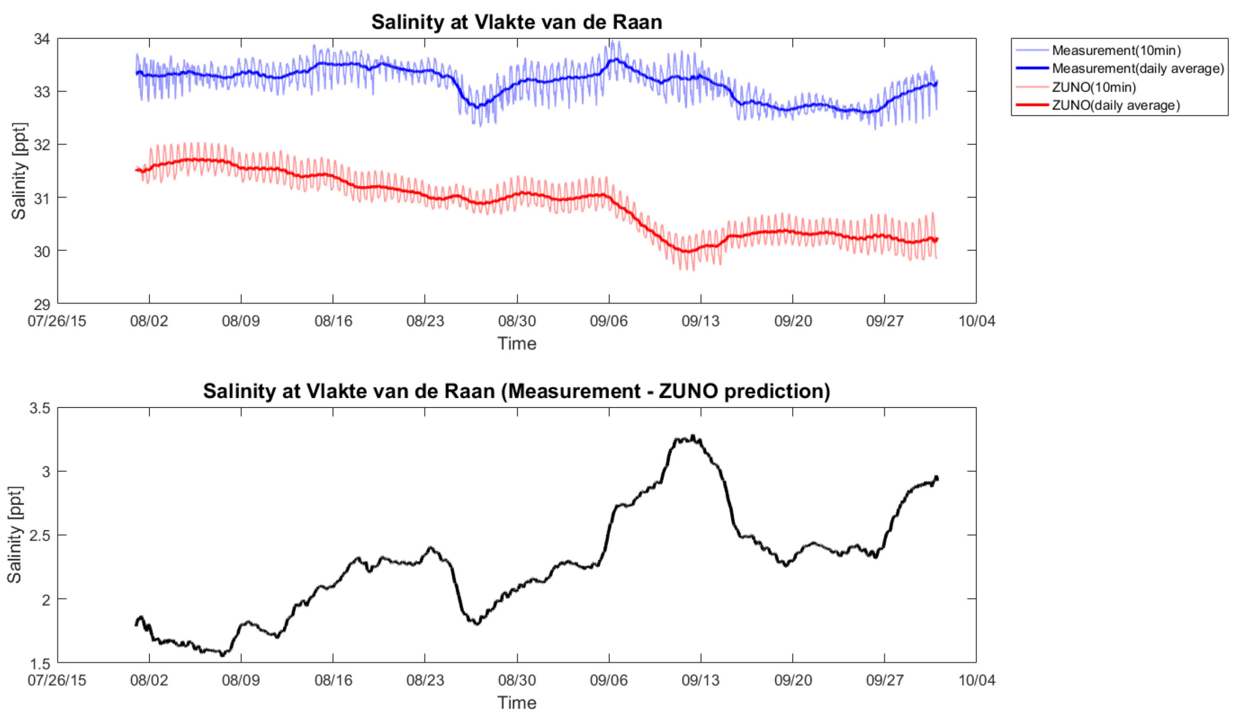

5.3 NEVLA 3D

The existing NEVLA3D model was recently calibrated and validated by Vanlede et al (2015) and is used as a basis for this study. The same model settings are applied for this study (Table 12). The existing NEVLA3D model is updated to the year of 2015 with the most recent bathymetry (see §4.1 and Figure 13), initial salinity conditions (see §4.4 and Figure 7), river discharge boundary conditions (see §4.5) and wind forcing (see §4.6.2). The open sea water level and salinity boundary conditions are corrected based on analysis of model output from ZUNO model (details are referred to §5.2.1 and §5.2.2).

Table 12 – Model parameters NEVLA model

Model parameter	**Value**
Global diffusion coefficient	10 m^2s^{-1}
Dynamic water viscosity	0.01 $kg.m^{-1}s^{-1}$
Water density	1023 kgm^{-3}
Air density	1.205 kgm^{-3}
Gravity	9.813 ms^{-2}
Wind stress coefficient	0.0026
Wind field	constant
Time step	0.125 min
Type of convergence criterion for the continuity equation	Water level
Convergence criterion for water levels in continuity equation	0.0005 m
Maximum number of iterations for the continuity equation	16
Maximum number of iterations for the momentum equation	32
Threshold value for drying/flooding checks at velocity points	0.3 m
Threshold value for drying/flooding checks at water level points	0.3 m
Friction formula	varying roughness field (Figure 12)
Time interval to compute Chézy values from given friction values	10 min
Eddy viscosity coefficient	1 m^2s^{-1}
Vertical velocity profile in the velocity boundary points	Logarithmic
Relation for the calculation of Chezy_3D	Velocity-ratio
Time integration of the vertical terms in the mass transport equation	Central
Modelled constituents	Salinity
Turbulence model	k-ε model

Figure 12 – The bottom roughness field (Manning coefficient unit: $m^{-1/3}s$) of the NEVLA3D model.

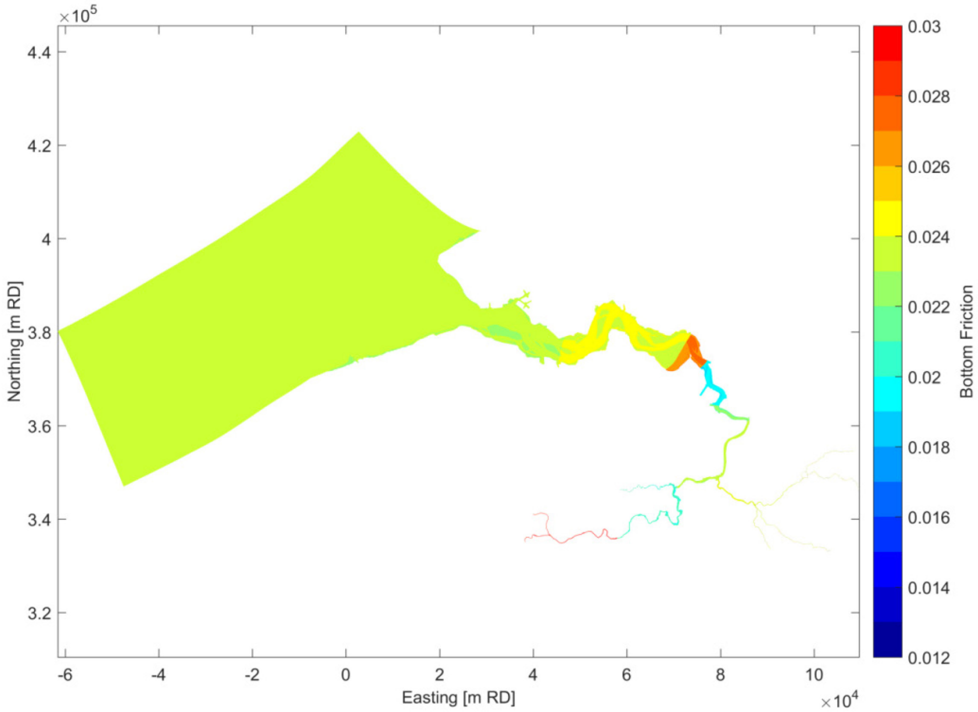

Figure 13 – Bathymetry of NEVLA3D model (positive downward).

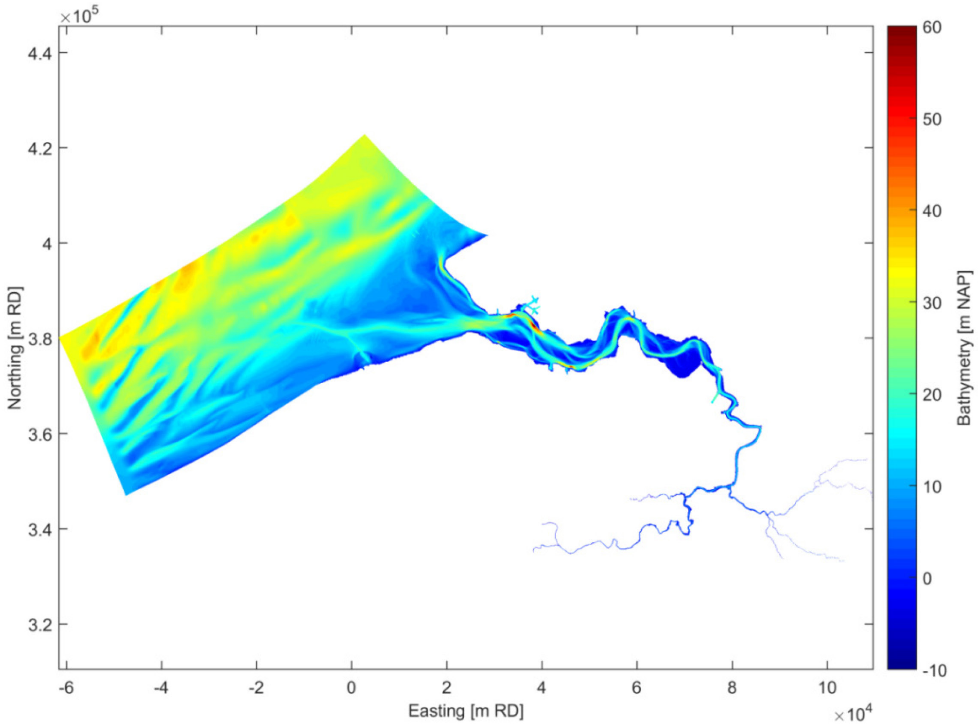

5.4 Boudewijn – Kallo

A detailed Delft3D model has been constructed for the entrances of the locks Boudewijn, Van Cauwelaert and Kallo. For these areas it is important to have a well refined grid which can represent the flow in the locks' entrances correctly. This detailed model has been calibrated and validated based on the available ADCP measurements at Liefkenshoek and Kallo (Maximova et al. 2011) and it is therefore used as a basis for this study. The same parameter settings are applied on this study (Table 13).

Table 13 – Model parameters of the Boudewijn-Kallo model.

Model parameter	**Value**
Time step	3 s
Secondary Flow	On
Initial condition water level	2 m NAP
Initial condition velocity	0 ms^{-1}
Horizontal eddy viscosity (background value)	1 m^2s^{-1}
HLES	On
Number of layers in the vertical (KMAX)	1 (2D model)
Salt transport	Off
Wind	Off
Roughness formula	Manning
Bed roughness value	0.028 $m^{-1/3}s$

Figure 14 shows the model grid with domain decomposition. For the Boudewijn-Kallo region, the cells of the first sub-domain are about 115 x 50 m (length x width) near Schaar van de Noord, 120 x 100 m near Bath and 100 x 50 m at the Land van Saeftinge. The grid becomes finer near the Deurganck dock. The grid resolution there varies from 90 x 50 m to 60 x 40 m. The cell size is about 80 x 40 m at Antwerp and 100 x 35 m at Hemiksem. The second model sub-domain with a refined grid includes the area from Liefkenshoek to Oosterweel. The cell size near the Boudewijn – Van Cauwelaert locks varies from 25 x 15 m to 35 x 20 m. Near the Kallo lock the cell size changes from about 30 x 15 m to 40 x 18 m.

The bathymetry has been updated with the most recent bathymetric measurements (§4.1) and shown in Figure 15.

The boundary conditions are nested from NEVLA3D model. The selection of boundary types is taken from Maximova et al. 2011. The downstream boundary is located at Walsoorden and has been divided into three sections between the points that never become dry (Figure 16) and total discharges are imposed. A linear water level profile is defined at the upstream boundary which is located at Schelle. The boundary condition is prescribed at two so-called boundary support points. Points that lie in between these two support points are calculated by linear interpolation of the forcing at both ends (WL/Delft Hydraulics, 2007). Two points closest to the river banks that never get dry are used as support points in the detailed model. 10 minute time series of the water level (calculated in the NEVLA model) are defined in these points.

There are in total 43 ADCP transect measurements available within the Boudewijn-Kallo model domain, among which 34 ADCP measurements are located within the far field domain and 9 ADCP measurements (at Kallo and Liefkenshoek) are located within the near field domain (see locations in Figure 17).

Figure 14 – Boudewijn-Kallo - detailed model with domain decomposition (Delft3D).
Red - first sub-domain (NEVLA grid resolution), Green - second sub-domain (4x4 grid refinement).

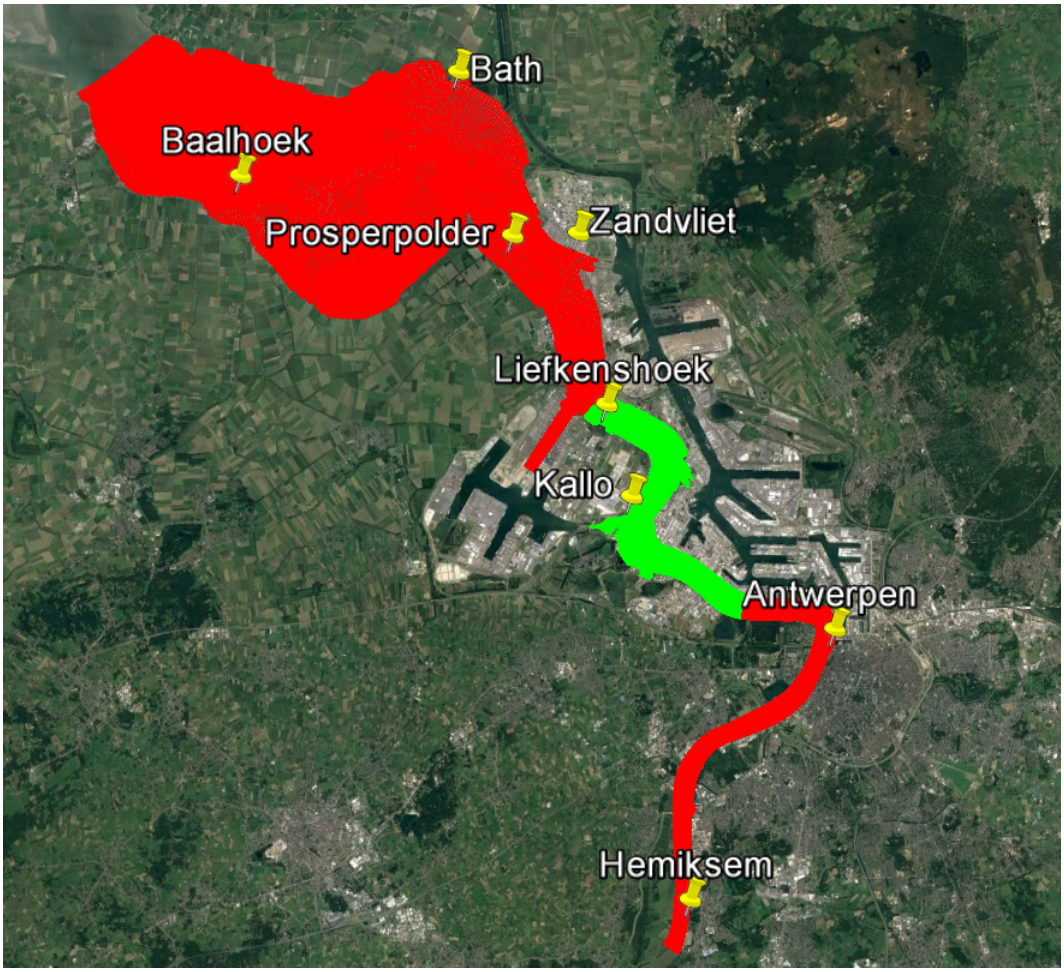

Figure 15 – Bathymetry of the Boudewijn-Kallo model (positive downward).

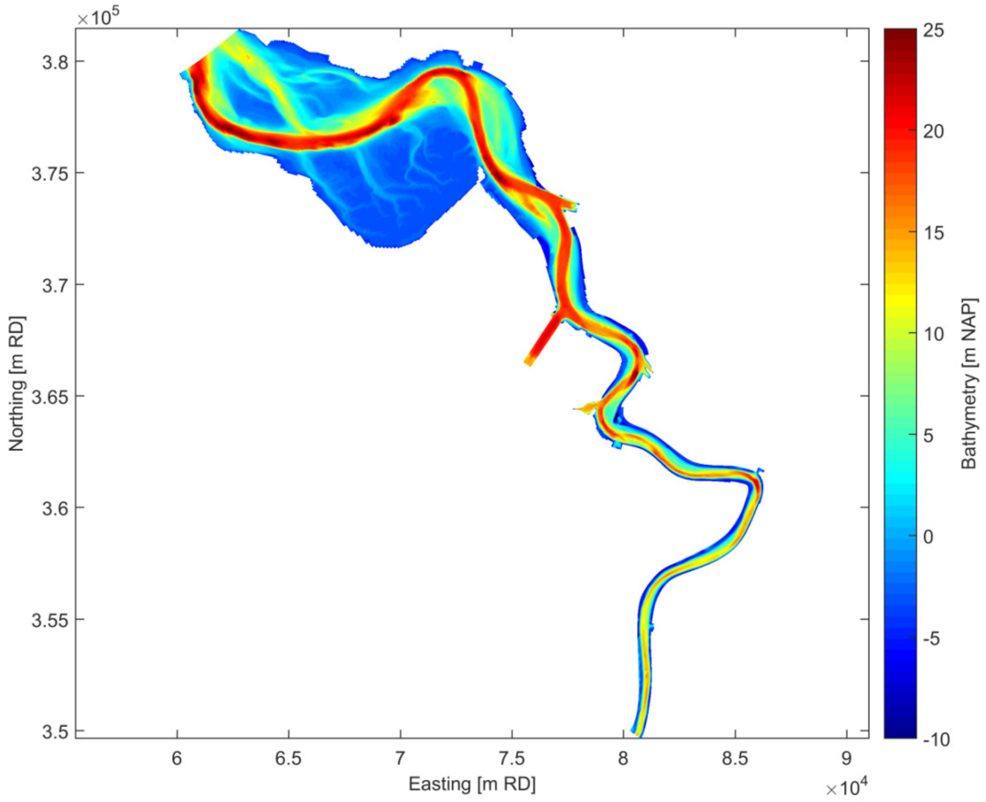

Figure 16 – Left panel: Downstream discharge boundary; Right panel: Upstream water level boundary.

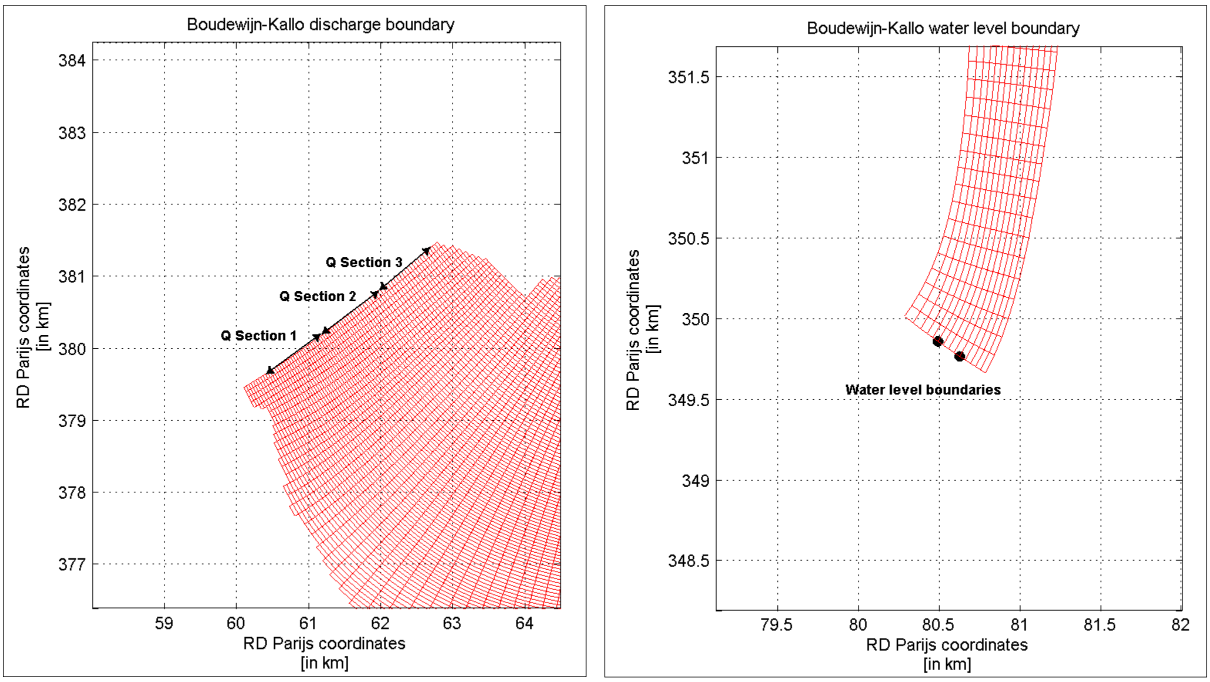

Figure 17 – Available ADCP measurements within the Boudewijn-Kallo model domain.
Note: for the purpose of concision, different ADCP transects (executed on different dates) at the same locations (e.g. Oostwerweel, DGD, Liefkenshoek etc) are labeled only once.

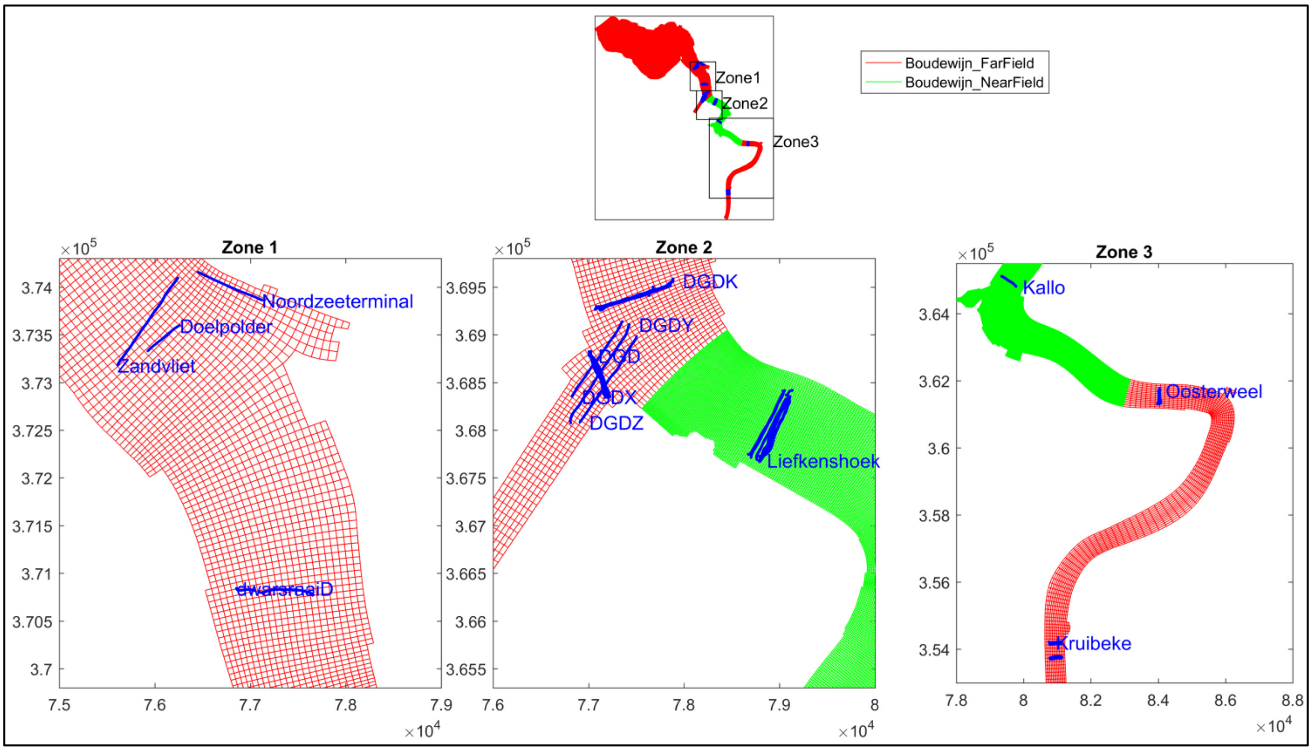

5.5 Zandvliet-Berendrecht

The detailed Delft3D Zandvliet- Berendrecht model has been calibrated and reported by Decrop et al (2010) and it is used as a basis for this study. The same parameter settings are applied on this study (Table 14).

Table 14 – Model parameters of the Zandvliet model.

Model Parameter	**Value**
Time step	3.75 s
Secondary Flow	On
Initial condition water level	2.35 m NAP
Initial condition velocity	0 ms^{-1}
HLES	On
Number of layers in the vertical	1 (2D model)
Salt transport	Off
Wind	Off
Roughness formula	Manning
Bed roughness value	0.024 $m^{-1/3}s$
Horizontal eddy viscosity	1.0E-6 m^2s^{-1}

For the Zandvliet- Berendrecht model, the domain is also divided into two sub-domains as presented in Figure 18. The grid resolution is about 20x23 m (width x length) to 11x30 m in the study area (near field) and 47x57 to 80x110 m near the boundaries (far field).

The bathymetry has been updated with the most recent bathymetric measurements (§4.1) and shown in Figure 19.

The boundary conditions are nested from NEVLA3D model. The discharge per cell is used as downstream boundary condition and water level for the upstream boundaries (Figure 20). An individual discharge was defined for each cell (except permanently dry cells) as it was calculated for this width across the river by the overal model. At the upstream boundary a linear water level profile was imposed. The water level time series were defined at two so-called boundary support points. Points that lie in between two support points were calculated by linear interpolation.

There are in total 4 ADCP transect measurements available within the Zandvliet model domain, among which one ADCP measurements are located within the far field domain and 3 ADCP measurements are located within the near field domain (see locations in Figure 21).

Figure 18 – Zandvliet - detailed model with domain decomposition (Delft3D).
Red - first sub-domain (original grid resolution), Green - second sub-domain (4x4 grid refinement).

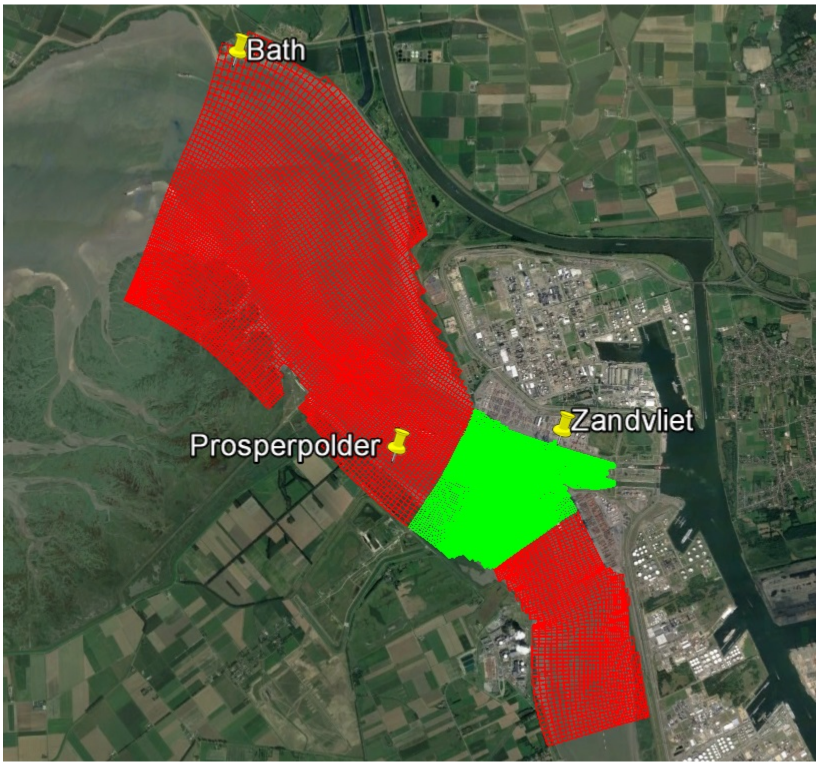

Figure 19 – Bathymetry of the Zandvliet model (positive downward).

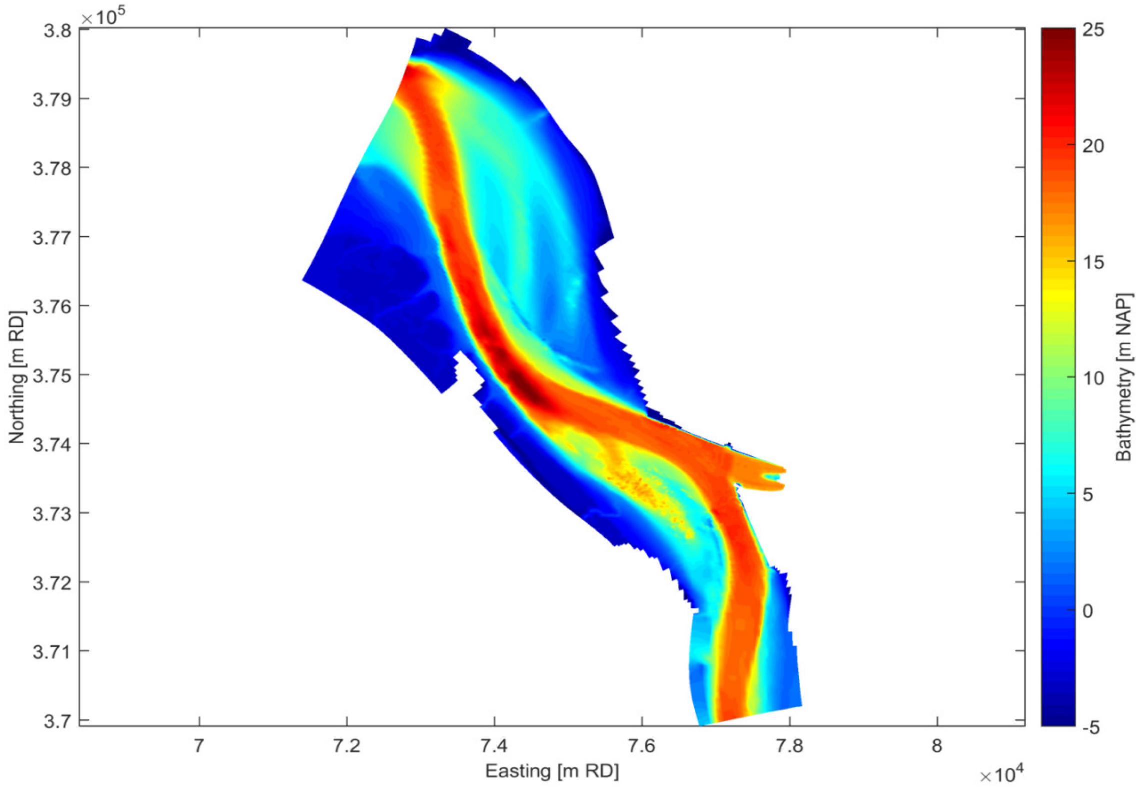

Figure 20 – Left panel: Downstream discharge boundary per cell; Right panel: Upstream water level boundary.

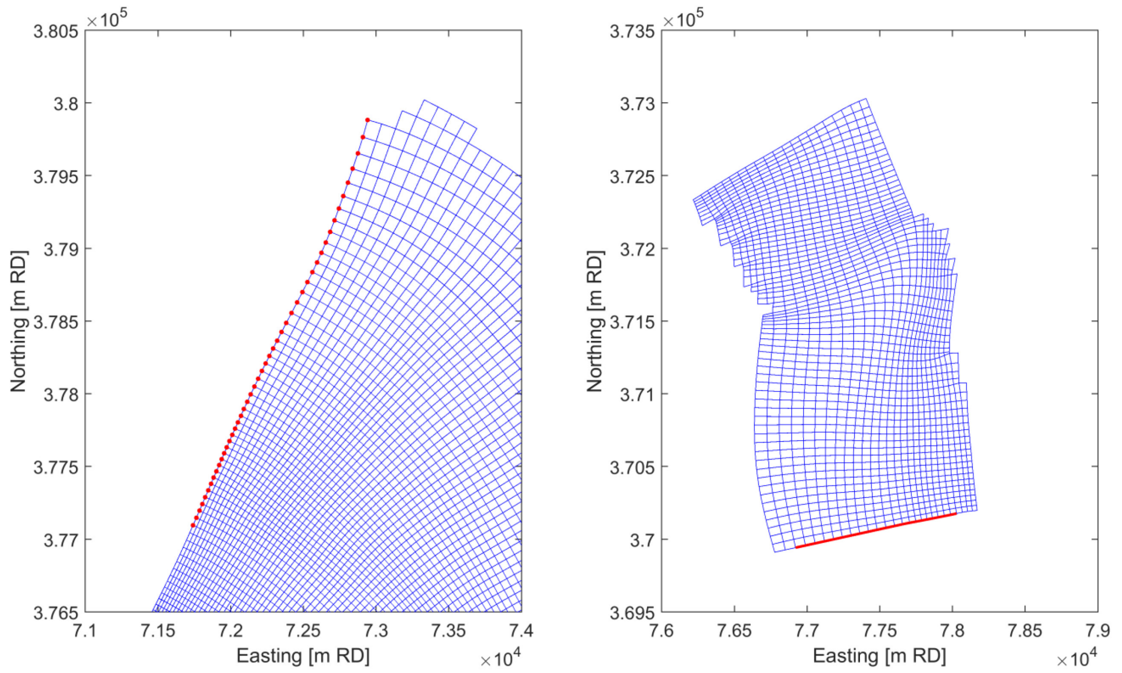

Figure 21 – Available ADCP measurements within the Zandvliet model domain.

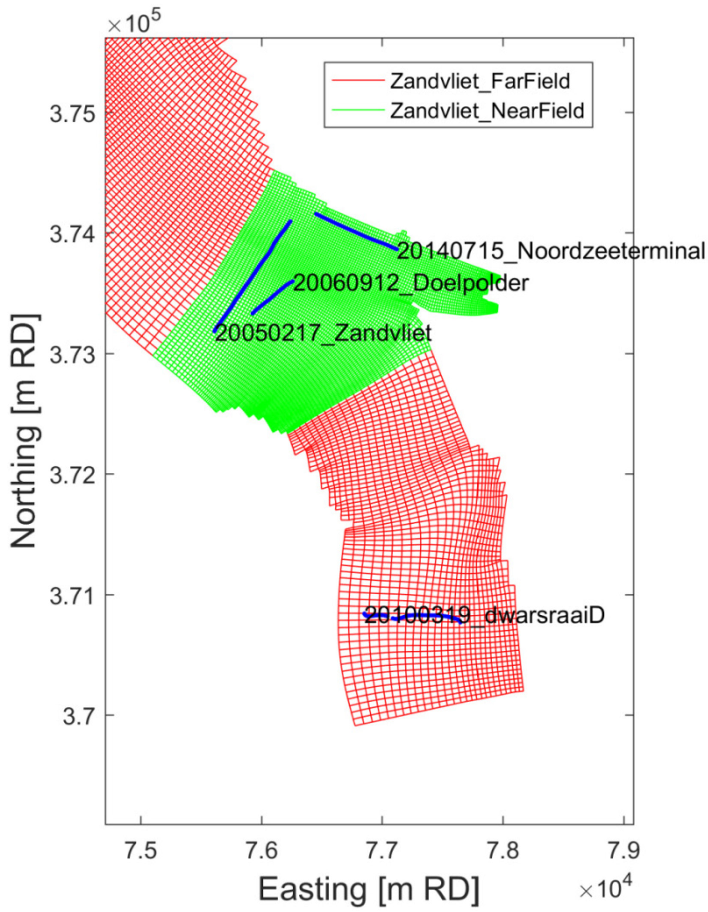

5.6 Wintam

A detailed TELEMAC model has been constructed for the lock of Wintam. For this area it is important to have a well refined grid which can represent the flow to the lock correctly. The model has been calibrated based on the available water level, velocity and discharge measurements (Maximova et al, 2014) and it is therefore used as a basis for this study. The same parameter settings are applied on this study (Table 15).

Table 15 – Model parameters of the Wintam model.

Parameter	**Value**
Time step	3 s
Initial condition	7 m NAP
Number of layers in the vertical	1 (2D model)
Version TELEMAC	TELEMAC 5.9 (Linux)
Salt transport	Off
Wind	Off
Roughness formula	Manning
Bed roughness value	0.017 $m^{-1/3}s$ uniform
Velocity diffusivity	10^{-4} m^2s^{-1}
Treatment of the linear system	2: wave equation
Free surface gradient compatibility	0.9
Continuity correction	true
Turbulence model	1: Constant viscosity
Type of advection	Method of characteristics
Solver	7: GMRES

The model grid is presented in Figure 22. The grid resolution near the lock of Wintam is 10 m. The bathymetry has been updated with the most recent bathymetric measurements (§4.1) and shown in Figure 23.

The boundary conditions are nested from NEVLA3D model. The downstream boundary is located between Kallo lock and Oosterweel and it is forced with water levels. The model has four upstream river discharge boundaries (Figure 24). The upstream boundaries are simulated with 10 minutes discharge time series extracted from the NEVLA model. The discharge at Durme is zero and therefore no boundary condition is defined there. The discharges from NEVLA are multiplied by -1 because the ebb flow is negative in SIMONA at these locations while it is positive in TELEMAC (the inflow at the upstream boundary is positive). There are in total 16 ADCP transect measurements available within the Wintam model domain (see locations in Figure 25).

Figure 22 – Overall grid of the Wintam model (upper) and zoom in to the Wintam lock (lower).

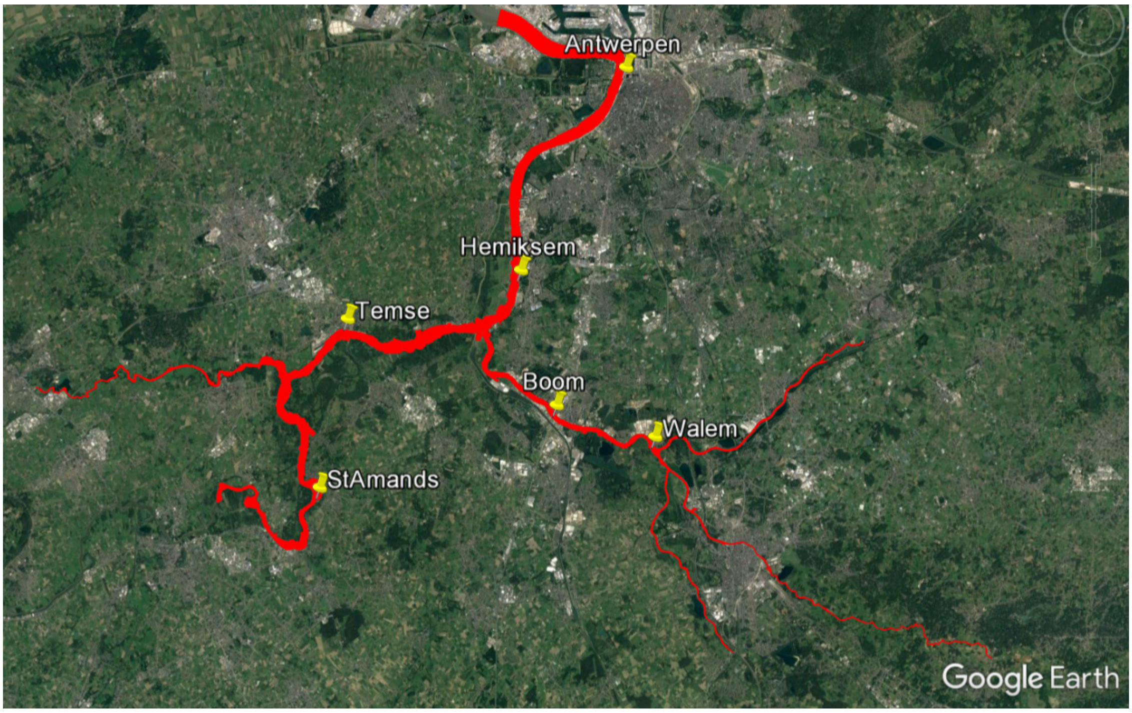

Figure 23 – Bathymetry of the Wintam model (positive downward).

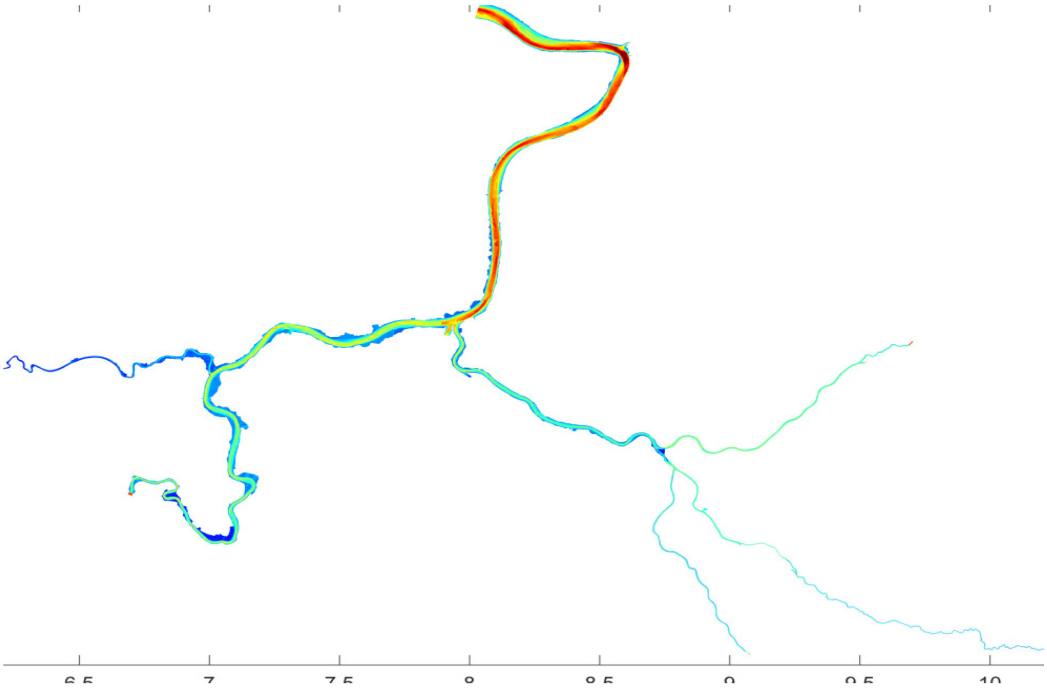

Figure 24 – Boundary conditions of the Wintam model.

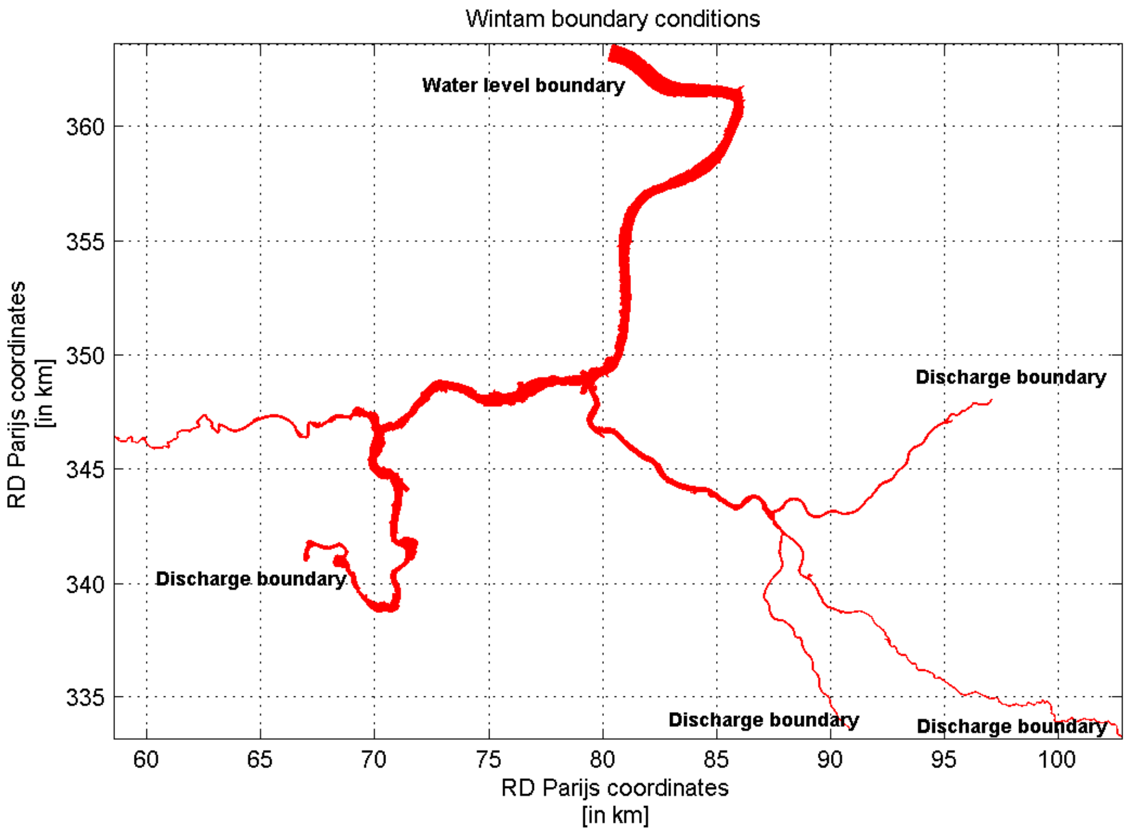

Figure 25 – Available ADCP measurements within the Wintam model domain.
Note: for the purpose of concision, different ADCP transects (executed on different dates) at the same locations (e.g. Kruibeke and Oosterweel etc) are labelled only once.

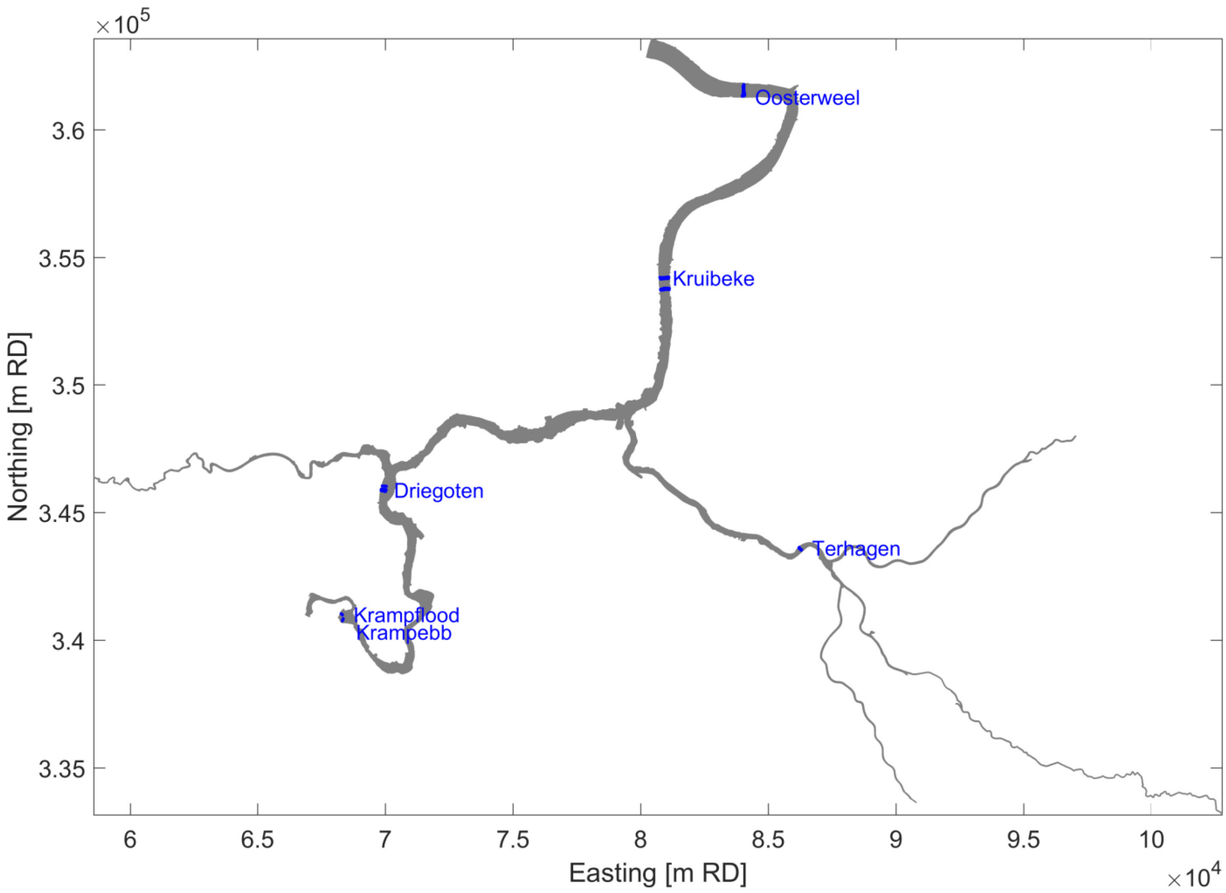

5.7 Terneuzen

A detailed TELEMAC model has been constructed for the port of Terneuzen. For this area it is important to have a well refined grid which can represent the flow to the locks correctly. The model has been calibrated based on the available water level, velocity and discharge measurements (Maximova et al, 2013) and it is therefore used as a basis for this study. The same parameter settings are applied on this study (Table 16).

Table 16 – Model parameters of the Terneuzen model.

Parameter	**Value**
Time step	3 s
Initial condition	2 m NAP
Number of layers in the vertical	1 (2D model)
Version TELEMAC	TELEMAC 5.9 (Linux)
Salt transport	Off

Wind	Off
Roughness formula	Manning
Bed roughness value	varying roughness field (0.021 to 0.023 $m^{-1/3}s$)
Velocity diffusivity	2 m^2s^{-1}
Graphic printout period	200 time steps (=10 min)
Treatment of the linear system	2: wave equation
Free surface gradient compatibility	0.9
Continuity correction	True
Turbulence model	1: Constant viscosity
Type of advection	Method of characteristics
Solver	7: GMRES

The model grid is presented in Figure 26. The grid resolution is 100 m at the model boundaries, 50 m in the area around the port of Terneuzen and 10 m at Terneuzen. Hard lines were used at the downstream and upstream model boundary to force the boundaries of the TELEMAC model to follow the lines of the NEVLA model. Soft lines were used to define the flow guiding structures of Ballastplaat and Ouden Doel (“leidam en strekdam” in Dutch) in the Lower Sea Scheldt.

The bathymetry has been updated with the most recent bathymetric measurements (§4.1) and shown in Figure 27.

The boundary conditions are nested from NEVLA3D model. The downstream boundary is located at Vlissingen; the upstream boundary is located at Liefkenshoek. The downstream boundary is total discharge and the upstream boundary is water level (Figure 28).

There are in total 42 ADCP transect measurements available within the Terneuzen model domain (see locations in Figure 29).

Figure 26 – Overall grid of the Terneuzen model (upper) and zoom in to Terneuzen (lower).

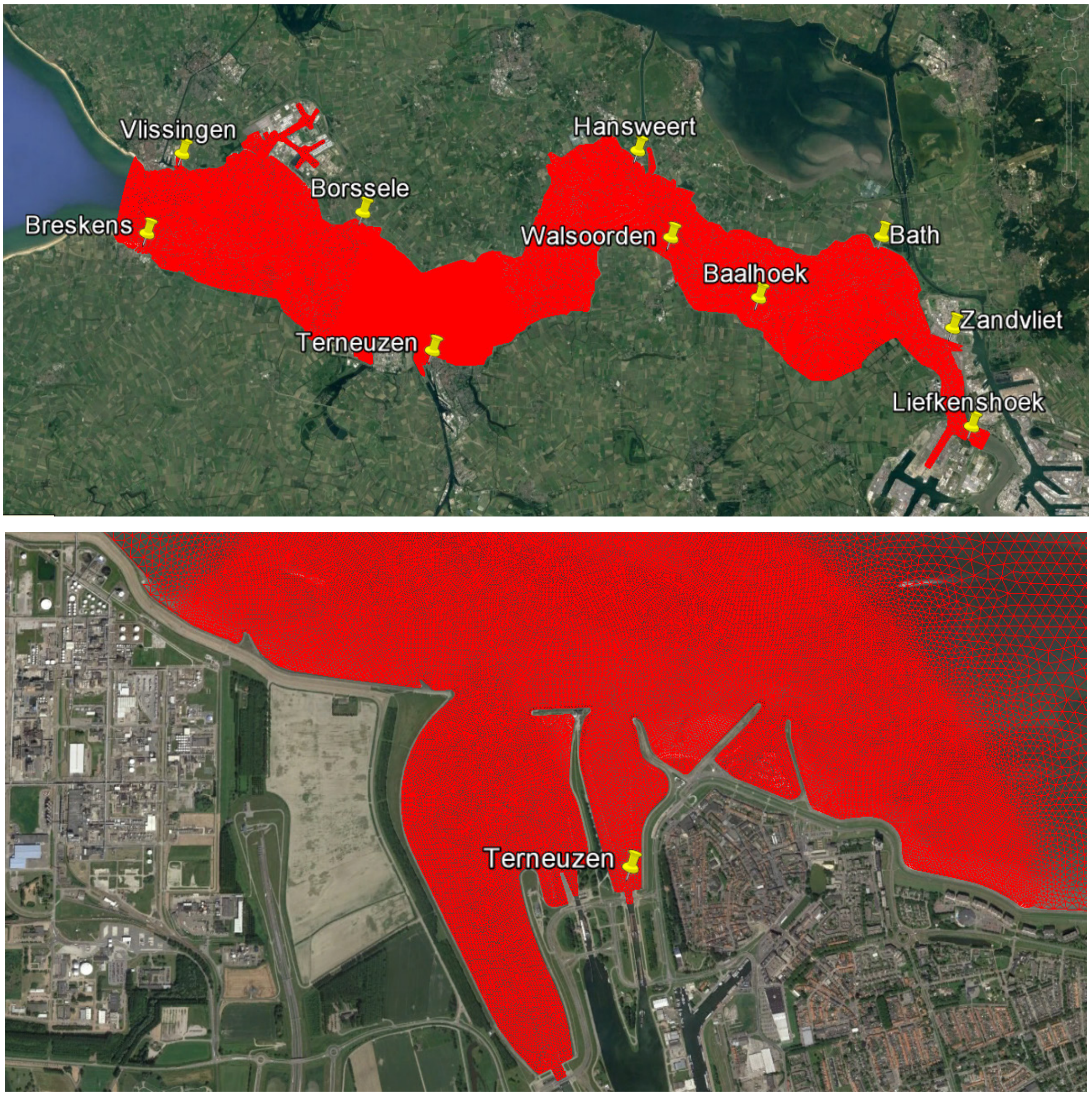

Figure 27 – Bathymetry of the Terneuzen model (positive downward).

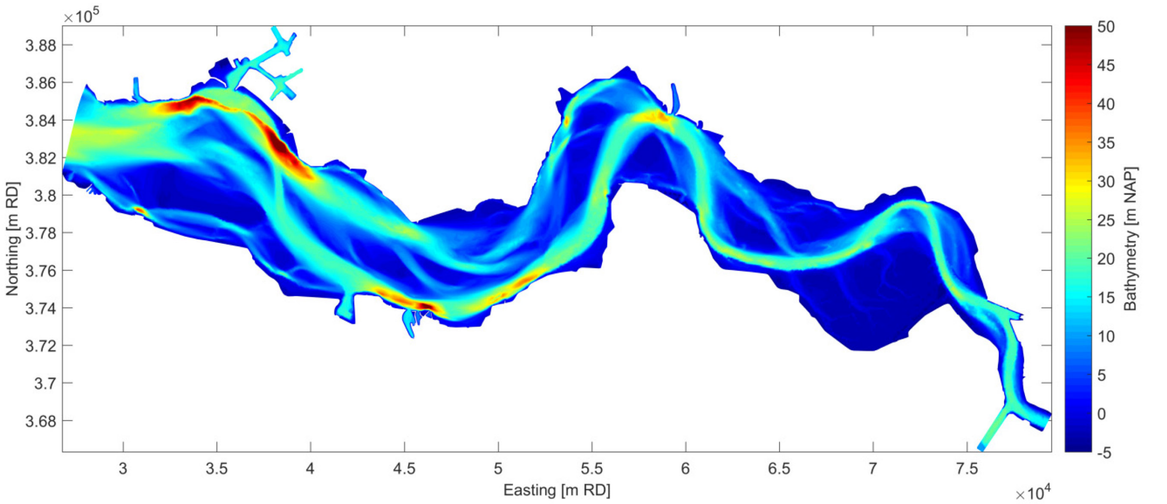

Figure 28 – Left panel: Downstream discharge boundary; Right panel: Upstream water level boundary.

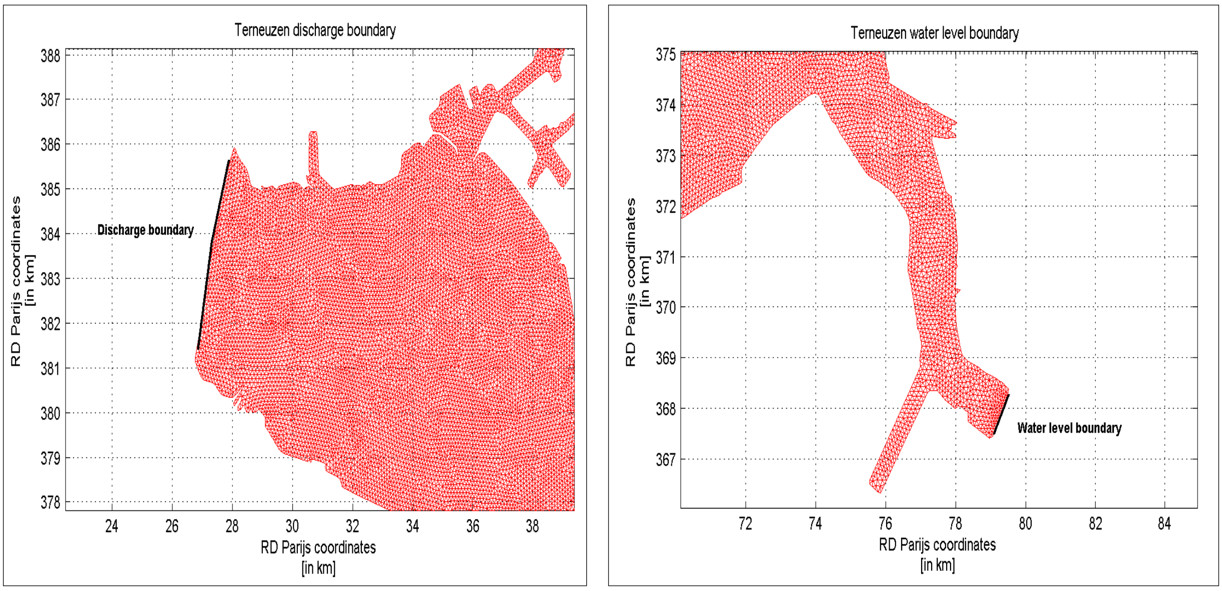

Figure 29 – Available ADCP measurements within the Terneuzen model domain.
Note: for the purpose of concision, different ADCP transects (executed on different dates) at the same locations (e.g. DGD and Liefkenshoek etc) are labelled only once.

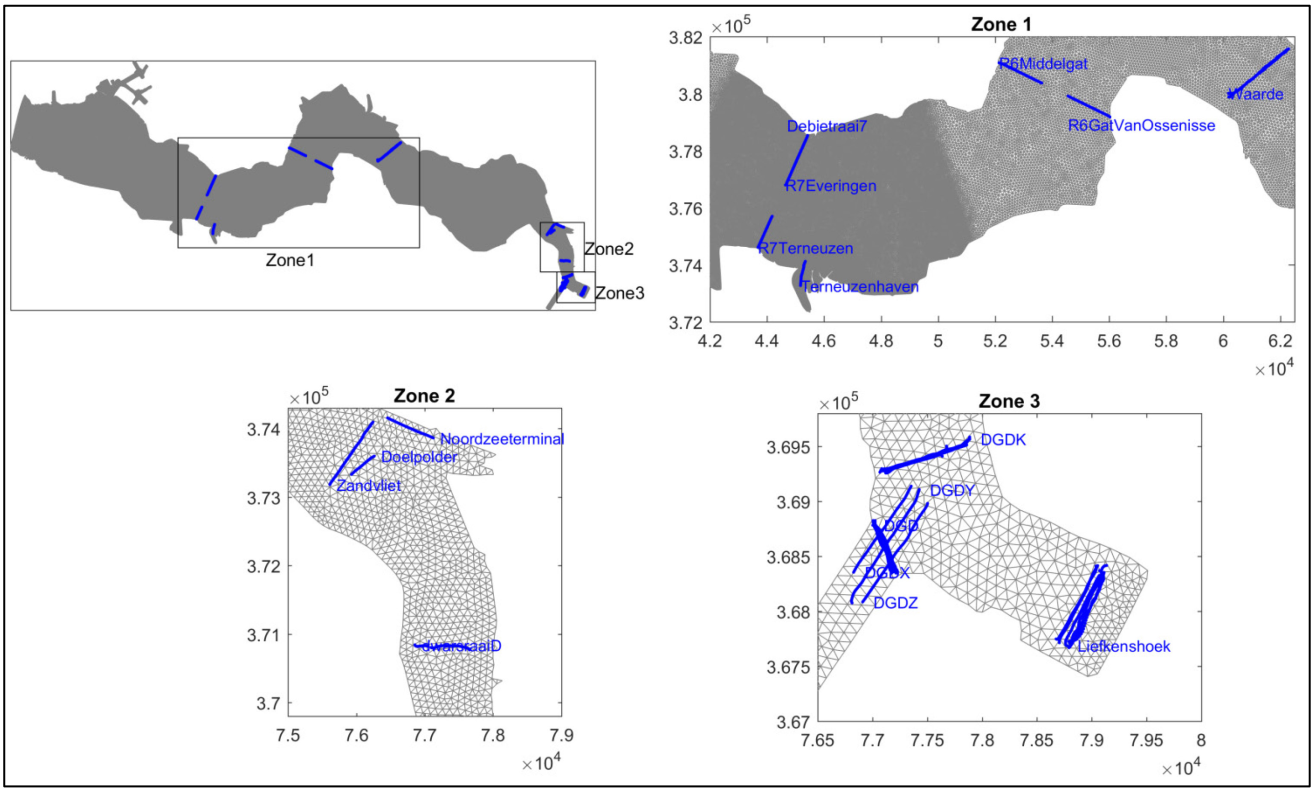

5.8 Quality Check of Nesting

The four above-mentioned detailed models are all nested with NEVLA model. Therefore it is necessary to check the nesting quality before performing scenario runs. .

Figure 30 present the RMSE of the complete time series of water level along the estuary, compared with NEVLA model predictions.

The location of the water level boundary of the detailed model that is nested in the water levels of NEVLA is indicated with a box in .

Figure 30.

A perfect nesting would mean that the RMSE of water level between mother and daughter model is zero at the boundary. Differences between water levels in mother and daughter model can occur due to a different model schematisation between mother and daughter, the influence of the other boundary condition of the daughter model (typically a discharge boundary condition), different software platforms and different model parametrizations (roughness in particular).

Figure 30 – Comparison of RMSE0 (versus NEVLA model) of the complete time series of water level along the estuary.

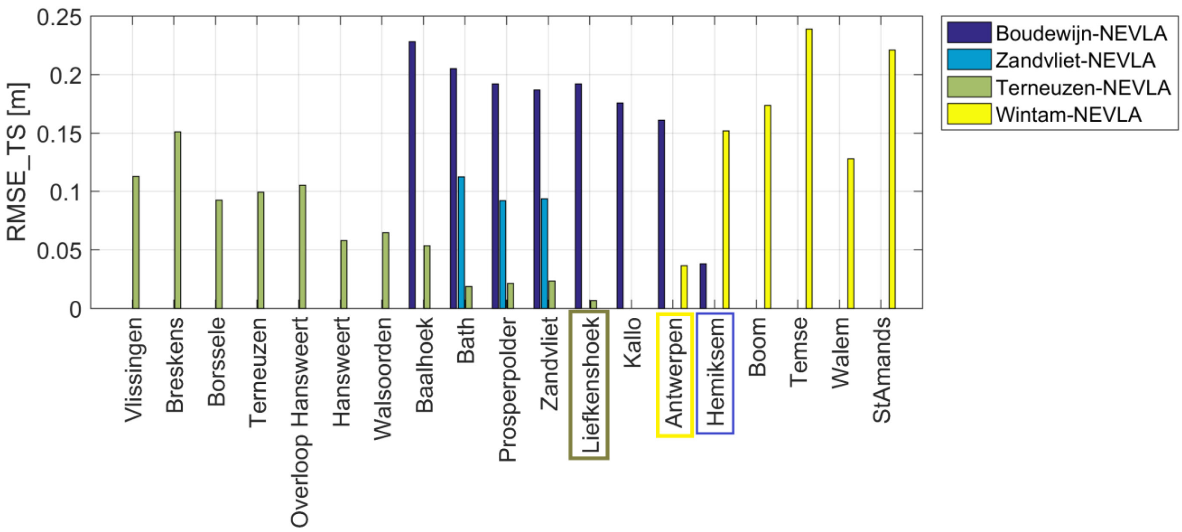

The closest water level station from the nested water level boundary section between Boudewijn-Kallo model and the NEVLA model is at **Hemiksem** where the RMSE is less than 5 cm. The nesting quality is considered as good. However the RMSE increases substantially to ~20 cm from boundary to inside model domains.

The closest water level station from the nested water level boundary section between Zandvliet model and the NEVLA model is at **Liefkenshoek** which is however just outside of the Zandvliet domain. Threfore the nesting quality for the Zandvliet model is not checked here.

The closest water level station from the nested water level boundary section between Terneuzen model and the NEVLA model is at **Liefkenshoek** where the RMSE is less than 2 cm. The nesting quality is good. The RMSE slightly increases to 5-15 cm from boundary to further downstream.

The closest water level station from the nested water level boundary section between Wintam model and the NEVLA model is at **Antwerpen** where the RMSE is less than 5 cm. The nesting quality is good. The RMSE substantially increases to ~25 cm from boundary to further upstream.

5.9 SCALDIS

The existing in-house SCALDIS3D model was recently calibrated and validated by Smolders et al (2016) and is used as a basis for this study. The same model settings are applied for this study (Table 17). The existing SCALDIS model is updated to the year of 2015 with the most recent bathymetry (see §4.1 and Figure 32), initial salinity conditions (§4.4 and Figure 33), river discharge boundary conditions (§4.5) and wind forcing (§4.6.2).

Similar to NEVLA3D model, the open sea water level and salinity boundary conditions are corrected based on analysis of model output from ZUNO model (details are referred to §5.2.1 and §5.2.2).

Table 17 – Model parameters SCALDIS model

Parameter	**Value**
Time step	4 s
Initial condition	1 m NAP
Number of vertical levels	5
Version TELEMAC	TELEMAC Balloonfish (Linux; in-house customised version)
Salt transport	On
Wind	On
Roughness formula	Manning
Bed roughness value	varying roughness field (Figure 31)
Option for the treatment of tidal flats	1: equations solved everywhere with correction on tidal flats
Treatment of negative depths	2: flux control
Free surface gradient compatibility	0.9
Vertical turbulence model	2: mixing length
Mixing length model	3: Nezu and Nakagawa
Horizontal turbulence model	4: Smagorinski
Scheme for advection of velocities	1: characteristics
Scheme for advection of depth	5: conservative scheme
Scheme for advection of tracers	13: Leo Postma for tidal flats
Scheme for diffusion of velocities	1: implicit (1 is default; 0 cancels the diffusion)
Scheme for diffusion of tracers	1: implicit
Solver	7: GMRES

Figure 31 – The bottom roughness field (Manning coefficient unit: $m^{-1/3}s$) of the SCALDIS model.

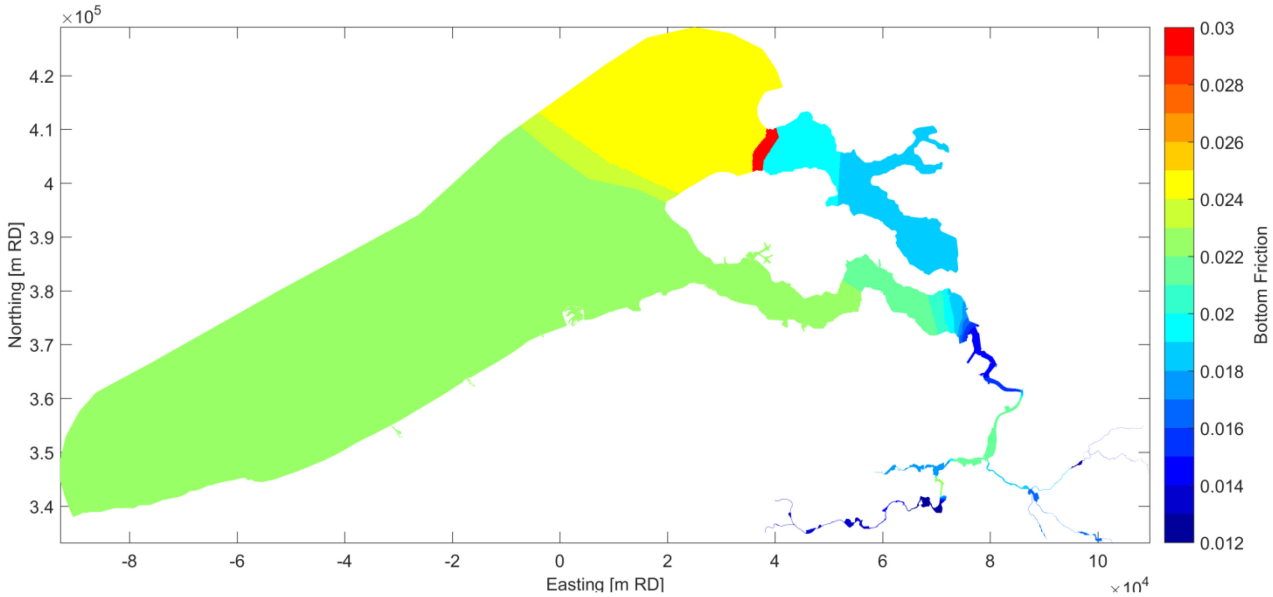

Figure 32 – Bathymetry of the SCALDIS model (positive downward).

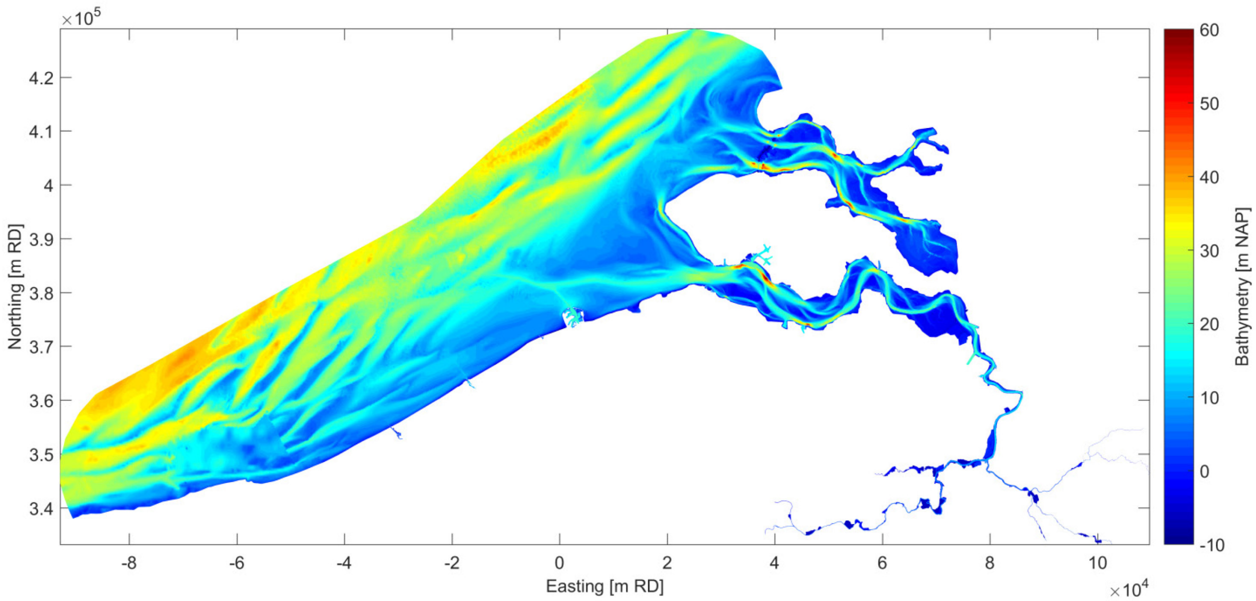

Figure 33 – Initial salinity field for the SCALDIS model.

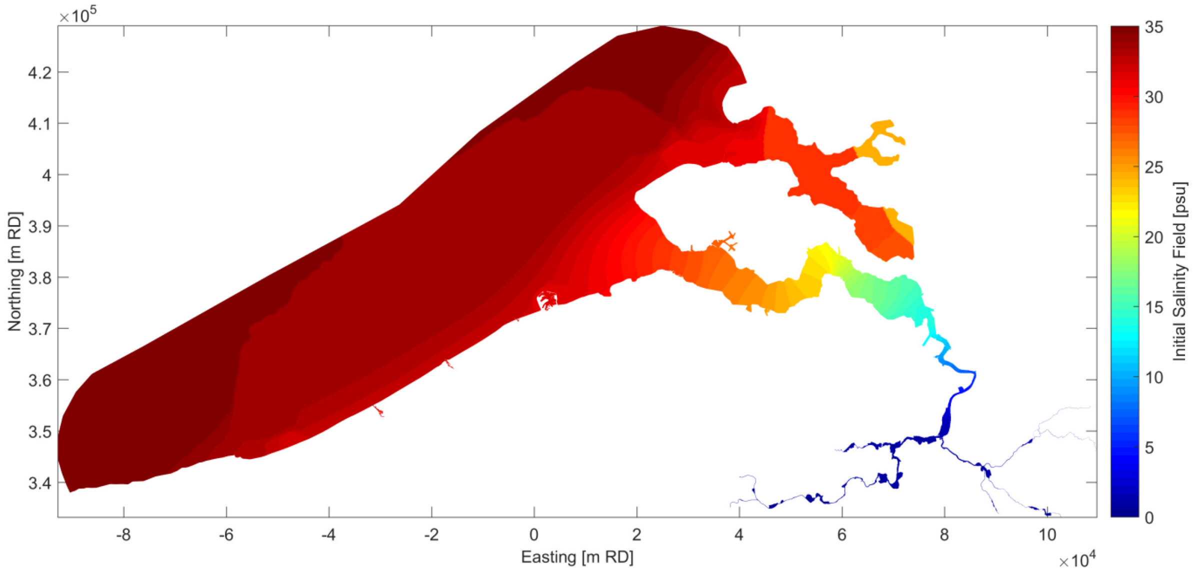

6 Model results

6.1 Stationary Velocity

3D modelled velocities from NEVLA3D and Scaldis3D are compared with the stationary velocity measurements at Buoy 84, Oosterweel and Driegoten at corresponding heights above the bottom (see Table 5). Figure 34 to Figure 38 exemplify the time series plot of velocity magnitude and direction between 01-09-2015 and 03-09-2015 at Buoy 84, Oosterweel and Driegoten respectively. The statistical parameters (MAE and RMAE of the velocity vector, bias and RMSE of the velocity magnitude and direction) were calculated to evaluate the model accuracy (Table 18).

Both of the Scaldis3D and NEVLA3D model reproduce the stationary velocity very well at Buoy 84 and Oosterweel. The RMSE of velocity magnitude are in general less than 0.2 m/s. This is in a line with the predictive abilities of Scaldis3D along ADCP transects (see Table 21).

The discrepancies at Driegoten are higher than at the other two stations. NEVLA3D overestimates the velocity magnitude at Driegoten substantially by about 0.40 m/s. The main reason is that the measurement location in reality is in a shallower area on the slope while the station placed in the NEVLA3D model is closer to the deep tidal channel (Figure 39). For future studies, the location of Driegoten is suggested to shift to a shallower location where closer to the river bank. Scaldis3D model shows slightly better results (e.g. bias of 0.18 m/s), but still with substantial overestimation. This has been reported by Smolders et al., 2016. The discrepancy can be originated from the inaccuracies in the bathymetry implemented in the model or to the location of the point (in the river bend).

Comparing modelled velocity with stationary velocity measurements is often challenging because the point velocity is very sensitive to the local bathymetry, which therefore requires finer mesh, good quality of bathymetry and accurate representation of the location in the model. Besides, the stationary velocities are usually measured on the side slope which introduce difficulties for the representation in the model. However the discrepancies of velocity at Dreigoten are not deemed problematic, because both models reproduce the velocity along ADCP transects at Dreigoten very well (Table 21) with e.g. RMSE of 0.16 m/s at 20140617_Driegoten from Scaldis3D run.

Table 18 – Statistical parameters for the stationary velocities. Color scaling according to Table 19 and Table 20

Location	Analysis vector				Magnitude				Direction			
	MAE TS [m/s]		RMAE TS [-]		BIAS TS [m/s]		RMSE TS [m/s]		BIAS TS [°]		RMSE TS [°]	
	Scaldis 3D	NEVLA 3D	Scaldis 3D	NEVLA 3D	Scaldis 3D	NEVLA 3D	Scaldis 3D	NEVLA 3D	Scaldis 3D	NEVLA 3D	Scaldis 3D	NEVLA 3D
Buoy 84 top	0.17	0.14	0.48	0.39	0.12	0.08	0.19	0.16	-3.70	-2.96	24.58	28.00
Buoy 84 bottom	0.14	0.12	0.31	0.27	0.08	0.07	0.14	0.13	-4.34	-1.55	26.51	28.83
Oosterweel top	0.15	0.17	0.27	0.32	-0.06	0.12	0.15	0.19	11.60	2.29	33.73	26.94
Oosterweel bottom	0.18	0.23	0.28	0.35	-0.11	0.12	0.18	0.23	2.69	-0.60	31.17	27.96
Driegoten	0.22	0.41	0.46	0.88	0.18	0.39	0.25	0.45	1.47	2.12	23.87	29.90
Total	0.18	0.22	0.36	0.45	0.06	0.16	0.19	0.27	0.41	-0.41	27.51	28.50

Figure 34 – Measured and modeled velocities at Buoy 84 (bottom)

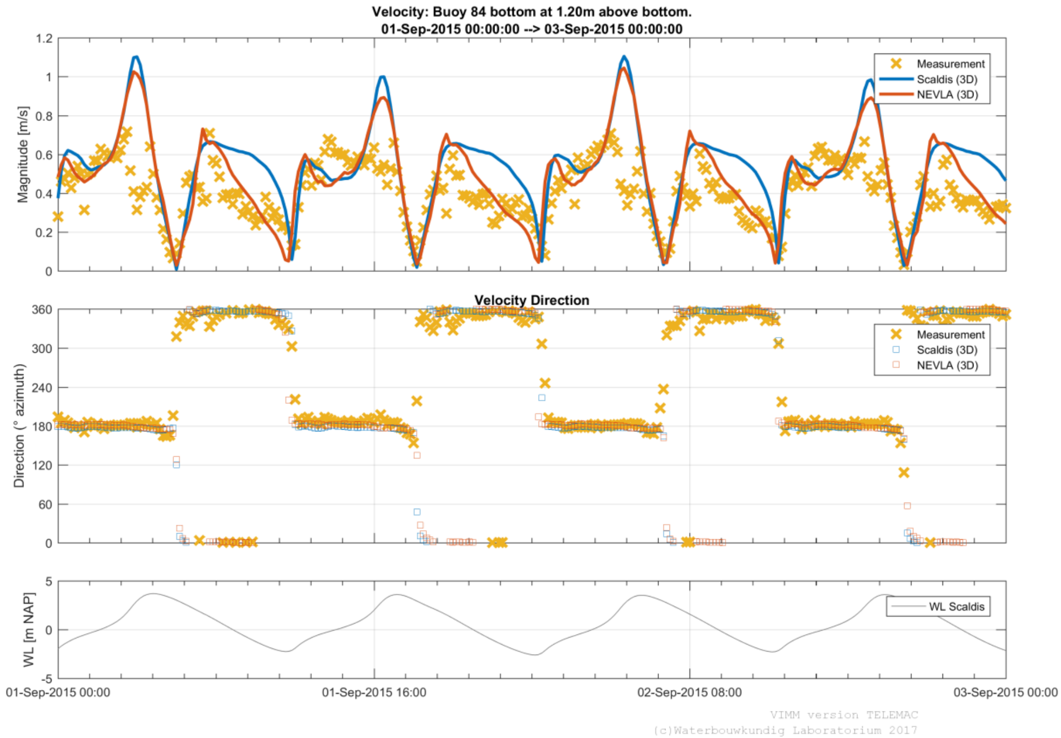

Figure 35 – Measured and modeled velocities at Buoy 84 (top)

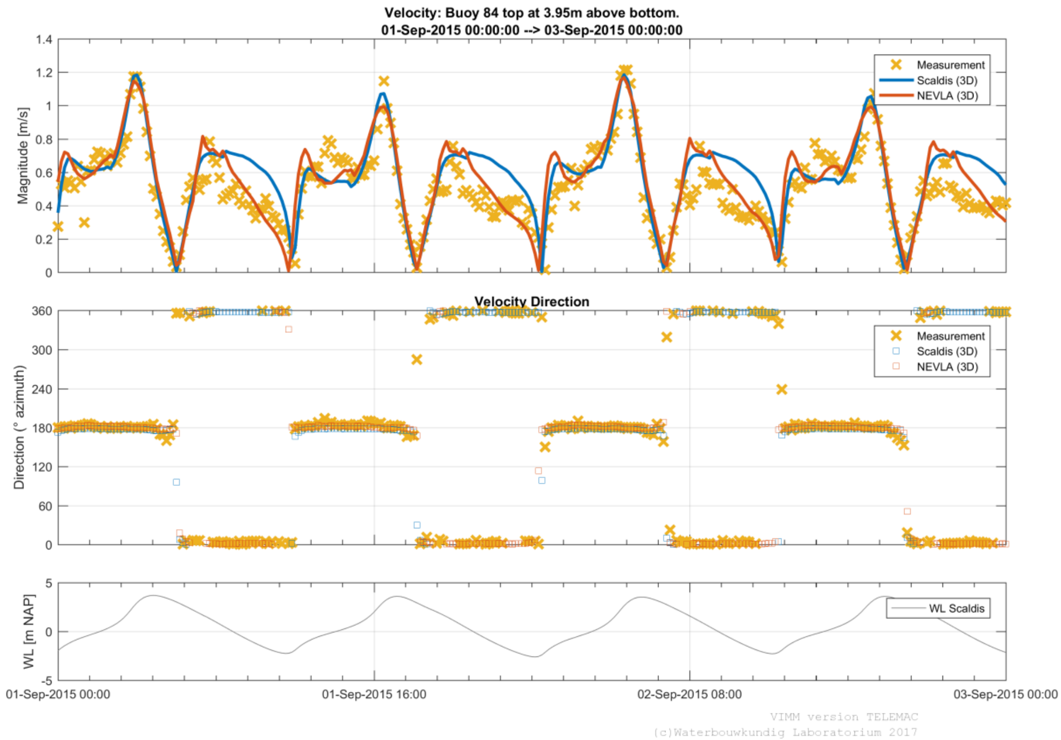

Figure 36 – Measured and modeled velocities at Oosterweel (bottom)

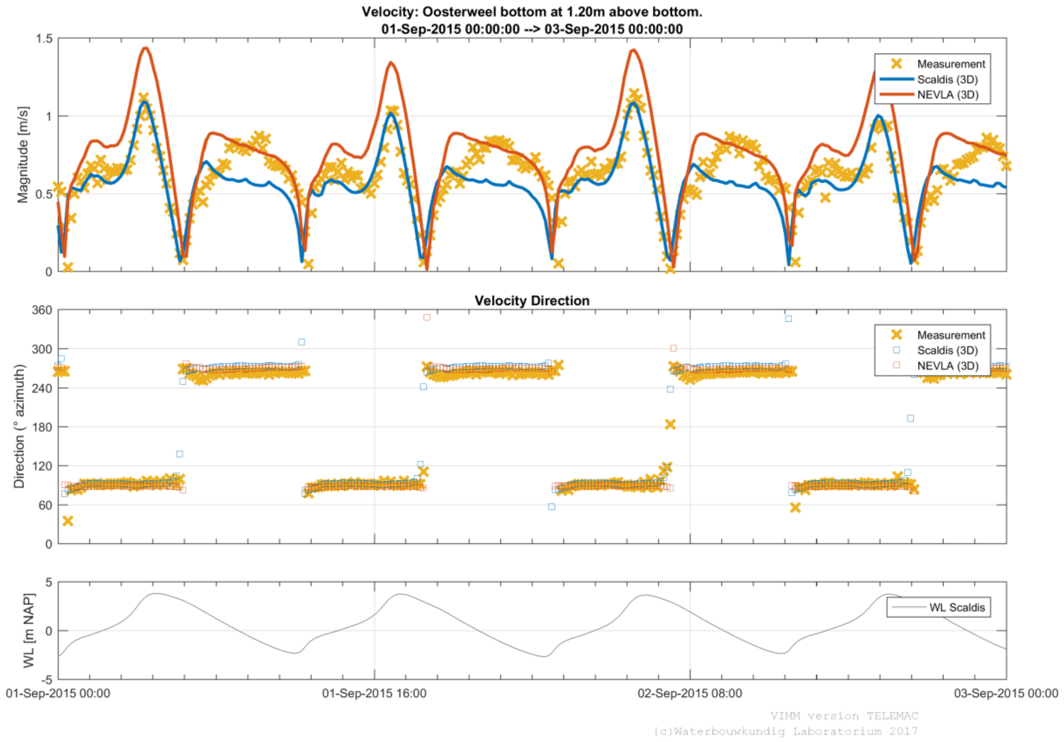

Figure 37 – Measured and modeled velocities at Oosterweel (top)

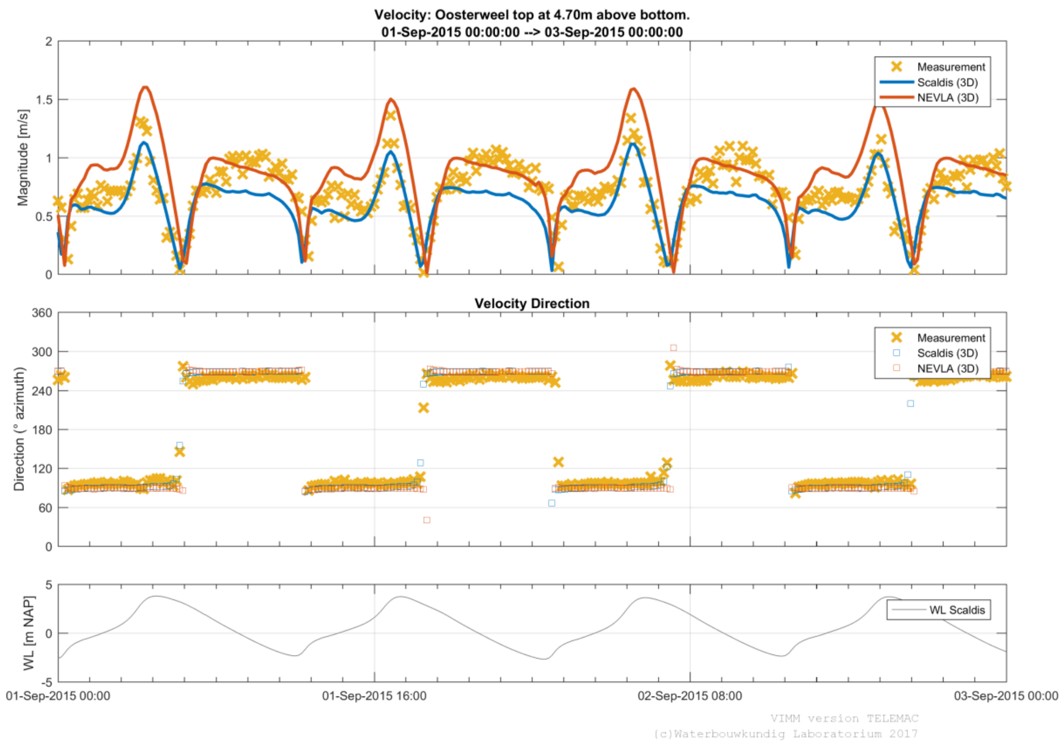

Figure 38 – Measured and modeled velocities at Driegoten.

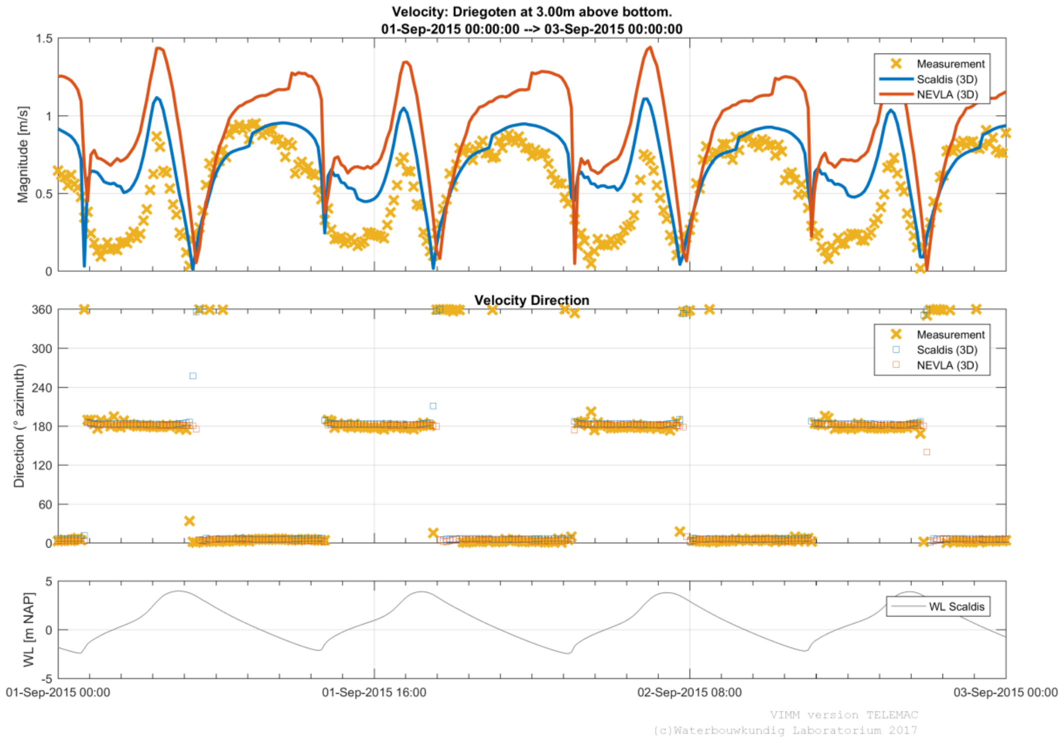

Figure 39 – Comparison of location of Driegoten in reality and in the NEVLA3D model with background of maximum velocity magnitude.

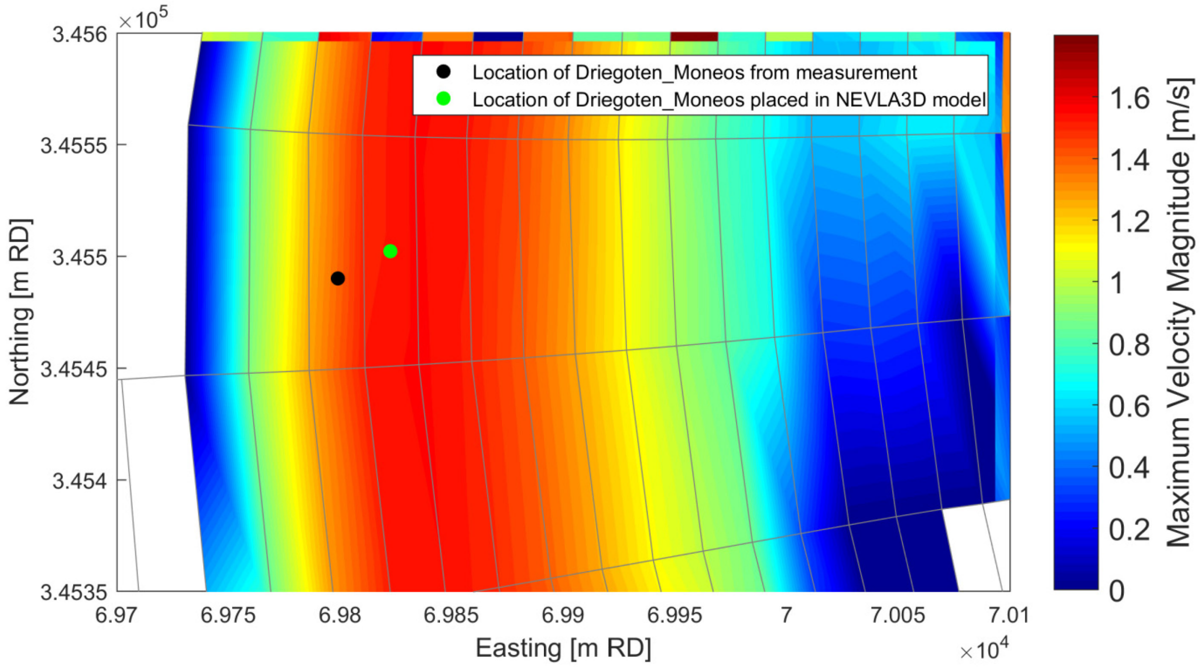

6.2 Velocity along transects

The modelling results are presented as a comparison between two modelling approaches. For the modelling approach of ‘Structured Grid with Boundary Nesting (**SG-BN**)’, the model results of the different domains are combined based on the priority for highest resolution to arrive at one flow field with the best accuracy at any given point. The SG-BN approach is compared to the modelling approach of using one Unstructured Grid (**UG**).

The depth averaged velocities predicted by both modelling approaches are compared with depth averaged velocity from ADCP measurements. Error statistics are calculated as RMSE of magnitude and RMAE in Table 21 (see Annex 1 for the definition of these statistical parameters). Note that RMAE includes the accuracy of both magnitude and direction. For the purpose of visualization, the RMSE is sorted by different colours with interval of every 0.1 m/s (Table 19). Model performance according to RMAE is qualified following Sutherland et al (2003) (Table 20). The full comparison of velocity predicted by all the 6 models and ADCP measurement are shown in Annex 3.

Table 19 – Model qualification based on RMSE of magnitude.

Model qualification	RMSE [m/s]
	<0.1
	0.1-0.2
	0.2-0.3
	>0.3
	-

Table 20 – Model qualification based on RMAE (Sutherland et al., 2003)

Model qualification		RMAE [-]
Excellent		<0.2
Good		0.2-0.4
Reasonable/fair		0.4-0.7
Poor		0.7-1.0
Bad		>1.0
Not Applicable		-

Table 21 – Comparison of RMSE and RMAE of velocities along the 67 ADCP transects.

Sl. No.		ADCP	RMSE Magnitude [m/s]		RMAE [-]	
			SG-BN	UG	SG-BN	UG
1	WES	20110706_R7_Terneuzen	0.20	0.23	0.48	0.52
2		20080604_Debietraai_7	0.17	0.17	0.26	0.27
3		20110705_R7_Everingen	0.13	0.13	0.35	0.35
4		20070321_Terneuzen_haven	0.10	0.11	0.38	0.39
5		20120508_R6_Middelgat	0.17	0.17	0.45	0.44
6		20120509_R6_GatVanOssenisse	0.17	0.16	0.36	0.35
7		20060323_Waarde	0.12	0.12	0.31	0.31
8		20060928_Waarde	0.13	0.13	0.42	0.42
		AVERAGE	**0.15**	**0.15**	**0.38**	**0.38**
9	BeZS1	20050217_Zandvliet	0.17	0.11	0.60	0.37
10		20060912_Doelpolder	0.16	0.17	0.51	0.69
11		20140715_Noordzeeterminal	0.19	0.21	0.57	0.56
12		20100319_dwarsraaiD	0.37	0.22	0.65	0.35
		AVERAGE	**0.22**	**0.18**	**0.58**	**0.49**
13	BeZS2	20060322_DGD	0.08	0.09	0.74	0.78
14		20060927_DGD	0.06	0.07	0.72	0.74
15		20071024_DGD	0.06	0.07	0.81	0.75
16		20080311_DGD	0.06	0.07	0.77	0.75
17		20080619_DGD	0.06	0.07	0.71	0.73
18		20080626_DGD	0.06	0.06	0.75	0.74
19		20080924_DGD	0.06	0.06	0.80	0.76
20		20080930_DGD	0.05	0.06	0.74	0.72
21		20081001_DGD_X	0.14	0.16	0.53	0.58
22		20081001_DGD_Y	0.14	0.17	0.54	0.64
23		20081001_DGD_Z	0.16	0.19	0.58	0.68
24		20081202_DGD	0.07	0.08	0.80	0.77
25		20081210_DGD	0.07	0.07	0.84	0.79
26		20090306_DGD	0.08	0.09	0.74	0.78
27		20090312_DGD	0.08	0.09	0.72	0.73
		AVERAGE	**0.08**	**0.09**	**0.72**	**0.73**
28	BeZS3	20050216_DGD_K	0.17	0.18	0.30	0.31
29		20050217_DGD_K	0.15	0.15	0.31	0.32
30		20060322_DGD_K	0.19	0.18	0.48	0.48
31		20060323_DGD_K	0.14	0.15	0.38	0.39
32		20060927_DGD_K	0.18	0.18	0.45	0.46
33		20060928_DGD_K	0.15	0.14	0.35	0.35
34		20080311_DGD_K	0.21	0.21	0.38	0.41
35		20050217_Liefkenshoek	0.15	0.15	0.33	0.32
36		20060322_Liefkenshoek	0.17	0.17	0.50	0.50
37		20060927_Liefkenshoek	0.16	0.15	0.36	0.36
38		20080311_Liefkenshoek	0.21	0.20	0.40	0.40
39		20090527_Liefkenshoek	0.21	0.21	0.48	0.48
40		20100430_Liefkenshoek	0.16	0.15	0.30	0.30
41		20130625_Liefkenshoek	0.16	0.15	0.31	0.31
42		20140514_Liefkenshoek	0.14	0.14	0.27	0.24

43		20050218_Kallo	0.12	0.11	0.58	0.55
		AVERAGE	**0.17**	**0.16**	**0.39**	**0.39**
44	BeZS4	20090529_Oosterweel	0.18	0.16	0.30	0.28
45		20100429_Oosterweel	0.19	0.18	0.33	0.32
46		20130627_Oosterweel	0.16	0.14	0.32	0.29
47		20140516_Oosterweel	0.18	0.17	0.29	0.28
48		20090526_Kruibeke	0.23	0.23	0.57	0.56
49		20100414_Kruibeke	0.14	0.13	0.23	0.21
50		20130530_Kruibeke	0.17	0.16	0.50	0.49
51		20140702_Kruibeke	0.16	0.15	0.35	0.33
		AVERAGE	**0.18**	**0.16**	**0.36**	**0.34**
52	BoZS1	20130529_Terhagen	0.20	0.18	0.36	0.32
53		20140630_Terhagen	0.19	0.15	0.38	0.35
54		20090623_Driegoten	0.17	0.14	0.25	0.21
55		20100415_Driegoten	0.19	0.15	0.40	0.35
56		20130612_Driegoten	0.22	0.21	0.48	0.47
57		20140617_Driegoten	0.18	0.16	0.32	0.30
58		20110218_Kramp_ebb	0.16	0.16	0.23	0.23
59		20110218_Kramp_flood	0.26	0.21	0.42	0.33
		AVERAGE	**0.20**	**0.17**	**0.36**	**0.32**
60	BoZS2	20140417_Dendermonde	0.19	0.12	0.36	0.23
61		20110801_Appels_downstream	0.17	0.15	0.72	0.68
62		20110801_Appels_upstream	0.17	0.18	0.65	0.66
63		20090625_Schoonaarde	0.19	0.20	0.42	0.56
64		20100414_Schoonaarde	0.13	0.09	0.25	0.20
65		20130527_Schoonaarde	0.18	0.15	0.32	0.28
66		20140703_Schoonaarde	0.19	0.16	0.42	0.33
67		20140415_Schellebelle	0.16	0.15	0.47	0.38
		AVERAGE	**0.17**	**0.15**	**0.45**	**0.42**
OVERALL			**0.15**	**0.15**	**0.49**	**0.46**

6.2.1 Western Scheldt

In the Western Scheldt (WES), both SG-BN and UG models in general show decent performance ('Good') on velocity predictions with average RMSE of 0.15 m/s and RMAE value of 0.38. All the models are equally functional in reproducing velocities in the Western Scheldt.

As discussed in §5.6, a detailed TELEMAC model has been constructed for the port of Terneuzen. The mesh resolution is refined to up to 10 m in the access entrance of the port (see Figure 26). However the SCALDIS3D model does not pay specific attention to the port of Terneuzen which leads to a relatively coarser mesh resolution of 40 m in this area. Therefore a direct comparison of the predictive ability of velocity along the transect of ***20070321_Terneuzen_haven*** (see location in Figure 4) between the SCALDIS3D model (UG) and the Terneuzen model (SG-BN) has been carried out. Figure 40 to Figure 42 present the comparison of Bias, RMSE and RMAE between the two models over one tidal cycle. The mean value of RMSE and RMAE over one tidal cycle are presented in Table 22.

Both models show equal skill in reproducing the flow field at Terneuzen. The bias generally within the range of 0.1 m/s which is within the error margin of the observations. The mean RMSE of magnitude is similar (0.10 vs 0.11 m/s) while SCALDIS shows slightly better predictions on flow direction (53.7 vs 58.3 degree). The comparison of RMAE (0.39 vs 0.38) indicates that both SCALDIS3D and the Terneuzen detail model show equal model skill in representing the flow field at Terneuzen port, even though the Terneuzen detail model had 4x higher resolution there.

Figure 40 – Comparison of Bias of velocity at Terneuzen between SCALDIS3D and Terneuzen model.

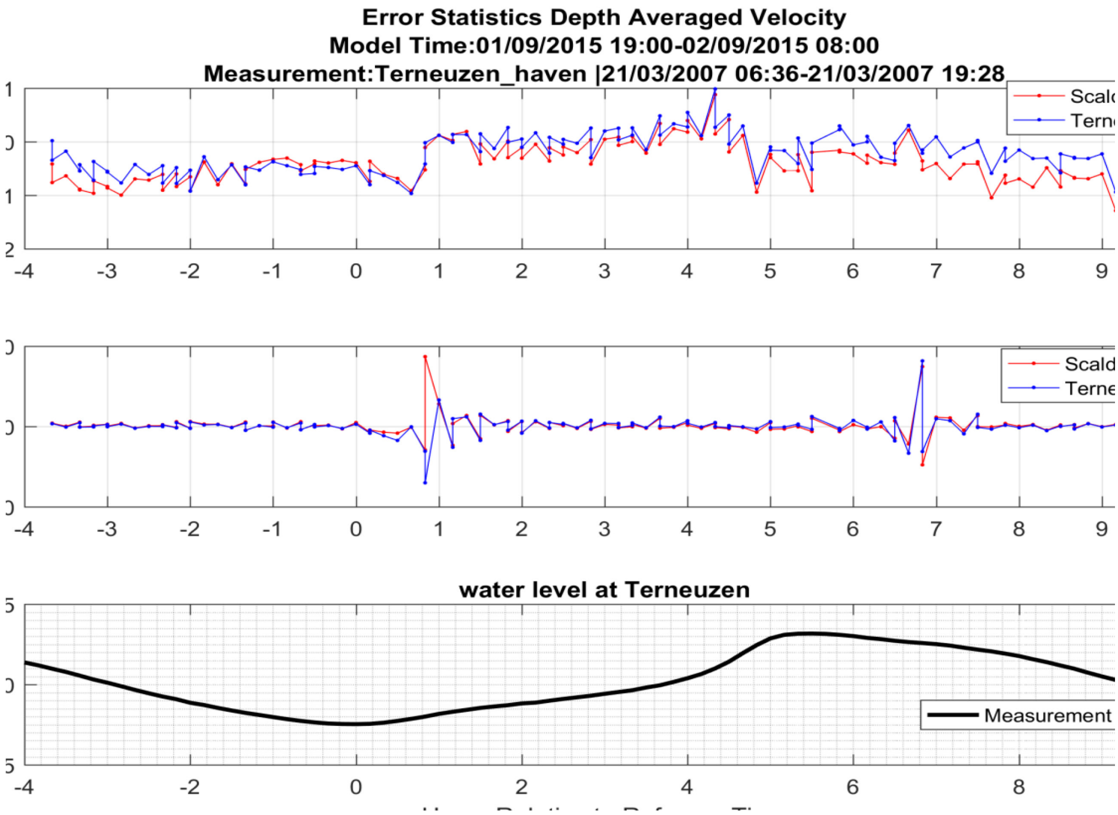

Figure 41 – Comparison of RMSE of velocity at Terneuzen between SCALDIS3D and Terneuzen model.

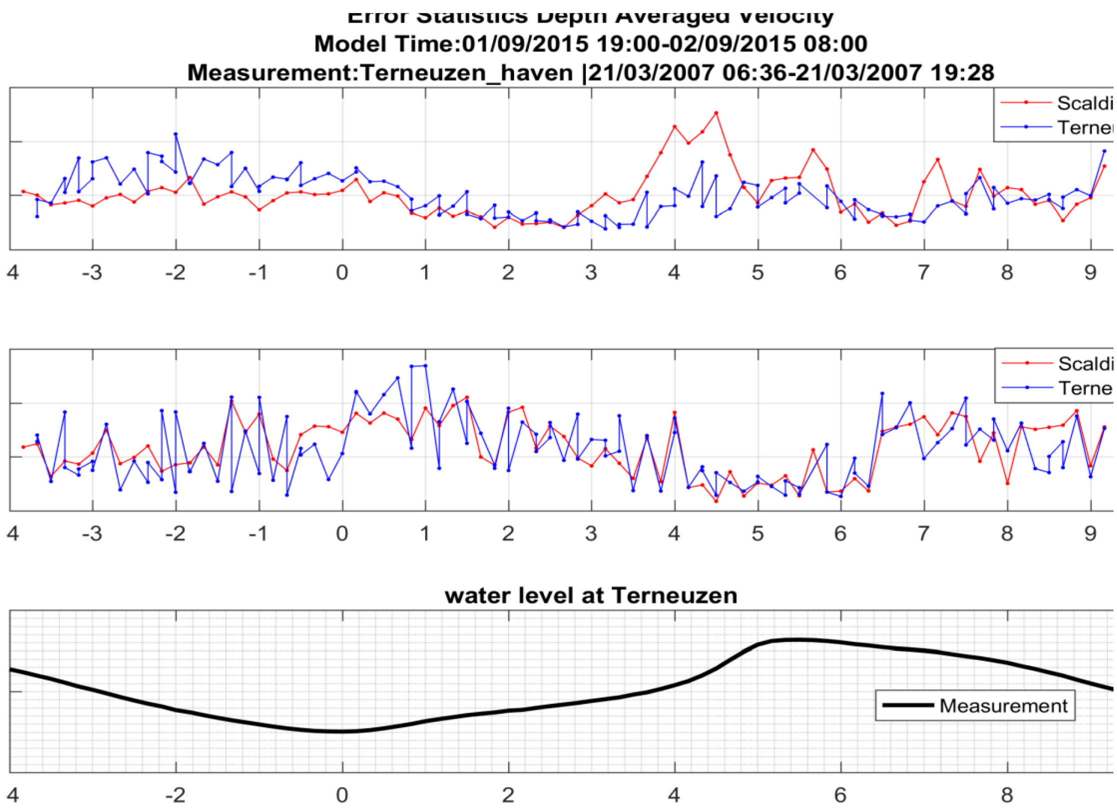

Figure 42 – Comparison of RMAE of velocity at Terneuzen between SCALDIS and Terneuzen model.

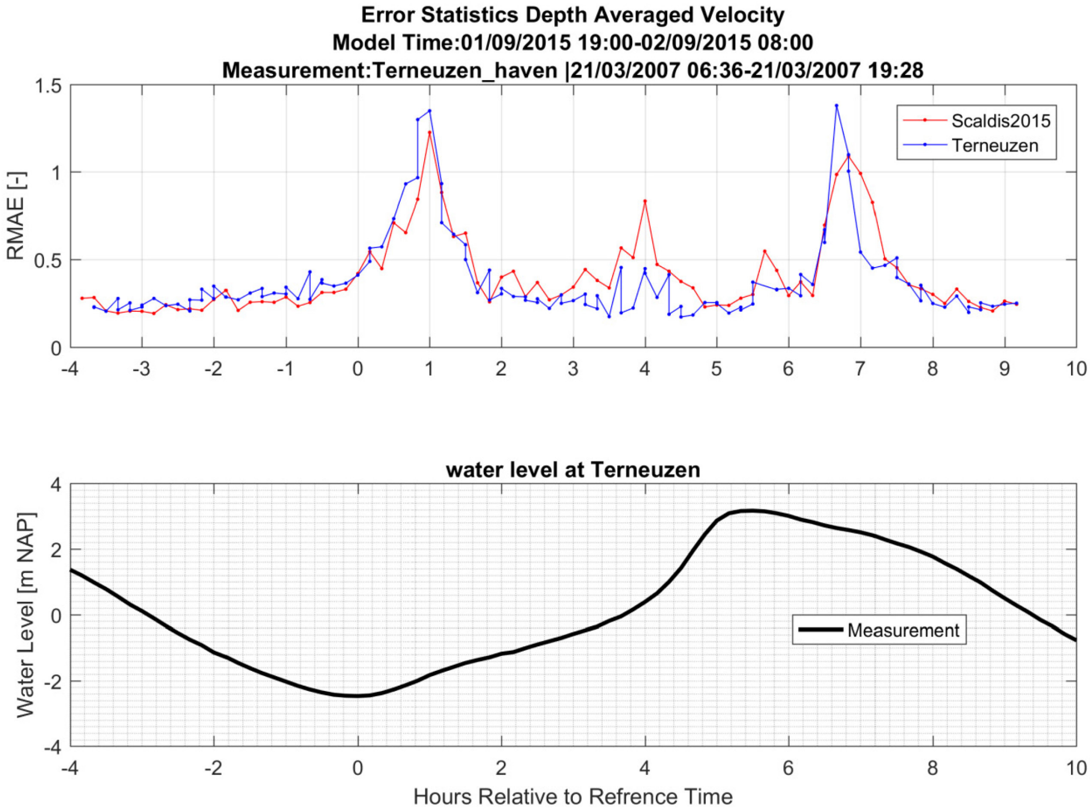

Table 22 – Comparison of statistical results between SCALDIS and Terneuzen model along the transect of 20070321_Terneuzen_haven.

Statistics	SCALDIS	Terneuzen model
RMSE Magnitude [m/s]	0.11	0.10
RMSE Direction [deg]	53.7	58.3
RMAE [-]	0.39	0.38

6.2.2 Lower Sea Scheldt

In the Lower Sea Scheldt from **Zandvliet** to **dwarsraaiD** (BeZS1), both SG-BN and UG models show 'Reasonable/Fair' performance with average RMSE of 0.18-0.19 m/s and RMAE value around 0.5.

In the vicinity of the **Noordzeeterminal**, the RMSE error in both models is substantial. Figure 43 shows a snapshot of the velocity field comparison between measurement and SCALDIS model. A pronounced hump-pattern of velocity along the transect is observed in the measurement while this is not being captured by the SCALDIS model. Surprisingly this hump-pattern of velocity is not captured by any of the available models (NEVLA3D, Boudewijn-Kallo and Zandvliet). A better resolved geometry with finer mesh resolution and higher resolution of bathymetry might overcome this malfunction. This is strongly recommended for future model improvements. Additionally, more ADCP measurement would be needed (e.g. during flood tide and in the transversal direction) for validation.

A point of attention are the eddies in the access channel to the Zandvliet/Berendrecht sluice complex. Figure 44 shows the modelled flow patterns in NEVLA3D and Scaldis3D and in the Zandvliet-Berendrecht detailed model. The detailed model has a local resolution of 20 m in the access channel. The mesh resolution near Berendrechtsluis for NEVLA3D and Scaldis3D model are about 70 m and 80 m respectively. This is deemed too coarse to reproduce an eddy in the access channel. For future studies, the mesh of the Scaldis3D model could be locally refined to enhance the predictive ability to capture local flow patterns. There is however no measurement of the eddy pattern in the Zandvliet/Berendrecht complex (see Figure 5 for available ADCP measurements), so we basically don't know yet whether an eddy occurs and how strong it would be. It would be advisable to collect additional measurements there before trying to re-calibrate a model to capture the eddy dynamics that might be occurring.

Figure 43 – Comparison of velocity pattern between measurement and the SCALDIS model.

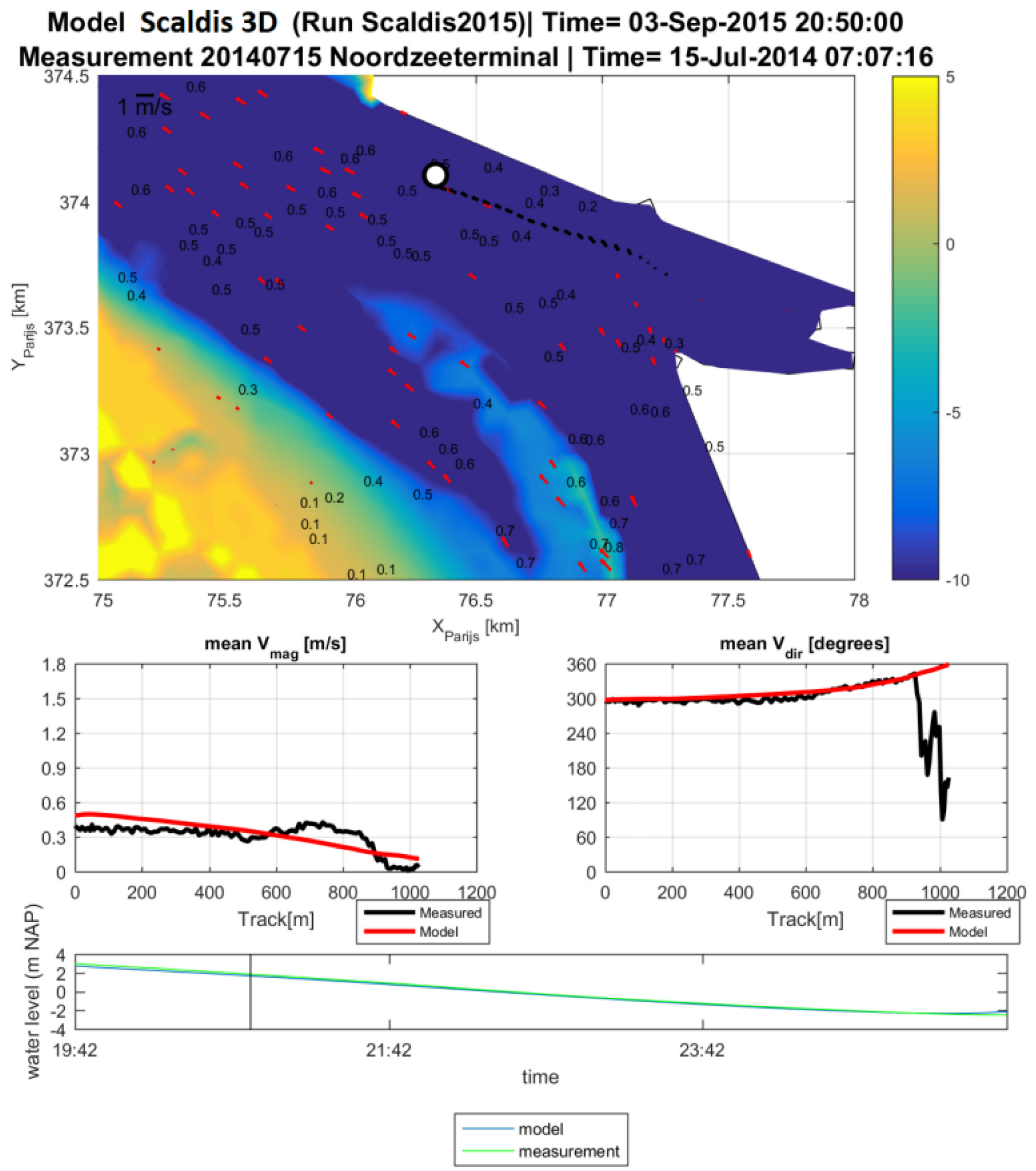

Figure 44 – Comparison of velocity patterns near Berendrechtsluis between Scaldis3D, NEVLA3D and Zandvliet2D model. The red lines represent the model mesh.

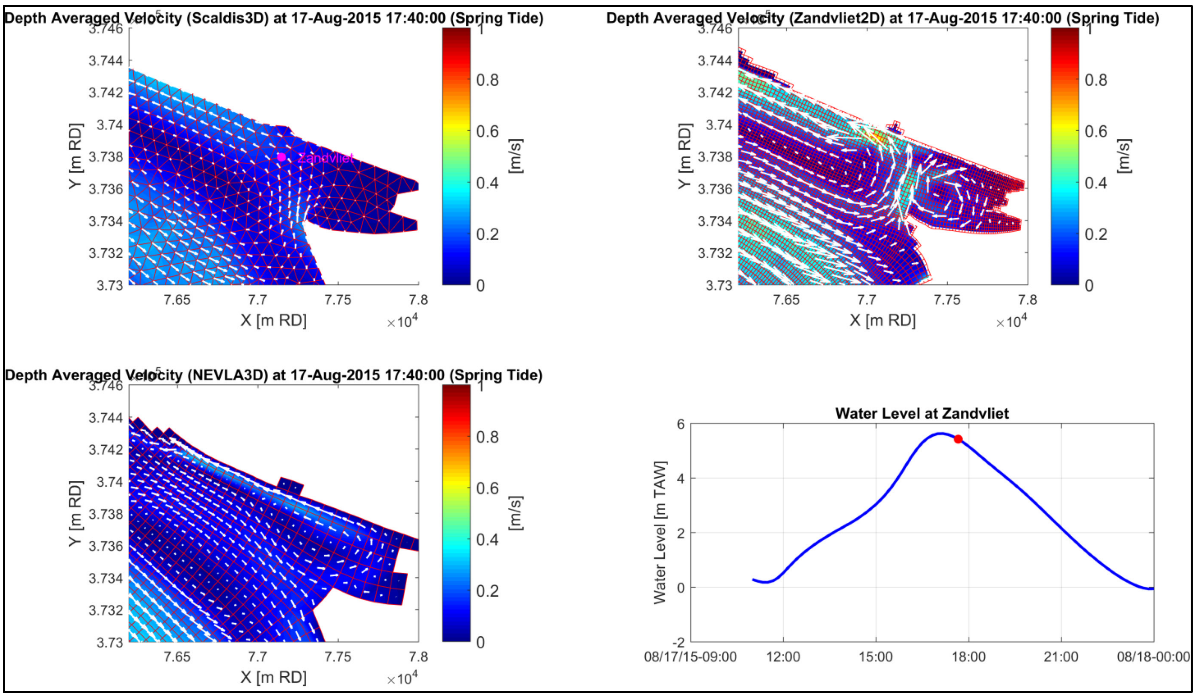

Modelling velocities inside the **Deurganckdok (BeZS2)** is challenging, and model performances are categorized as 'Poor' along most of the ADCP transects (average RMAE of 0.72 and 0.73 respectively). However this is not deemed problematic because the large values of RMAE is mainly due to the local low velocities inside the Deurganckdok where water depth is great (>20 m). The RMSE of velocities are relatively small (0.09 m/s).

Figure 45 exemplifies the evolution of RMAE over time of the Scaldis3D run against measurement 20090312_DGD.

Figure 45 – Time series of RMAE at 20090312_DGD from Scaldis3D run.

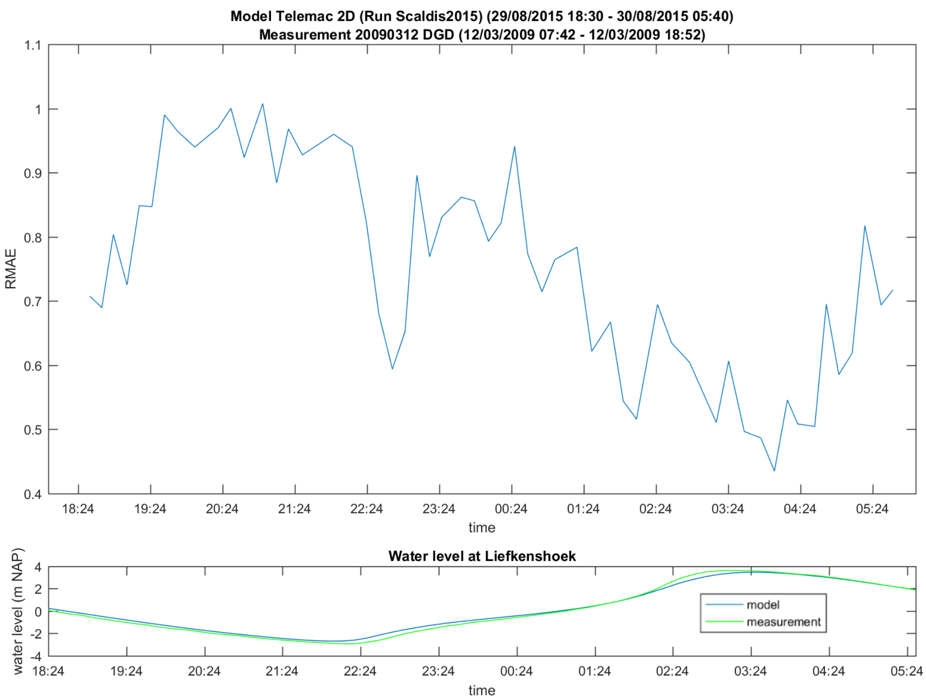

Figure 46 compares the eddy pattern predicted by SCALDIS3D model and measurements during flood at 20081001_DGD_Y. Although the model underestimates the velocity magnitude slightly, the direction changes of the eddy is quietly well captured by the model.

Figure 46 – Comparison of eddy patterns between measurements and Scaldis2015 prediction at 20081001_DGD_Y.

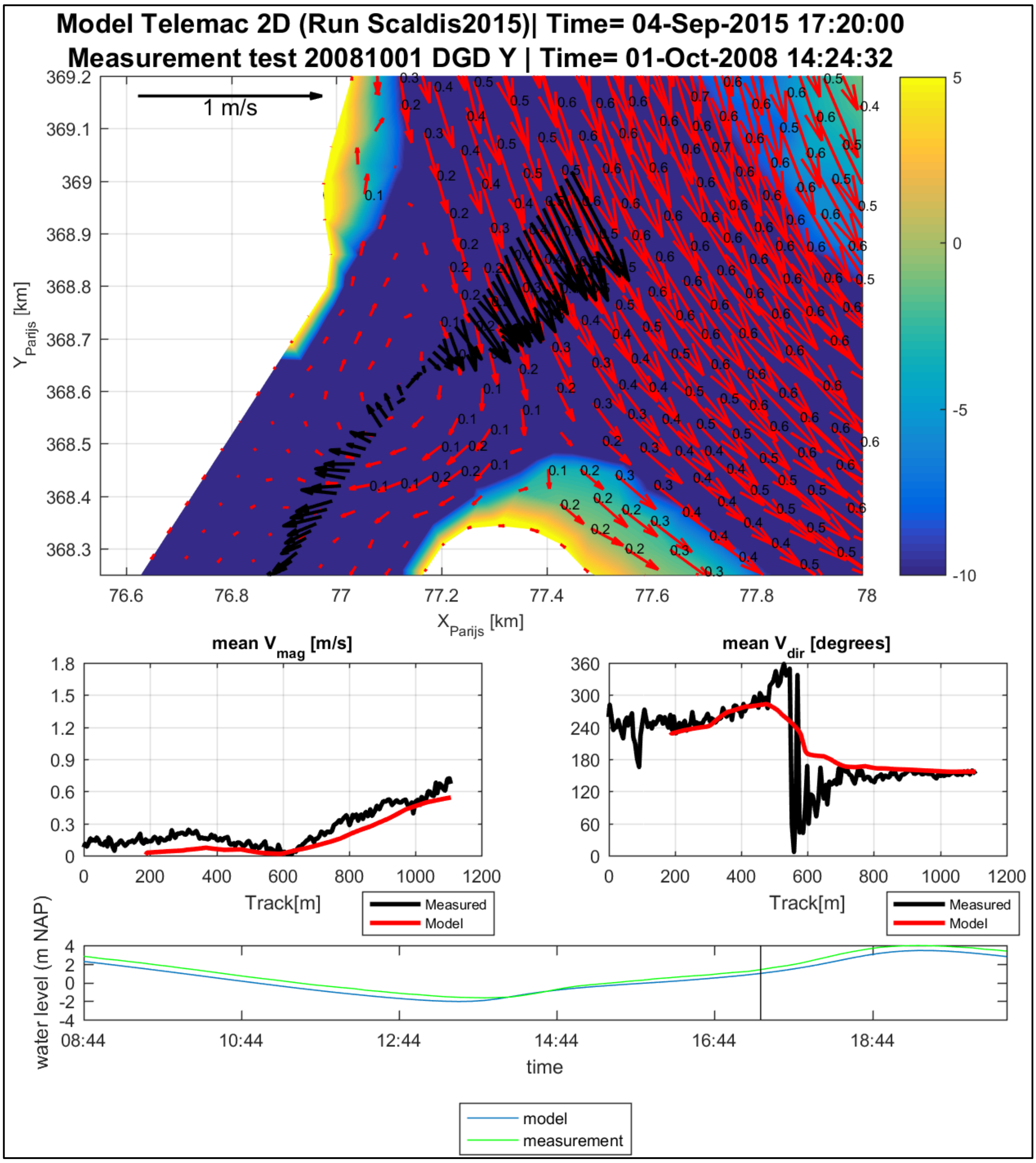

The density driven currents are well known and understood e.g. in (IMDC, 2014) and (Vanlede, 2014). Figure 47 presents the density current at high water at the dock entrance from measurements. Density currents arise from a horizontal density gradient which is compensated by a water level gradient. The imbalance of hydrostatic forces over the vertical drives a two-layer current with the near-bed current towards the lower density region and the surface current in opposing direction.

Figure 48 presents the density current simulated by SCALDIS model. The pattern of the vertical velocity profile is more or less reproduced by the SCALDIS model, with the near-bed current entering the dock and the surface current leaving the dock. However the magnitude of the density current predicted by the

SCALDIS model is relatively lower. This might be due to the fact that part of the density currents are caused by gradients in sediment concentration which are not simulated by the SCALDIS model.

Figure 47 – Example of density current at high water at the dock entrance (v>0 leaves the dock).

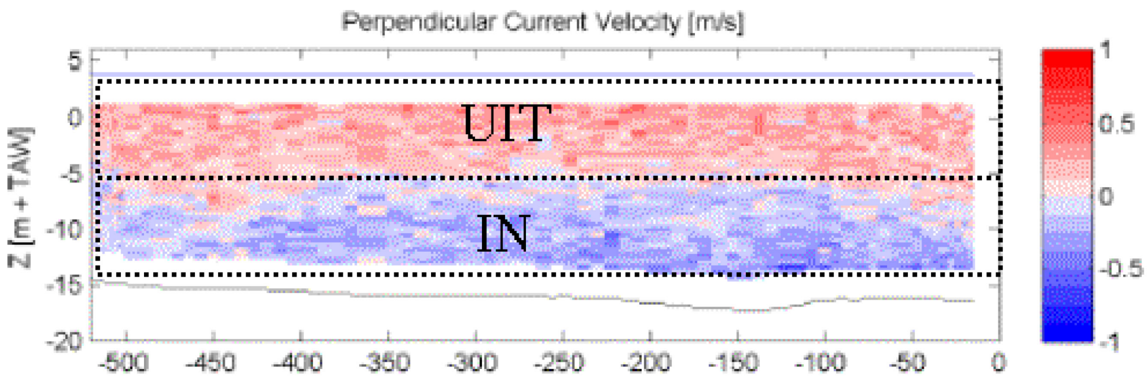

Figure 48 – Density current predicted by SCALDIS model at high water at the dock entrance (v>0 leaves the dock).

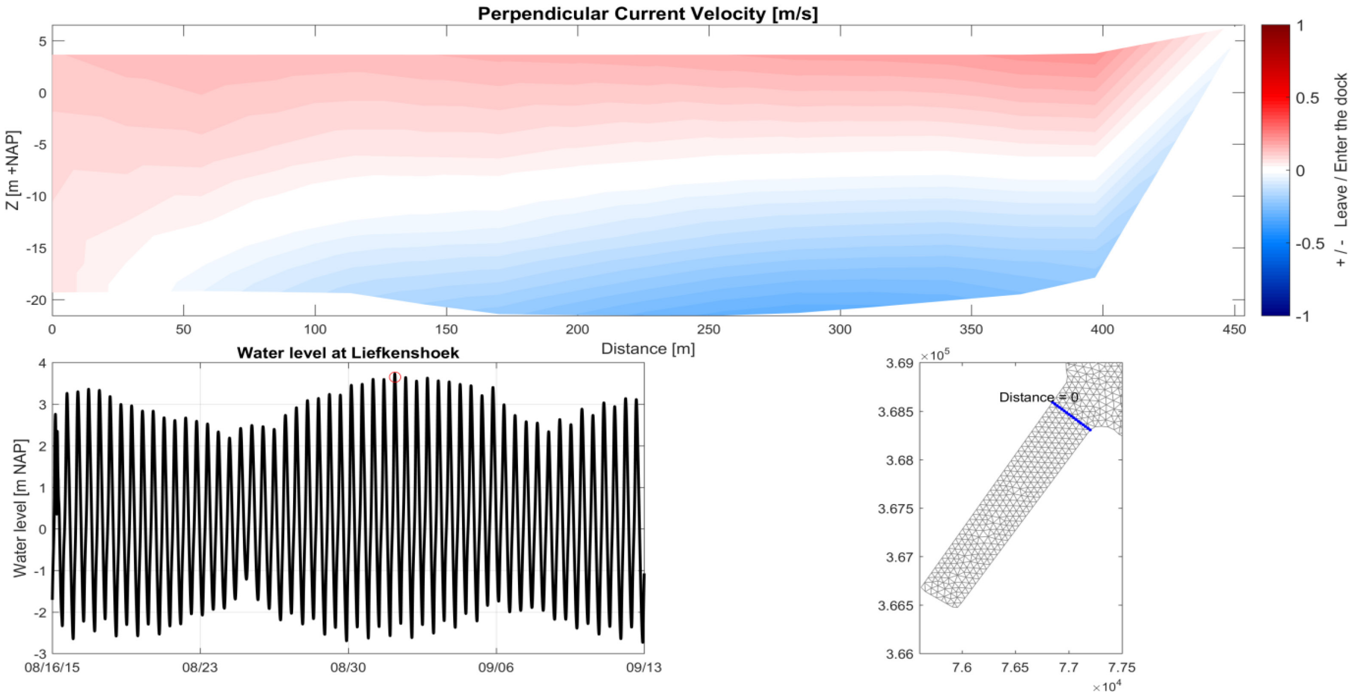

From outside **Deurganckdok** to **Kallo (BeZS3)**, both SG-BN and UG models show equally decent performance ('Good') on velocity predictions with average RMAE of 0.39. The average RMSE are 0.17 m/s and 0.16 m/s respectively.

For the area of **Oosterweel** and **Kruibeke (BeZS4)**, both SG-BN and UG models show equally decent performance ('Good') on velocity predictions with average RMAE of 0.36 and 0.34 respectively. The RMSE on velocity are 0.18 m/s and 0.16 m/s respectively.

6.2.3 Upper Sea Scheldt

In the Upper Sea Scheldt from **Terhagen** to **Kramp (BoZS1),** both SG-BN and UG models show in general decent performance ('Good') on velocity predictions with average RMAE of 0.36 and 0.32 respectively. The average RMSE are 0.20 m/s and 0.17 m/s respectively.

For the area of **Dendermonde** to **Schellebelle (BoZS2)**, both SG-BN and UG models are categorized as 'Reasonable/Fair' with average RMAE of 0.45 and 0.42 respectively. The average RMSE are 0.17 m/s and 0.15 m/s respectively.

6.2.4 Summary

The SG-BN and UG models in general show comparable predictive abilities on velocity. This is remarkable, given the fact that SG-BN and UG models were built totally independently from each other from the ground up by different teams. The update of all model schematisations to 2015 gives the first opportunity to compare both modeling approaches extensively.

The RMAE averaged along all ADCP transects throughout the estuary are 0.49 and 0.46 respectively. Both models are categorized as 'Reasonable/Fair'. The RMSE averaged along all ADCP transects throughout the estuary are 0.15 m/s for both models.

SCALDIS model uses unstructured grid, with which the detailed local geometry can be better resolved (e.g. quay walls). In a structured grid approach, following a geometric feature that doesn't align with the grid orientation leads to a "staircase" effect along the grid edges which adds additional momentum loss in the solution. It is also easier to have higher mesh resolutions in areas of interests using unstructured grids.

Based on these interesting grid properties, it is decided to produce the updated velocity fields from the SCALDIS model, following the unstructured grid approach.

6.3 Water Level

RMSE0 is the bias corrected RMSE which determines in a sense the tidal range/tidal shape and consequently the tidal volume passing by a certain location. Therefore RMSE0 is to some extent an 'indicator' of the local velocity field.

Figure 49 presents the comparison of RMSE0 of the complete time series of water levels (see values in Table 23) along the estuary between all the 6 models.

The RMSE0 values are similar from all the models (differences are less than 3 cm) from downstream station of Vlakte van de Raan to upstream station of Kallo. The NEVLA2015 model leads to lowest RMSE0 from Antwerp to Temse and StAmands (16 cm on average) while the Wintam model leads to substantially large RMSE0 values (up to 26 cm). In the upper sea Scheldt from Walem to Melle, the SCALDIS model shows smaller RMSE0 compared with NEVLA2015 by 5 cm on average. The main reason is that SCALDIS model has much finer grid resolution in the upstream part.

The complete set of water level analysis (time series plot; high water and low water analysis; harmonic analysis) files is presented in a CD in annex.

Figure 49 – Comparison of RMSE0 (versus measurement) of the complete time series of water level along the estuary.

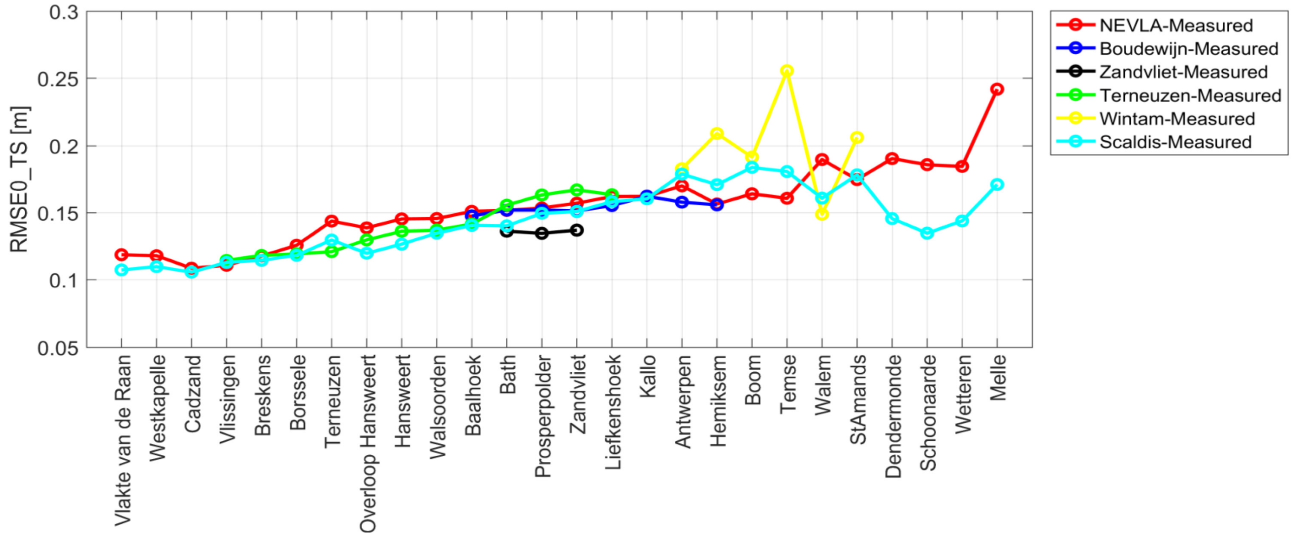

Table 23 – Statistics of RMSE0 of the complete time series of water level along the estuary.

Stations	NEVLA	Boudewijn	Zandvliet	Terneuzen	Wintam	SCALDIS
Vlakte van de Raan	0.12	-	-	-	-	0.11
Westkapelle	0.12	-	-	-	-	0.11
Cadzand	0.11	-	-	-	-	0.11
Vlissingen	0.11	-	-	0.11	-	0.11
Breskens	0.12	-	-	0.12	-	0.11
Borssele	0.13	-	-	0.12	-	0.12
Terneuzen	0.14	-	-	0.12	-	0.13
Overloop Hansweert	0.14	-	-	0.13	-	0.12
Hansweert	0.15	-	-	0.14	-	0.13
Walsoorden	0.15	-	-	0.14	-	0.13
Baalhoek	0.15	0.15	-	0.14	-	0.14
Bath	0.15	0.15	0.14	0.16	-	0.14
Prosperpolder	0.15	0.15	0.13	0.16	-	0.15
Zandvliet	0.16	0.15	0.14	0.17	-	0.15
Liefkenshoek	0.16	0.16	-	0.16	-	0.16
Kallo	0.16	0.16	-	-	-	0.16
Antwerpen	0.17	0.16	-	-	0.18	0.18
Hemiksem	0.16	0.16	-	-	0.21	0.17
Boom	0.16	-	-	-	0.19	0.18
Temse	0.16	-	-	-	0.26	0.18
Walem	0.19	-	-	-	0.15	0.16
StAmands	0.17	-	-	-	0.21	0.18
Dendermonde	0.19	-	-	-	-	0.15
Schoonaarde	0.19	-	-	-	-	0.13
Wetteren	0.18	-	-	-	-	0.14
Melle	0.24	-	-	-	-	0.17

6.4 Salinity

The comparison of the modelled and measured salinity time series are presented in Figure 50 to Figure 56. Salinity is in general well reproduced by both models of NEVLA3D and SCALDIS along the estuary. The statistical analysis results are presented in Table 24. The RMSE are smaller than 2 psu for all stations from both models. The differences between the calculated and measured salinity are smaller than 2 psu (NEVLA3D) and 4 psu (SCALDIS) for most stations except at Hemiksem where both models overestimate salinity substantially. The discrepancies are considered mainly attribute to the less accurate initial salinity (§4.4) due to lack of data in space.

Figure 50 – Comparison of salinity between measurement, NEVLA and SCALDIS at Vlakte Van De Raan.

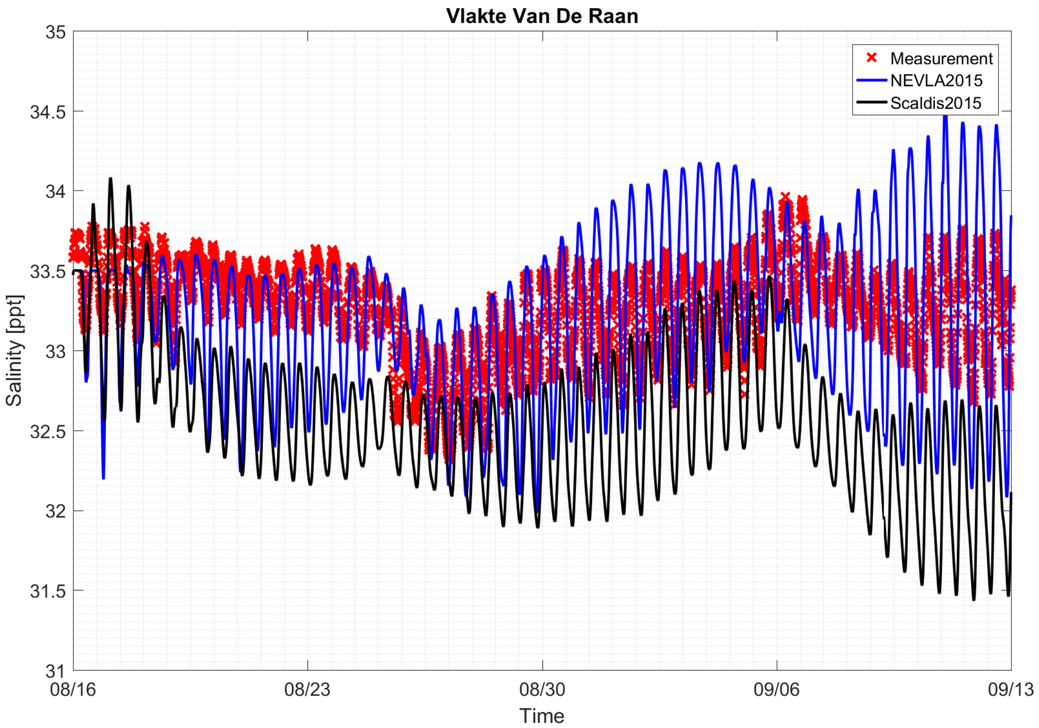

Figure 51 – Comparison of salinity between measurement, NEVLA and SCALDIS at Overloop Hansweert.

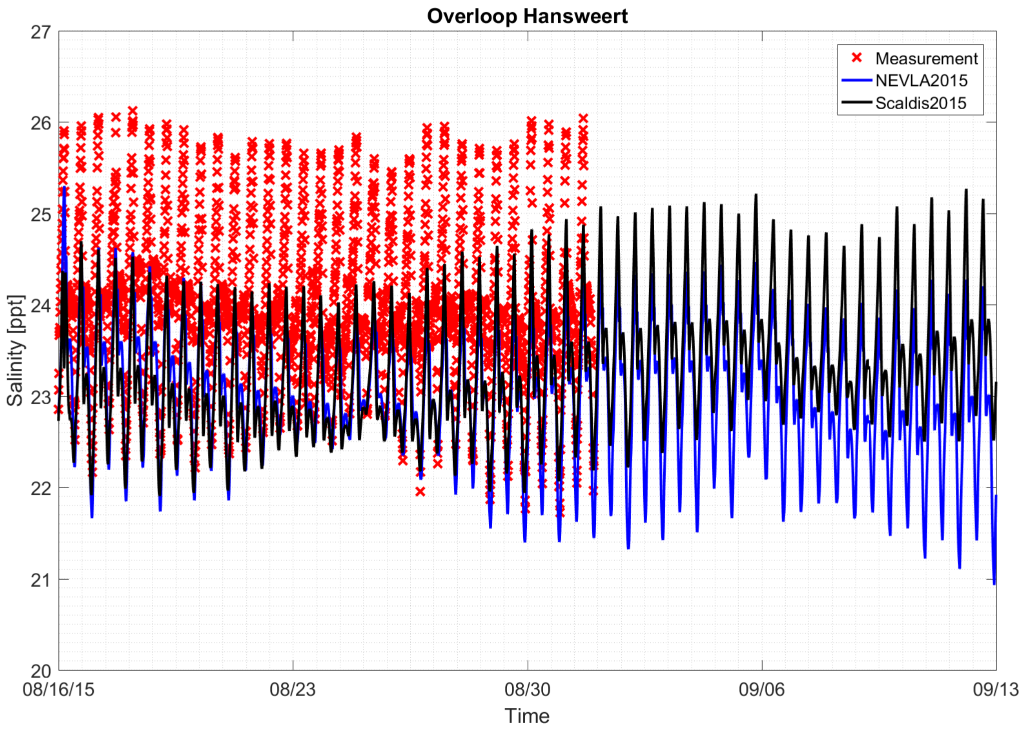

Figure 52 – Comparison of salinity between measurement, NEVLA and SCALDIS at Baalhoek.

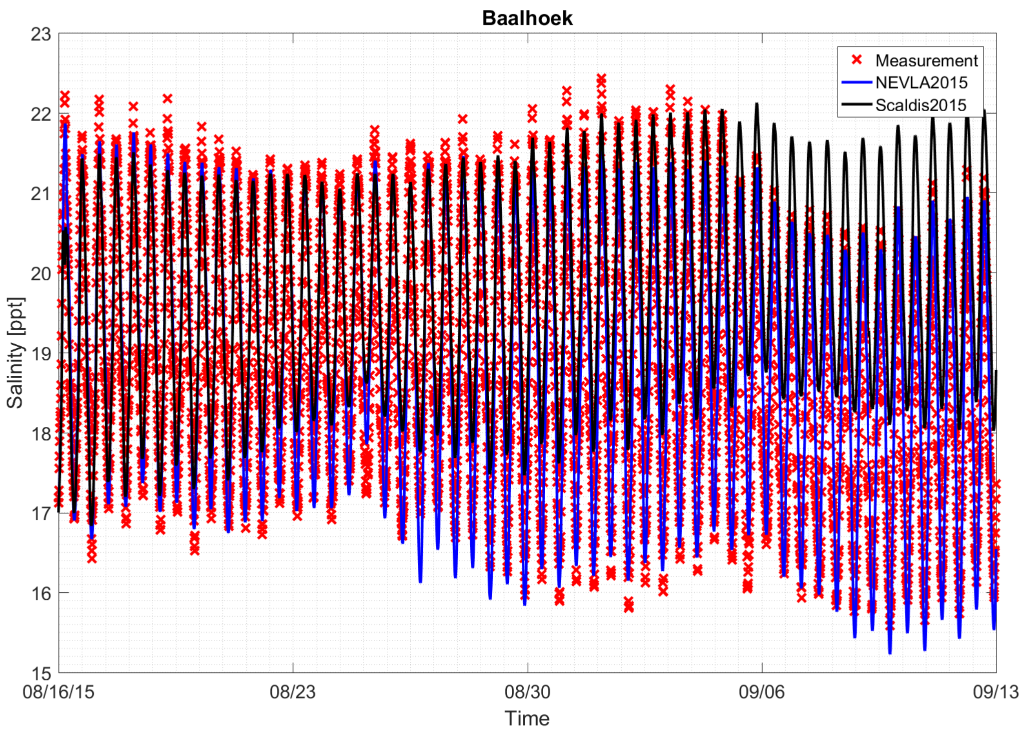

Figure 53 – Comparison of salinity between measurement, NEVLA and SCALDIS at Prosperpolder.

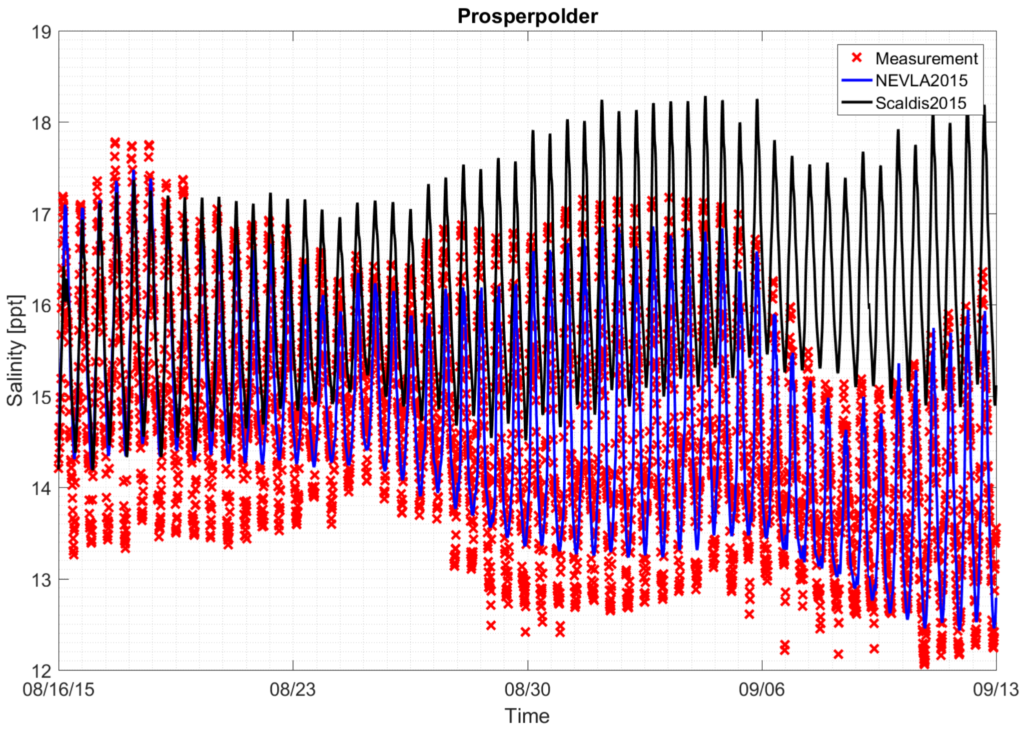

Figure 54 – Comparison of salinity between measurement, NEVLA and SCALDIS at Boei 84.

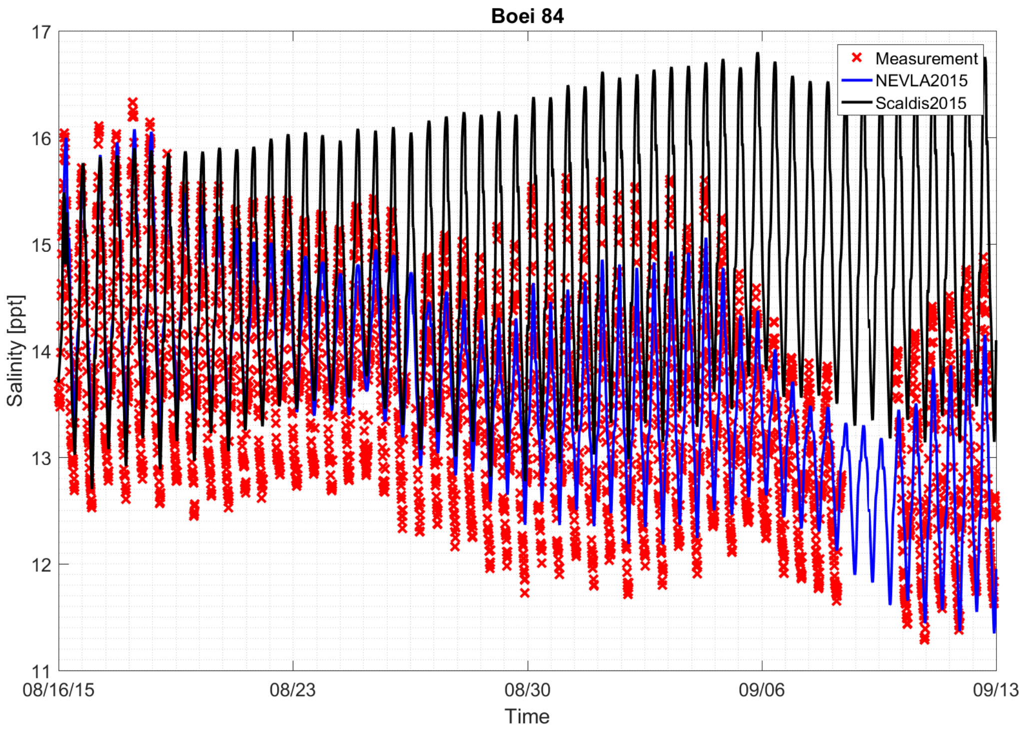

Figure 55 – Comparison of salinity between measurement, NEVLA and SCALDIS at Liefkenshoek.

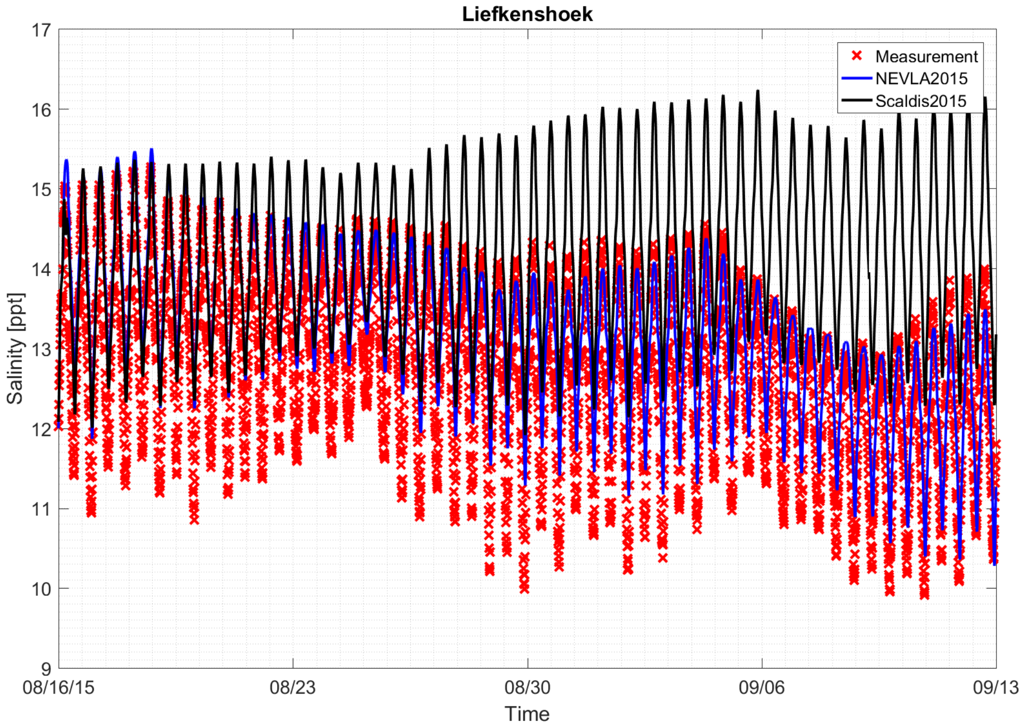

Figure 56 – Comparison of salinity between measurement, NEVLA and SCALDIS at Hemiksem.

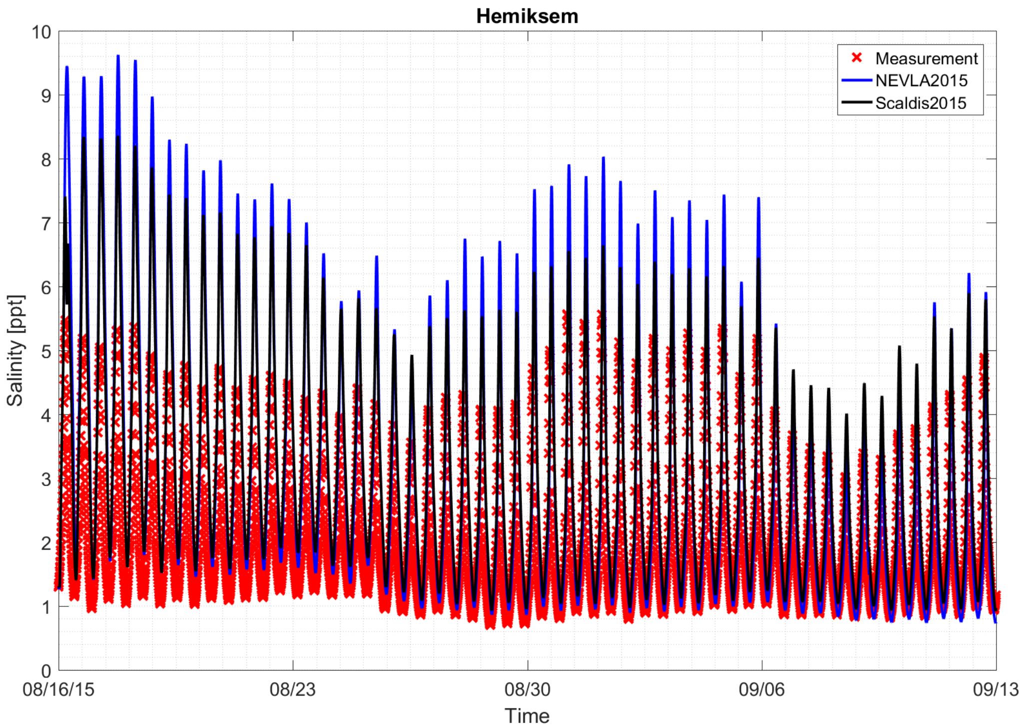

Table 24 – Statistic analysis of salinity between NEVLA, SCALDIS and measurements.

Nr	**Measuring station**	**Correlation Coefficient R [-]**		**RMSE [psu]**		**NEVLA2015 minus Measurement**			
						Max [psu]		**Min [psu]**	
		NEVLA	SCALDIS	NEVLA	SCALDIS	NEVLA	SCALDIS	NEVLA	SCALDIS
1	Vlakte Van De Raan	0.70	0.69	0.38	0.78	0.92	0.37	-1.15	-1.64
2	Overloop Hansweert	0.85	0.87	1.04	1.05	0.71	1.05	-2.00	-2.60
3	Baalhoek	0.97	0.88	0.39	1.15	1.40	2.80	-1.11	-2.04
4	Prosperpolder	0.87	0.58	0.60	1.74	1.70	3.64	-2.28	-1.65
5	Boei 84	0.86	0.66	0.52	1.39	1.17	3.50	-1.86	-1.14
6	Liefkenshoek	0.91	0.76	0.64	1.58	1.89	3.26	-1.01	-0.54
7	Hemiksem	0.73	0.80	1.73	1.47	6.35	4.99	-2.40	-1.45
8	Driegoten	Not enough Data		Not enough Data		Not enough Data		Not enough Data	

7 Updated flow field

The flow field is generated from modelled flow fields from the SCALDIS model. The inputs for the ship simulator are generated with in-house matlab toolbox **Mod2ShipSim** which is linked to the sub-versioning system (https://wl-subversion.vlaanderen.be/svn/repoSpNumMod/Matlab/Mod2ShipSim/branches/Mod2ShipSimv2)

The velocity data calculated by the SCALDIS model are exported as ASCII files over one tidal cycle during spring tide and neap tide respectively (Table 25). The spring and neap tide are defined by using tidal coefficient (see §Annex 2).

Table 25 – Periods to export velocity field for spring and neap tide from the model.

Tide	Period	Time Interval	Tidal coefficient at Antwerp
Spring Tide	17/08/2015 11:00 to 18/08/2015 00:00	10 minutes	1.12
Neap Tide	23/08/2015 02:00 to 23/08/2015 15:00	10 minutes	0.84

As a cross-check, the updated velocity field is compared against the existing flow field from the ship simulator. The velocity data provided by the nautical group are at 2 instantaneous moments at 03:10 and 07:10 on 09/09/2006 (during flood and ebb tide respectively). Associated with the velocity data, the water level data at Zandvliet is also provided for one tidal cycle from 08/09/2006 22:30 to 09/09/2006 11:00 (see Figure 57). The calculation of the tidal coefficient at Zandvliet has been carried out and presented in Table 26. The resulted tidal coefficient of 1.24 at Zandvliet implies that this tidal cycle is an extreme spring tide.

Table 26 – Analysis of water level at Zandvliet associated with the velocity from ship simulator.

Station Zandvliet	
High water level [m NAP]	3.23
Low water level [m NAP]	-2.99
Tidal Range [m]	6.22
Average tidal amplitude [m] (2001 to 2010) (Vanlierde, E. et al. 2016)	5.01
Tidal coefficient	1.24
Period	08/09/2006 22:30 to 09/09/2006 11:00

A comparable tide analysis is carried out to find the best-match tidal cycle within the model simulation period of 2015. The best-match tidal period is found between **16/08/2015 23:10 and 17/08/2015 11:40** which leads to tidal coefficient of **1.16** at Zandvliet and that is substantially lower than the tidal coefficient associated with the data from ship simulator (**1.24**, see Table 26). Therefore an additional tidal cycle is selected from **31/08/2015 23:00 to 01/09/2015 11:30**, which leads to a higher tidal coefficient of **1.23.**

The comparison of water level at Zandvliet over one tidal cycle is shown in Figure 57. The best match tidal cycle (16/08/2015 23:10 - 17/08/2015 11:40) still leads to substantial differences: **Bias of 0.27 m; RMSE of 0.31 m and RMSE0 of 0.14 m.** The tidal range in 2006 that is implemented in the simulator is relatively higher to the tidal range captured in this modelled period. The tidal cycle from 31/08/2015 23:00 to 01/09/2015 11:30 leads to statistical comparison of **Bias of 0.53 m; RMSE of 0.55 m and RMSE0 of 0.14 m.**

The flow field that is implemented now is compared to the modelled flow field in Figure 58 to Figure 65. Compared with the flow condition implemented in the simulator (year 2006), the modelled velocity magnitude (year 2015) in general decreases considerable (even up to 1 m/s) during both flood and ebb tide. The difference is most pronounced in the tidal channel. Even for a stronger spring tide (tidal coefficient of 1.23), the modelled velocity magnitude is still lower than the flow condition implemented in the simulator (year 2006) substantially. Be aware that the flow condition implemented in the simulator is with a multiplication factor of 1.4 to the extreme spring tide.

Figure 57 – Comparison of water level at Zandvliet between Nautical data and SCALDIS model data.

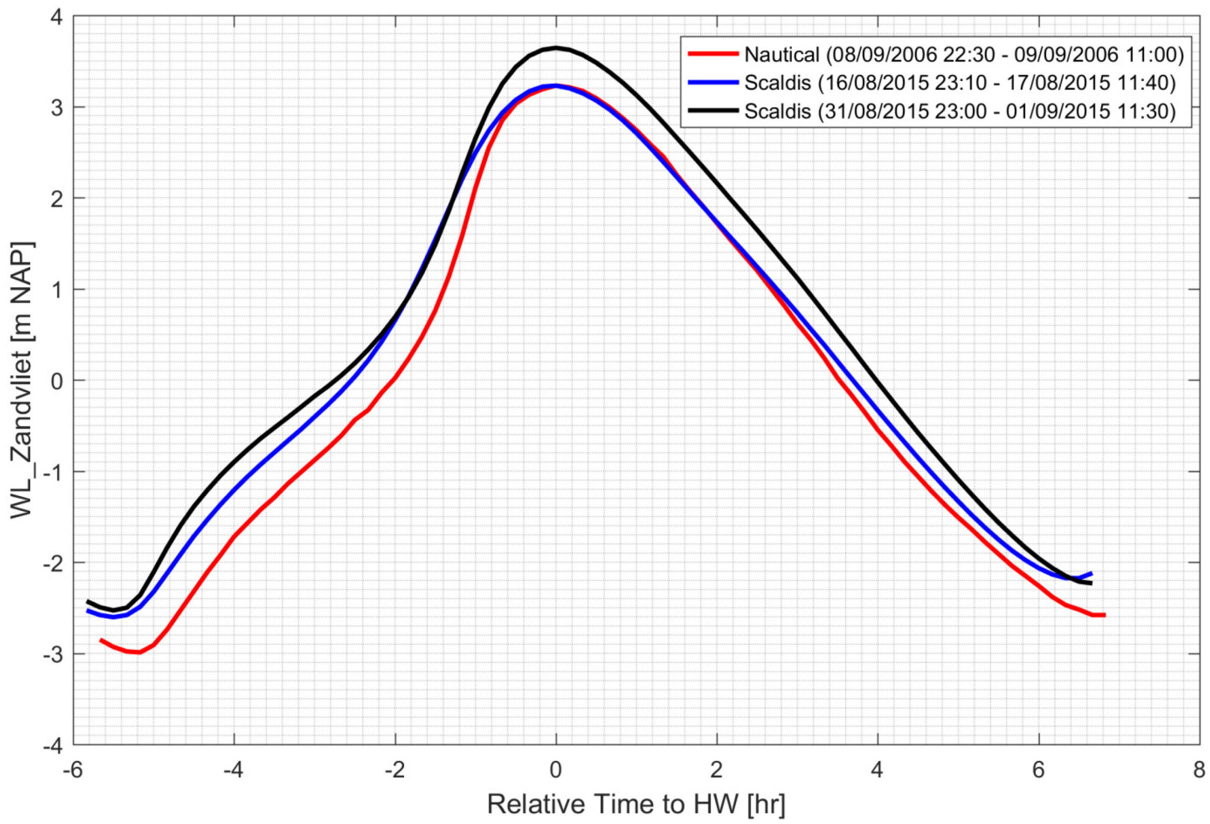

Figure 58 – Velocity field during flood (09/09/2006 03:10) from nautical ship simulator.

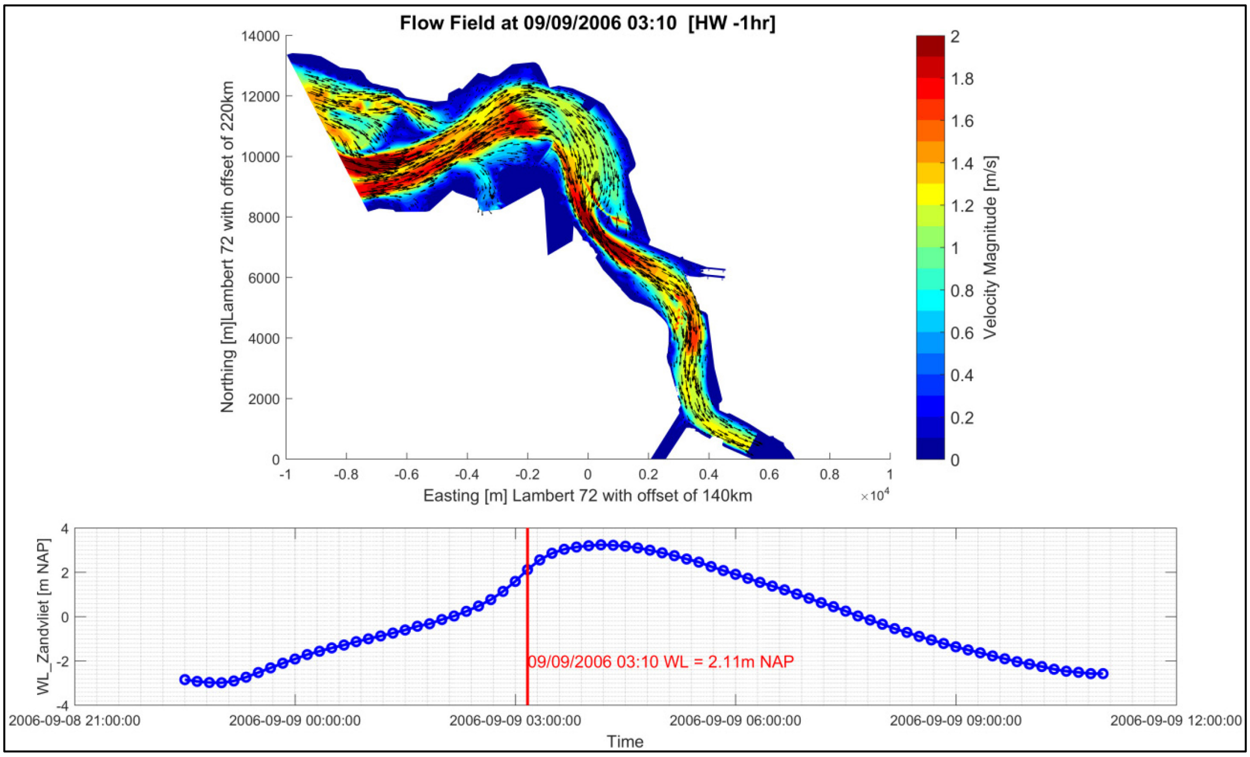

Figure 59 – Velocity field during flood (17/08/2015 04:00) from SCALDIS 2015 Run.

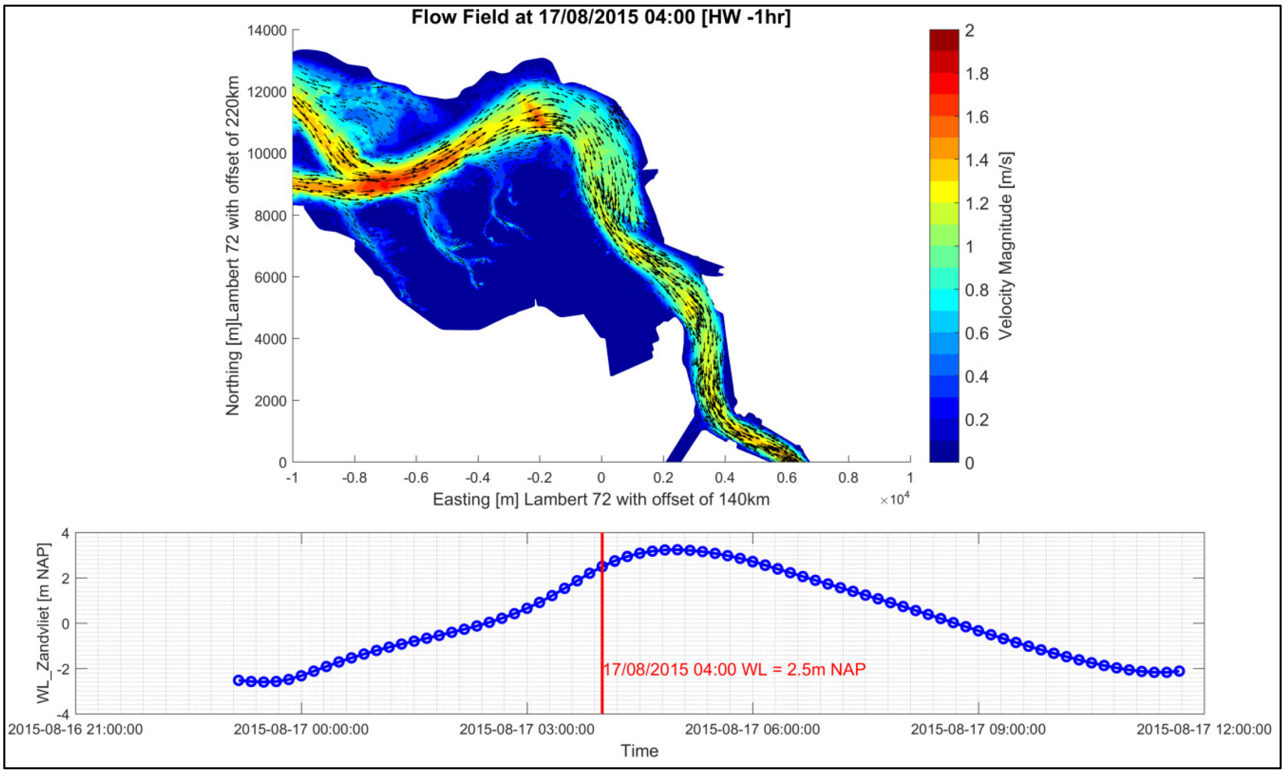

Figure 60 – Velocity field during flood (01/09/2015 03:50) from SCALDIS 2015 Run.

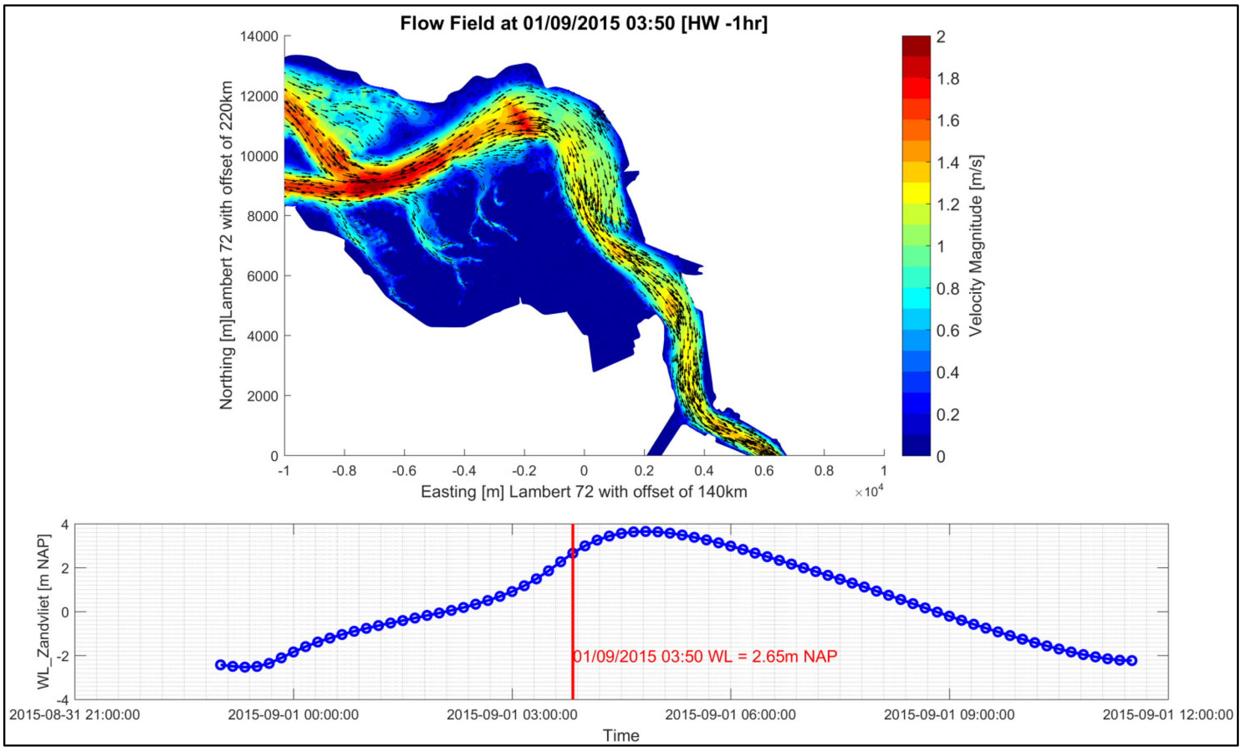

Figure 61 – Difference map of velocity (SCALDIS – Nautical) during flood.

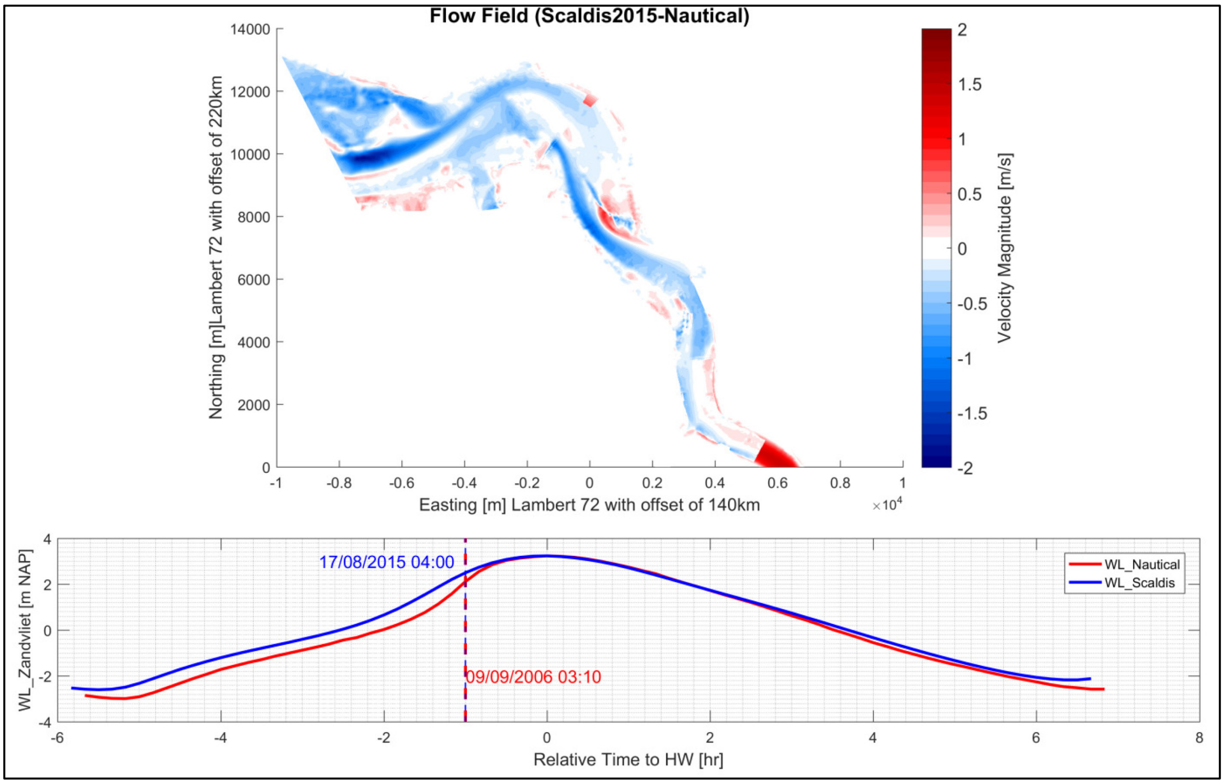

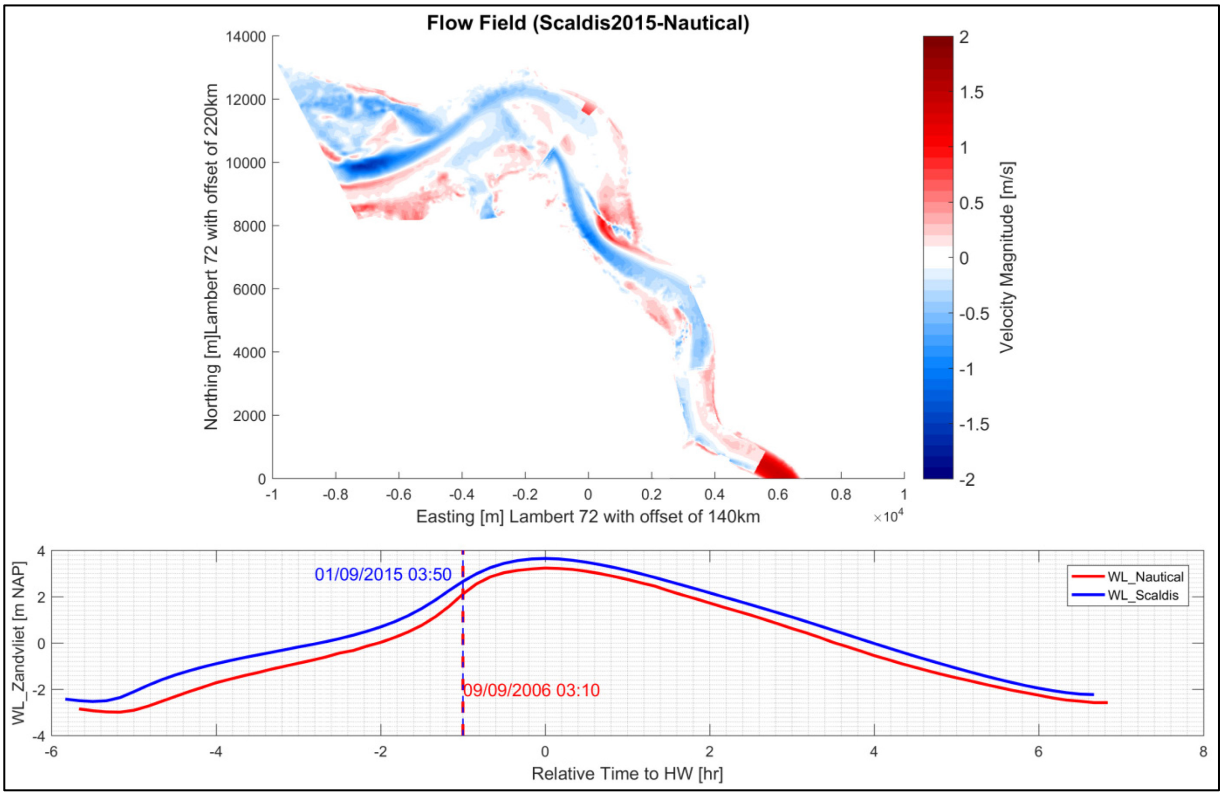

Figure 62 – Velocity field during ebb (09/09/2006 07:10) from nautical ship simulator.

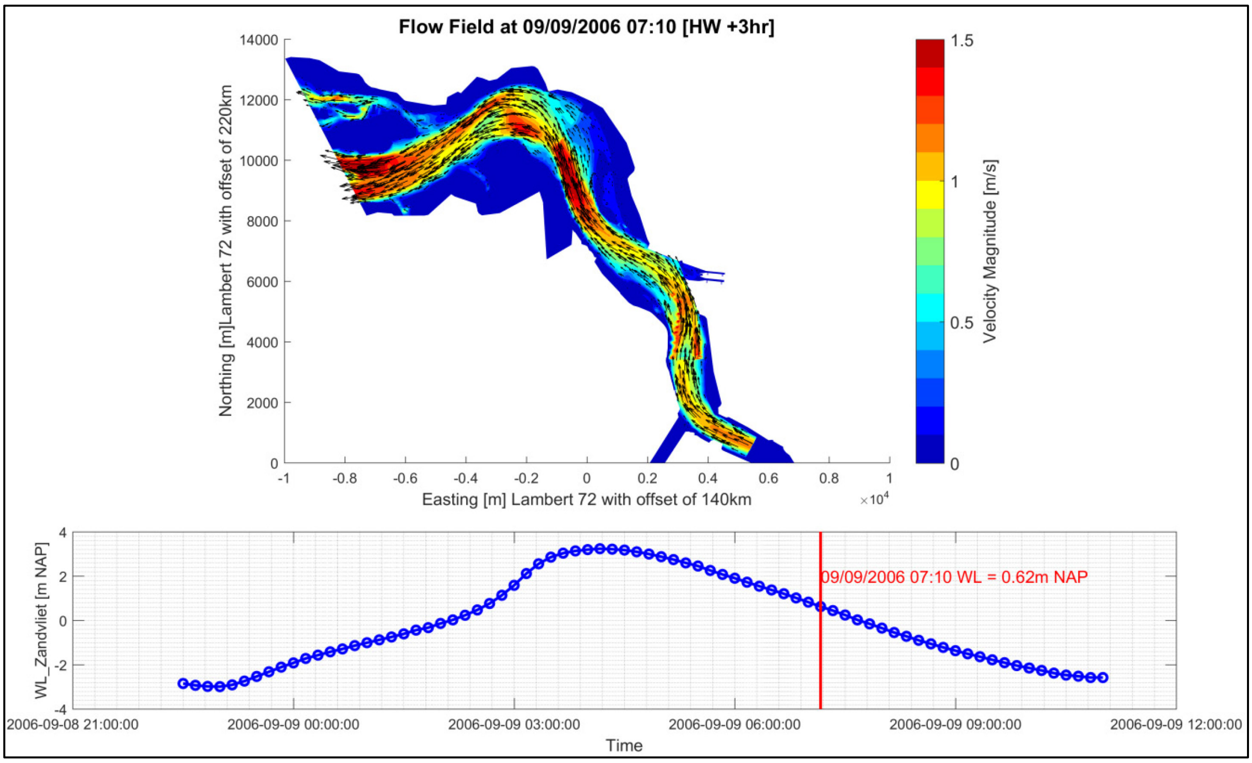

Figure 63 – Velocity field during ebb (07/08/2015 08:00) from SCALDIS 2015 Run.

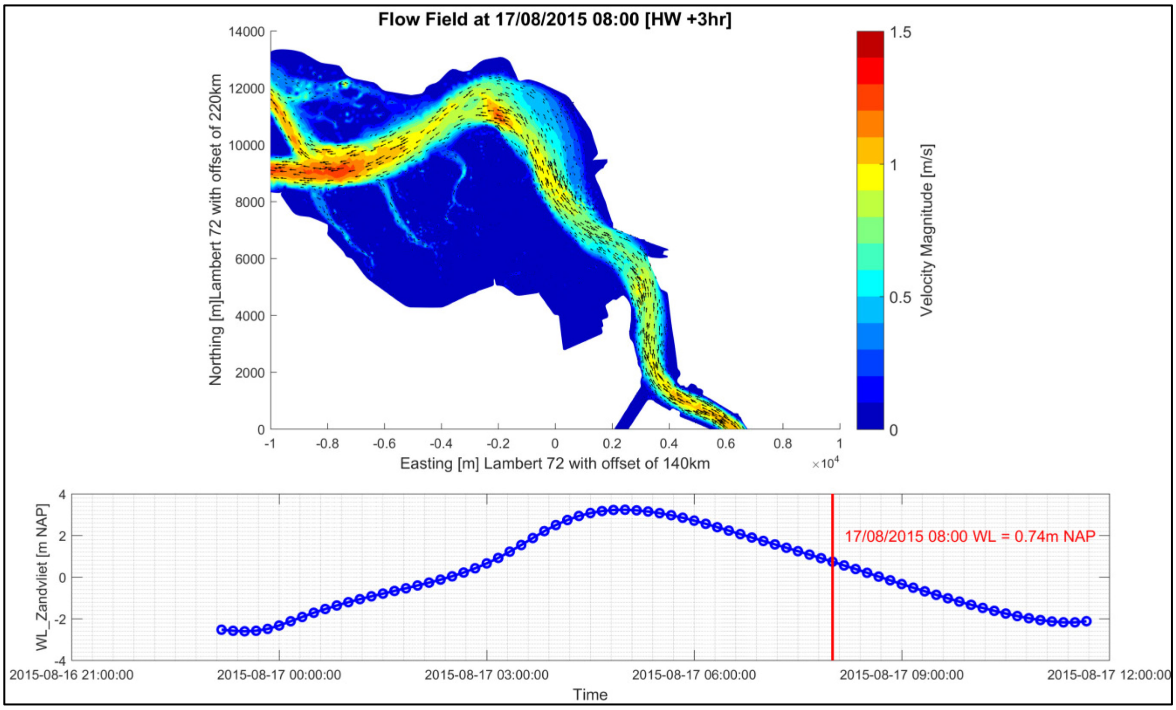

Figure 64 – Velocity field during ebb (01/09/2015 07:50) from SCALDIS 2015 Run.

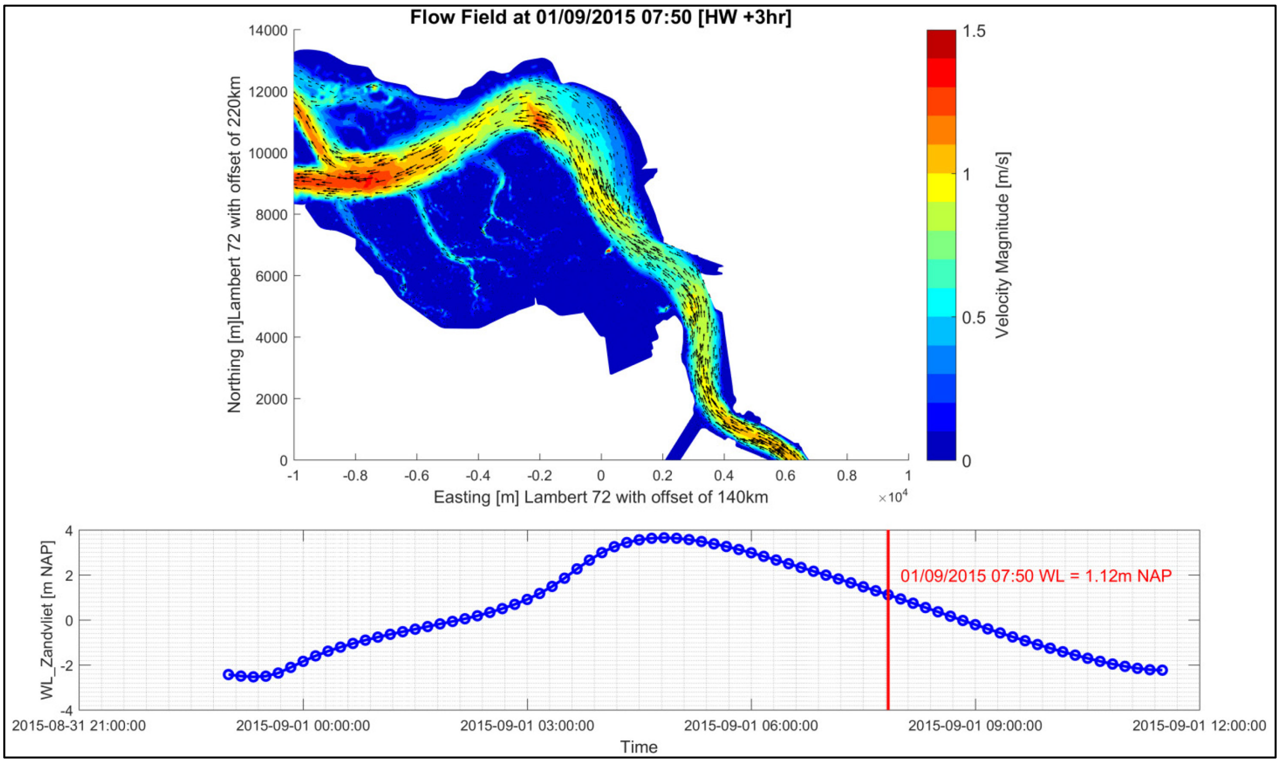

Figure 65 – Difference map of velocity (SCALDIS – Nautical) during ebb.

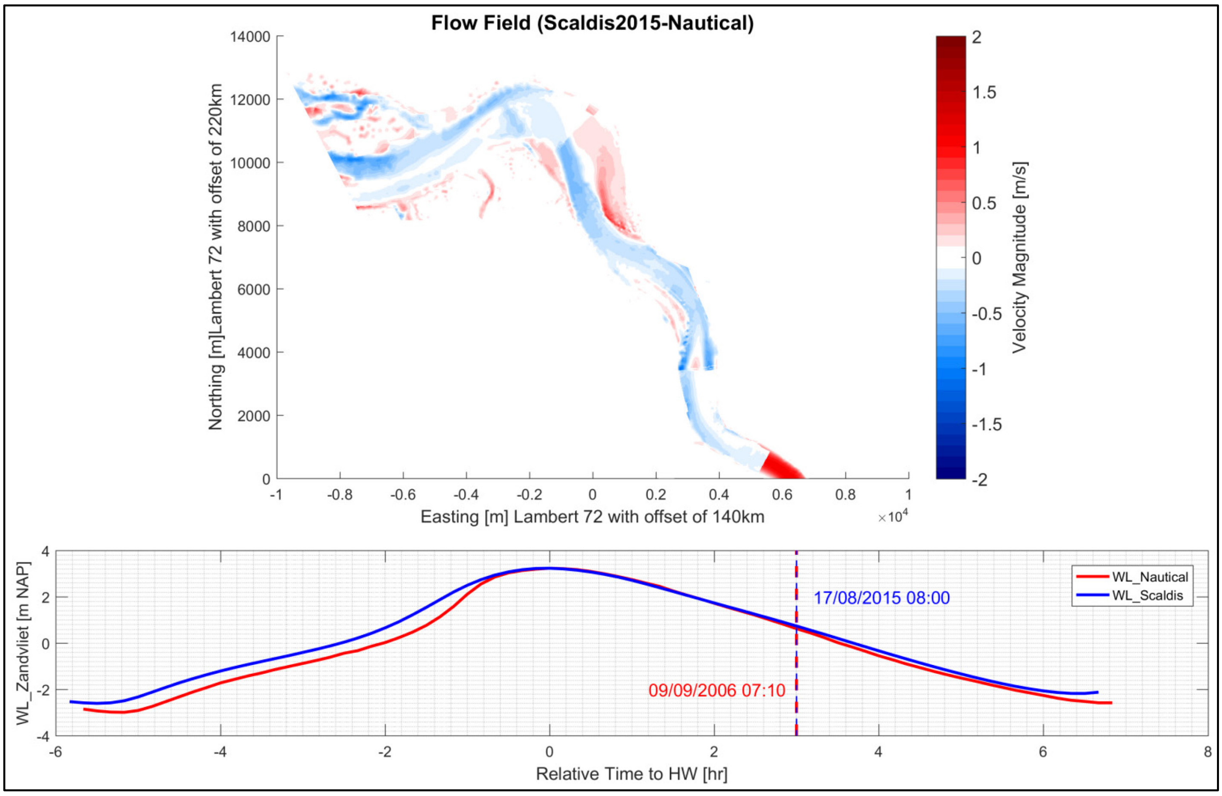

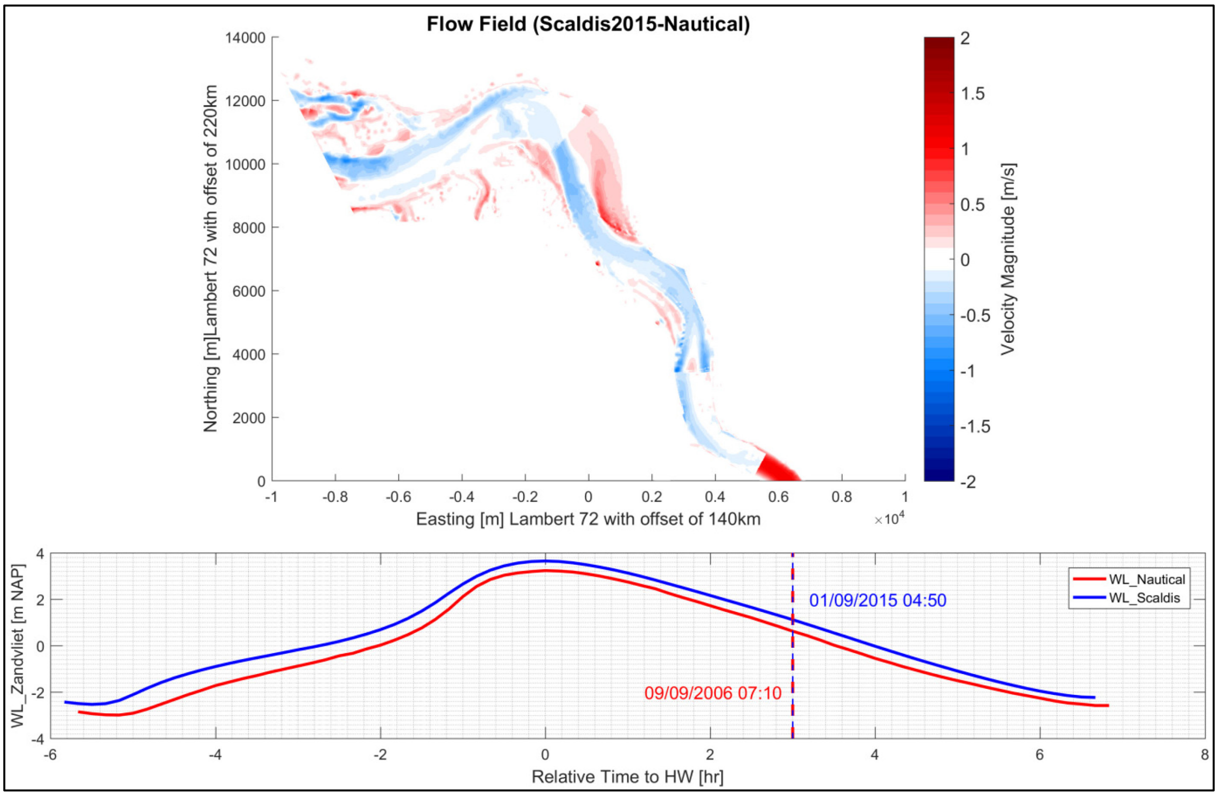

A curve is placed along the river Scheldt (Figure 66), the cross and tangential currents during both fold and ebb along this curve are compared and shown in Figure 67.

The cross current predicted by SCALDIS3D model during both mean and extreme spring tide are very similar to the cross current implemented in the ship simulator.

However, the discrepancies of tangential current are substantial, especially between 130 km and 135 km. The tangential currents are much greater from ship simulator compared with SCALDIS model predictions, during both flood and ebb.

Figure 66 – Distance along the curve (unit: km).

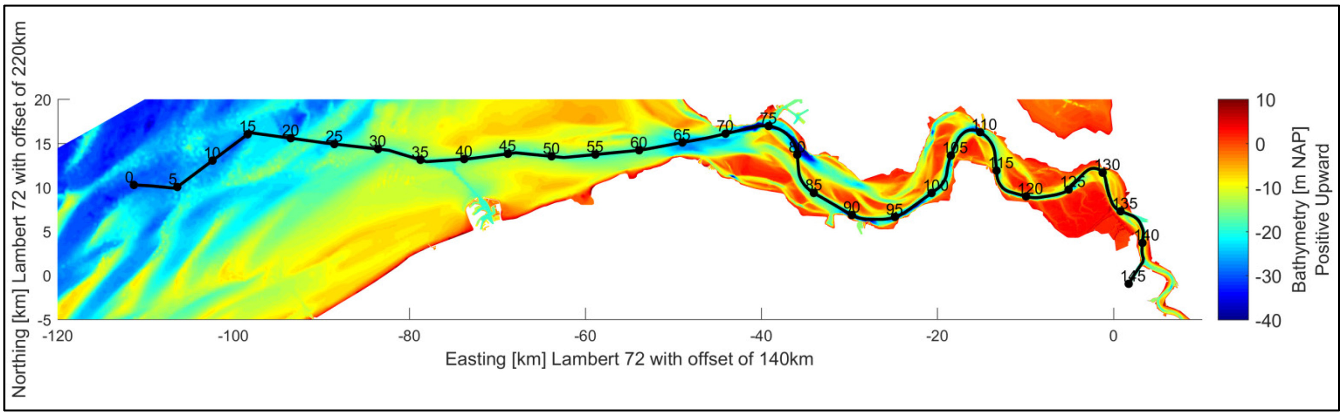

Figure 67 – Cross and tangential currents during flood (top) and ebb (bottom) along the river Scheldt.

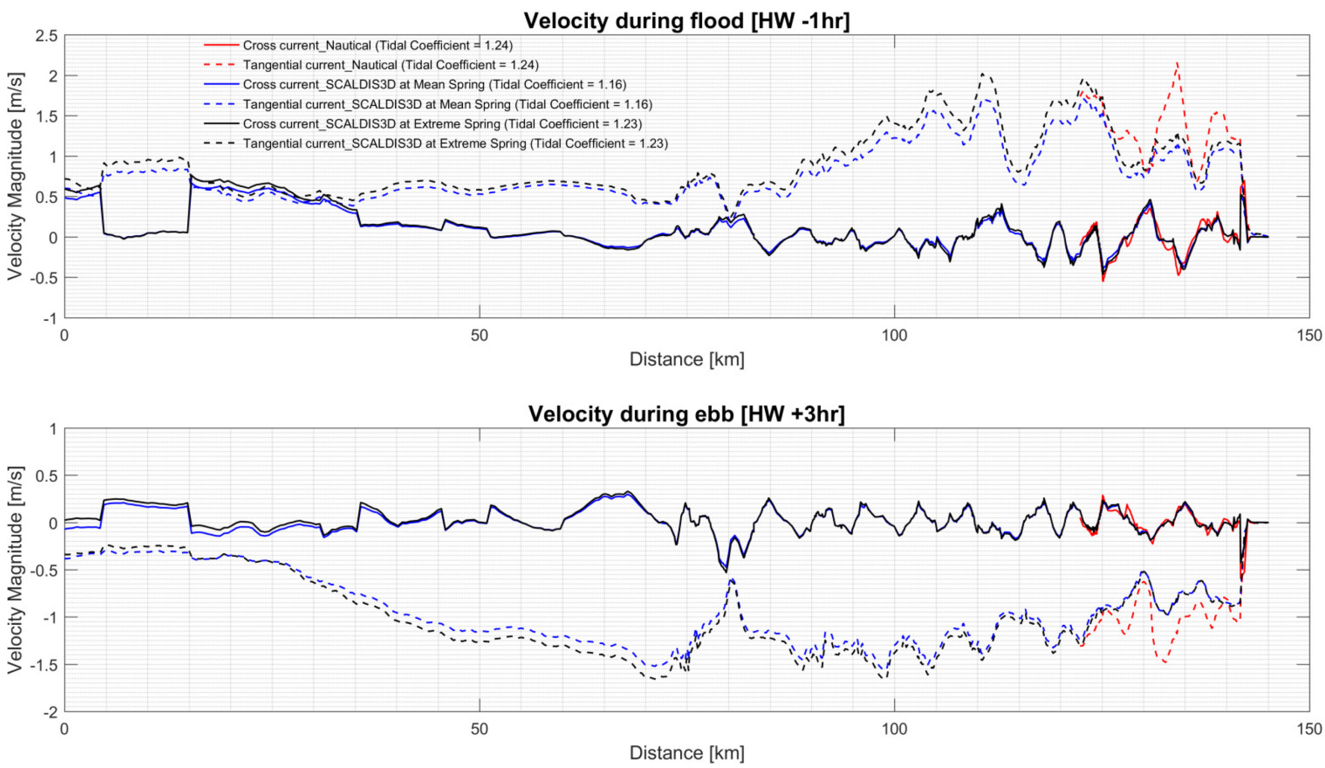

8 Conclusions and Recommendations

This study aims to update the flow field in the Sea Scheldt River using numerical model simulations. It calls for extensive modelling activities involving different modelling software and updates of existing well-calibrated models to a more recent year of 2015.

The modelling results are presented as a comparison between two modelling approaches. For the modelling approach of 'Structured Grid with Boundary Nesting (**SG-BN**)', the model results of the different domains are combined based on the priority for highest resolution to arrive at one flow field with the best accuracy at any given point. The SG-BN approach is compared to the modelling approach of using one Unstructured Grid (**UG**).

Velocities predicted by SG-BN and UG models over 2 spring-neap cycles in the year of 2015 are systematically compared with ADCP measurements along 67 transects. An extensive statistical analysis has been carried out of the error in modelled velocities, expressed both as RMSE and RMAE (see Annex 1 for definition of the error statistics).

The main findings are listed below:

- The SG-BN and UG models in general show comparable predictive abilities on velocity. This is remarkable, given the fact that SG-BN and UG models were built totally independently from each other from the ground up by different teams. The update of all model schematisations to 2015 done in this project, gives the first opportunity to compare both modelling approaches extensively.
- The unstructured grid approach (SCALDIS) can better resolve detailed local geometry (e.g. quay walls). In a structured grid approach, following a geometric feature that doesn't align with the grid orientation leads to a "staircase" effect along the grid edges. It is also easier to have higher mesh resolutions in areas of interests using unstructured grids. Based on these interesting grid properties, it is decided to produce the updated velocity fields from the SCALDIS model, following the unstructured grid approach.
- Velocity predicted by SCALDIS model and Terneuzen model along ***Terneuzen_haven*** are systematically compared. Both the SCALDIS and Terneuzen model show equally good abilities on flow predictions at Terneuzen port, even though the Terneuzen detail model had 4x higher resolution there.
- At **Noordzeeterminal** a pronounced velocity pattern during ebb is observed in the measurement which cannot be captured by either modelling approach. It is recommended to perform a new version of SCALDIS run with finer mesh resolution and higher resolution of bathymetry, to resolve the geometry in a better way. More ADCP measurement would also be needed (e.g. during flood tide and in the transversal direction) for validation.
- The updated velocity field is compared against the existing flow field from the ship simulator for both flood and ebb tide. The comparison of water level at Zandvliet between the considered periods in 2006 and 2015 shows that the best comparable tides have significant differences: Bias of 0.27 m; RMSE of 0.31 m and RMSE0 of 0.14 m. The hydrodynamic conditions are therefore different between the 2006 and 2015 flow fields. The tidal range is smaller in the 2015 period compared to the existing flow fields of 2006. Consequently the flow magnitude decreases by up to 1 m/s during both flood and ebb tide in 2015.
- Be aware that the ADCP measurements along Zuidergat and Platen van Hansweert in the WES are not considered in this study. The cross currents in these two areas are important for navigation, this can be done in a separate study in the future.
- Currently FHR has no code base available that can simulate the effect of a current deflection wall on the flow. It is advisable to have this functionality available in at least one code base. This entails implementation in source code and validation of the modelled effects.

9 References

Decrop, B.; De Clercq, B.; Vanlede, J.; Van Holland, G.; Ides, S.; Plancke, Y.; De Mulder, T.; Mostaert, F. (2009). Dwarsstromingen Ossenisse-Zuidergat. Rapport numeriek modelonderzoek. WL Rapporten, 753_07. Waterbouwkundig Laboratorium en IMDC rapport nr. I/RA/11313/09.009/BDC, Antwerpen, België

Decrop, B.; Vanlede, J.; Verwilligen, J.; van Holland, G. Mostaerd, F. (2010): Permanente verbetering modelinstrumentarium. Stroming aan de toegang tot het Zandvliet-Berendrecht sluizencomplex. Rapport 2D numeriek modelonderzoek. WL Rapporten, 753_10. Waterbouwkundig Laboratorium en IMDC rapport nr. I/RA/11313/09.090/BDC, Antwerpen, België

Deltares (2011). Delft3D-RGFGRID. User Manual.

IMDC (2014). Evaluation of the external effects on the siltation in Deurganckdok. Report 1.8: Analysis of external effects on siltation processes and factors. I/RA/11354/10.105/MBO/ANF.

Leyssen, G.; Vanlede, J.; Decrop, B.; Mostaert, F. (2012). Modellentrein CSM-ZUNO. Deelrapport 2: Validatie. WL Rapporten, 753_12. Waterbouwkundig Laboratorium & IMDC: Antwerpen, België

Leyssen, G.; Vanlede, J.; Mostaert, F. (2011). Modellentrein CSM-ZUNO. Deelrapport 1: Opzet en gevoeligheidsanalyse. Versie 2-0. WL Rapporten, 753_12. Waterbouwkundig Laboratorium & IMDC: Antwerpen, België.

Maximova, T.; Vanlede, J.; Eloot, K.; Mostaert, F. (2011). Ontwikkeling detailmodel omgeving Boudewijn-Van Cauwelaert- en Kallosluis: Numeriek 2D model. WL Rapporten, 753_13. Flanders Hydraulics Research: Antwerp, Belgium.

Maximova, T.; Vanlede, J.; Smolders, S.; Verwaest, T.; Mostaert, F. (2013). Terneuzen - detailmodel van de sluistoegang: Numeriek 2D model. Version 2_0. WL Rapporten, 00_080. Flanders Hydraulics Research: Antwerp, Belgium.

Maximova, T.; Vanlede, J.; Verwaest, T; Mostaert, F. (2014). Stroomatlas sluis van Wintam: Subreport 1 – Numerical 2D model. Version 2.0. WL Rapporten, 12_101. Flanders Hydraulics Research: Antwerp, Belgium.

Maximova, T.; Vanlede, J.; Verwaest, T; Mostaert, F. (2016). Vervolgonderzoek bevaarbaarheid Bovenzeeschelde: Subreport 4 – Modellentrein CSM – ZUNO: validatie 2013. Version 3.0. WL Rapporten, 13_131. Flanders Hydraulics Research: Antwerp, Belgium.

Smolders, S.; Maximova, T.; Vanlede, J.; Plancke, Y.; Verwaest, T.; Mostaert, F. (2016). Integraal Plan Bovenzeeschelde: Subreport 1 – SCALDIS: a 3D Hydrodynamic Model for the Scheldt Estuary. Version 5.0. WL Rapporten, 13_131. Flanders Hydraulics Research: Antwerp, Belgium.

Vanlede J., De Clercq B., Decrop B. et al. (2008): Verbetering randvoorwaardenmodel Schelde, Deelrapport 2: Afregeling van het Scheldemodel. WL2008R753_09rev1. Waterbouwkundig Laboratorium en IMDC: Borgerhout, België.

Vanlede, J.; Dujardin, A. (2014). A geometric method to study water and sediment exchange in tidal harbors. Ocean Dyn. (11): 1631–1641. doi:10.1007/s10236-014-0767-9

Vanlede, J.; Delecluyse, K.; Primo, B.; Verheyen, B.; Leyssen, G.; Plancke, Y.; Verwaest, T.; Mostaert, F. (2015). Verbetering randvoorwaardenmodel: Subreport 7 - Calibration of NEVLA 3D. Version 4.0. WL Rapporten, 00_018. Flanders Hydraulics Research & IMDC: Antwerp, Belgium.

Vanlierde, E.; Michielsen, S.; Vereycken, K.; Hertoghs, R.; Meire, D.; Deschamps, M.; Verwaest, T.; Mostaert, F. (2016). Tienjarig overzicht van de tijwaarnemingen in het Zeescheldebekken: Decennium 2001-2010. Versie 5.0. WL Rapporten, 12_071. Waterbouwkundig Laboratorium: Antwerpen, België.

Vanlierde, E.; Ferket, B.; Pauwaert, Z.; Michielsen, S.; Van De Moortel, I.; Levy, Y.; Plancke, Y.; Meire, D.; Deschamps, M.; Verwaest, T.; Mostaert, F. (2016). MONEOS - jaarboek monitoring WL 2015: Factual data rapportage van monitoring hydrodynamiek en fysische parameters zoals gemeten door WL in het Zeescheldebekken in 2015. Versie 3.0. WL Rapporten, 12_070. Waterbouwkundig Laboratorium: Antwerpen, België.

Wang, Z.B.; van der Kaaij, T.; Sas, M. (2015). Driedimensionaal modelleren van de waterbeweging en slibtransporten in het Beneden-Zeeschelde estuarium. Hydrodynamisch modelleren. WLDelft rapport Z3824.20: Delft, Nederland

Annex 1: Definition of Statistics

Water levels

The **Bias** of water level represents the average deviation of the differences between model predicted water level and measurement.

The **RMSE** of water level is a measure of the spread of the predicted values level around the measurement. It corresponds to a sample standard deviation.

The **RMSE0** is the bias corrected root mean square error which describes the forecast errors not associated with the bias.

The mathematical expressions are listed below. *y* and *x* represent modeled and measured values respectively and *n* is the number of samples.

$$Bias = \overline{y} - \overline{x}$$

$$RMSE = \sqrt{\frac{\sum_{1}^{n}(y_i - x_i)^2}{n}}$$

$$RMSE0 = \sqrt{\frac{\sum_{1}^{n}((y_i - x_i) - (\overline{y} - \overline{x}))^2}{n}}$$

ADCP velocities

Average velocity magnitude and direction for each transect are calculated as the magnitude and direction of the average vector (based on the average U and V components), (average means the combination of the depth average and average over the transect). This means that both magnitude and direction of velocities are taken into account. For example, a direction of the velocity with a higher magnitude has more weight in the calculation of an average direction than a direction of the velocity with a smaller magnitude.

$$\overrightarrow{V_{met}}(x,z,t) = \overrightarrow{e_x} U_{met}(x,z,t) + \overrightarrow{e_y} V_{met}(x,z,t)$$

$$\overrightarrow{V_{\mathrm{mod}}}(x,z,t) = \overrightarrow{e_x} U_{\mathrm{mod}}(x,z,t) + \overrightarrow{e_y} V_{\mathrm{mod}}(x,z,t)$$

where $\overrightarrow{V_{met}}(x,z,t)$ is the vector of the measured velocity;

$\overrightarrow{V_{\mathrm{mod}}}(x,z,t)$ is the vector of the modeled velocity.

Average velocity magnitude and direction:

$$MAG_{met}(t) = \left\| \frac{\sum_{x} \left\langle \overrightarrow{V_{met}} \right\rangle}{n} \right\| \qquad DIR_{met}(t) = dir\left(\frac{\sum_{x} \left\langle \overrightarrow{V_{met}} \right\rangle}{n} \right)$$

$$MAG_{\mathrm{mod}}(t) = \left\| \frac{\sum_{x} \left\langle \overrightarrow{V_{\mathrm{mod}}} \right\rangle}{n} \right\| \qquad DIR_{\mathrm{mod}}(t) = dir\left(\frac{\sum_{x} \left\langle \overrightarrow{V_{\mathrm{mod}}} \right\rangle}{n} \right)$$

where $\left\langle \overrightarrow{V_{\mathrm{mod}}} \right\rangle(x,t)$ and $\left\langle \overrightarrow{V_{met}} \right\rangle(x,t)$ are depth average modeled and measured velocities.

The **bias of magnitude and direction** is calculated as the difference between the calculated and measured average velocity magnitude and direction.

$$BIAS_{mag}(t) = MAG_{\mathrm{mod}} - MAG_{met}$$

$$BIAS_{dir}(t) = DIR_{\mathrm{mod}} - DIR_{met}$$

The **RMSE of velocity magnitude and direction** is calculated based on the depth average velocity magnitude and direction for each point along the transect. Magnitude is not taken into account for the calculation of the RMSE of velocity direction and vice-versa. Therefore, the RMSE plots show more variation between the model and measurements than the plots of average velocity magnitude and direction for all transects.

$$RMSE_{mag}(t) = \sqrt{\frac{\sum_{x} \left(\left\| \left\langle \overrightarrow{V_{\mathrm{mod}}} \right\rangle \right\| - \left\| \left\langle \overrightarrow{V_{met}} \right\rangle \right\| \right)^2}{n}}$$

$$RMSE_{dir}(t) = \sqrt{\frac{\sum_{x} \left(dir\left(\left\langle \overrightarrow{V_{\mathrm{mod}}} \right\rangle \right) - dir\left(\left\langle \overrightarrow{V_{met}} \right\rangle \right) \right)^2}{n}}$$

The **MAE** (mean absolute error) is calculated based on the calculated (Y_1,Y_2) and observed (X_1,X_2) components of the current. The **RMAE** (relative mean absolute error) is derived to identify the order of magnitude of the error compared to the observed velocities. A table was proposed in which the RMAE was used to identify the model quality to represent the current.

$$MAE = \left\langle \left\| \vec{Y} - \vec{X} \right\| \right\rangle = \frac{1}{N} \sum_{n=1}^{N} \sqrt{\left(Y_{1,n} - X_{1,n}\right)^2 + \left(Y_{2,n} - X_{2,n}\right)^2}$$

$$RMAE = \frac{\left\langle \left\| \vec{Y} - \vec{X} \right\| \right\rangle}{\left\langle \left\| \vec{X} \right\| \right\rangle} = \frac{MAE}{\left\langle \left\| \vec{X} \right\| \right\rangle}$$

Model qualification based on (*Sutherland et al.,* 2003)

Model qualification	RMAE
Excellent	<0.2
Good	0.2-0.4
Reasonable/fair	0.4-0.7
Poor	0.7-1.0
Bad	>1.0

Annex 2: Tidal coefficients

A tidal coefficient is calculated as a ratio of the tidal amplitude during the analysed period to the amplitude of the average tide for the period from 1991 to 2000. Tidal coefficients are calculated for all analysed tides based on the measured water levels at Antwerp.

Table below shows the typical values of the tidal coefficients corresponding to the neap, average and spring tides. Tides with coefficients higher than 1.06 are considered to be spring tides; tides with coefficients lower than 0.92 are neap.

Table 27 – Typical values of the tidal coefficients for neap, average and spring tides

Tide	Amplitude at Antwerp [m]	Tidal Coefficient k [-]
Neap	4.43	0.84
Average	5.29	1
Spring	5.95	1.12

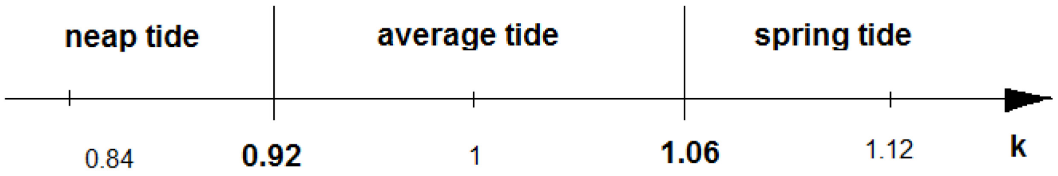

Annex 3: Full comparison of velocities

Table 28 – Comparison of RMSE and RMAE of velocities between all the 6 models along the 67 ADCP transects.

No.		ADCP	RMSE Magnitude [m/s]						RMAE [-]					
			NEVLA	Scaldis	Boudewijn	Zandvliet	Terneuzen	Wintam	NEVLA	Scaldis	Boudewijn	Zandvliet	Terneuzen	Wintam
1	WES	20110706_R7_Terneuzen	0.27	0.23	-	-	0.20	-	0.47	0.52	-	-	0.48	-
2		20080604_Debietraai_7	0.17	0.17	-	-	0.17	-	0.27	0.27	-	-	0.26	-
3		20110705_R7_Everingen	0.17	0.13	-	-	0.13	-	0.37	0.35	-	-	0.35	-
4		20070321_Terneuzen_haven	0.10	0.11	-	-	0.10	-	0.41	0.39	-	-	0.38	-
5		20120508_R6_Middelgat	0.21	0.17	-	-	0.17	-	0.43	0.44	-	-	0.45	-
6		20120509_R6_GatVanOssenisse	0.24	0.16	-	-	0.17	-	0.39	0.35	-	-	0.36	-
7		20060323_Waarde	0.11	0.12	-	-	0.12	-	0.29	0.31	-	-	0.31	-
8		20060928_Waarde	0.12	0.13	-	-	0.13	-	0.42	0.42	-	-	0.42	-
		AVERAGE	**0.17**	**0.15**	**-**	**-**	**0.15**	**-**	**0.38**	**0.38**	**-**	**-**	**0.38**	**-**
9	BeZS1	20050217_Zandvliet	0.11	0.12	0.12	0.17	0.12	-	0.38	0.39	0.40	0.60	0.41	-
10		20060912_Doelpolder	0.15	0.17	0.20	0.16	0.21	-	0.58	0.73	0.65	0.51	1.48	-
11		20140715_Noordzeeterminal	0.16	0.29	0.23	0.19	0.29	-	0.42	0.70	0.68	0.57	0.70	-
12		20100319_dwarsraaiD	0.18	0.22	0.20	0.37	0.24	-	0.31	0.35	0.31	0.65	0.36	-
		AVERAGE	**0.15**	**0.20**	**0.19**	**0.22**	**0.22**	**-**	**0.42**	**0.54**	**0.51**	**0.58**	**0.74**	**-**
13	BeZS2	20060322_DGD	0.08	0.09	0.09	-	0.10	-	0.74	0.78	0.86	-	0.87	-
14		20060927_DGD	0.06	0.07	0.07	-	0.08	-	0.72	0.74	0.90	-	0.86	-
15		20071024_DGD	0.06	0.07	0.07	-	0.07	-	0.81	0.75	0.88	-	0.86	-
16		20080311_DGD	0.06	0.07	0.07	-	0.08	-	0.77	0.75	0.92	-	0.84	-
17		20080619_DGD	0.06	0.07	0.07	-	0.08	-	0.71	0.73	0.85	-	0.84	-
18		20080626_DGD	0.06	0.06	0.06	-	0.07	-	0.75	0.74	0.90	-	0.84	-
19		20080924_DGD	0.06	0.06	0.06	-	0.07	-	0.80	0.76	0.82	-	0.86	-
20		20080930_DGD	0.05	0.06	0.06	-	0.07	-	0.74	0.72	0.87	-	0.85	-
21		20081001_DGD_X	0.14	0.16	0.15	-	0.18	-	0.53	0.58	0.64	-	0.70	-
22		20081001_DGD_Y	0.14	0.17	0.14	-	0.19	-	0.54	0.64	0.59	-	0.75	-
23		20081001_DGD_Z	0.16	0.19	0.16	-	0.21	-	0.58	0.68	0.64	-	0.76	-
24		20081202_DGD	0.07	0.08	0.07	-	0.08	-	0.80	0.77	0.97	-	0.92	-
25		20081210_DGD	0.07	0.07	0.07	-	0.08	-	0.84	0.79	0.89	-	0.91	-
26		20090306_DGD	0.08	0.09	0.08	-	0.10	-	0.74	0.78	0.89	-	0.88	-
27		20090312_DGD	0.08	0.09	0.09	-	0.11	-	0.72	0.73	0.85	-	0.84	-
		AVERAGE	**0.08**	**0.09**	**0.09**	**-**	**0.10**	**-**	**0.72**	**0.73**	**0.83**	**-**	**0.84**	**-**
28	BeZS3	20050216_DGD_K	0.15	0.18	0.17	-	0.22	-	0.29	0.31	0.30	-	0.36	-
29		20050217_DGD_K	0.11	0.15	0.15	-	0.21	-	0.25	0.32	0.31	-	0.44	-
30		20060322_DGD_K	0.16	0.18	0.19	-	0.24	-	0.42	0.48	0.48	-	0.54	-
31		20060323_DGD_K	0.13	0.15	0.14	-	0.18	-	0.39	0.39	0.38	-	0.44	-

32		20060927_DGD_K	0.15	0.18	0.18	-	0.24	-	0.38	0.46	0.45	-	0.54	-
33		20060928_DGD_K	0.13	0.14	0.15	-	0.19	-	0.35	0.35	0.35	-	0.42	-
34		20080311_DGD_K	0.20	0.21	0.21	-	0.25	-	0.39	0.41	0.38	-	0.44	-
35		20050217_Liefkenshoek	0.11	0.15	0.15	-	0.22	-	0.23	0.32	0.33	-	0.46	-
36		20060322_Liefkenshoek	0.13	0.17	0.17	-	0.26	-	0.38	0.50	0.50	-	0.61	-
37		20060927_Liefkenshoek	0.13	0.15	0.16	-	0.24	-	0.29	0.36	0.36	-	0.48	-
38		20080311_Liefkenshoek	0.18	0.20	0.21	-	0.30	-	0.37	0.40	0.40	-	0.53	-
39		20090527_Liefkenshoek	0.18	0.21	0.21	-	0.27	-	0.41	0.48	0.48	-	0.58	-
40		20100430_Liefkenshoek	0.14	0.15	0.16	-	0.24	-	0.31	0.30	0.30	-	0.41	-
41		20130625_Liefkenshoek	0.14	0.15	0.16	-	0.26	-	0.33	0.31	0.31	-	0.43	-
42		20140514_Liefkenshoek	0.15	0.14	0.14	-	0.23	-	0.30	0.24	0.27	-	0.35	-
43		20050218_Kallo	0.10	0.11	0.12	-	-	-	0.55	0.55	0.58	-	-	-
		AVERAGE	0.14	0.16	0.17	-	0.24	-	0.35	0.39	0.39	-	0.47	-
44	BeZS4	20090529_Oosterweel	0.19	0.16	0.18	-	-	0.18	0.37	0.28	0.29	-	-	0.30
45		20100429_Oosterweel	0.17	0.18	0.20	-	-	0.19	0.27	0.32	0.35	-	-	0.33
46		20130627_Oosterweel	0.22	0.14	0.16	-	-	0.16	0.44	0.29	0.29	-	-	0.32
47		20140516_Oosterweel	0.21	0.17	0.20	-	-	0.18	0.39	0.28	0.28	-	-	0.29
48		20090526_Kruibeke	0.19	0.23	0.26	-	-	0.23	0.43	0.56	0.55	-	-	0.57
49		20100414_Kruibeke	0.14	0.13	0.21	-	-	0.14	0.27	0.21	0.31	-	-	0.23
50		20130530_Kruibeke	0.19	0.16	0.24	-	-	0.17	0.48	0.49	0.58	-	-	0.50
51		20140702_Kruibeke	0.17	0.15	0.19	-	-	0.16	0.31	0.33	0.45	-	-	0.35
		AVERAGE	0.19	0.16	0.21	-	-	0.18	0.37	0.34	0.39	-	-	0.36
52	BoZS1	20130529_Terhagen	0.18	0.18	-	-	-	0.20	0.38	0.32	-	-	-	0.36
53		20140630_Terhagen	0.14	0.15	-	-	-	0.19	0.28	0.35	-	-	-	0.38
54		20090623_Driegoten	0.17	0.14	-	-	-	0.17	0.33	0.21	-	-	-	0.25
55		20100415_Driegoten	0.19	0.15	-	-	-	0.19	0.45	0.35	-	-	-	0.40
56		20130612_Driegoten	0.17	0.21	-	-	-	0.22	0.40	0.47	-	-	-	0.48
57		20140617_Driegoten	0.20	0.16	-	-	-	0.18	0.34	0.30	-	-	-	0.32
58		20110218_Kramp_ebb	0.15	0.16	-	-	-	0.16	0.22	0.23	-	-	-	0.23
59		20110218_Kramp_flood	0.29	0.21	-	-	-	0.26	0.45	0.33	-	-	-	0.42
		AVERAGE	0.19	0.17	-	-	-	0.20	0.36	0.32	-	-	-	0.36
60	BoZS2	20140417_Dendermonde	0.19	0.12	-	-	-	-	0.36	0.23	-	-	-	-
61		20110801_Appels_downstream	0.17	0.15	-	-	-	-	0.72	0.68	-	-	-	-
62		20110801_Appels_upstream	0.17	0.18	-	-	-	-	0.65	0.66	-	-	-	-
63		20090625_Schoonaarde	0.19	0.20	-	-	-	-	0.42	0.56	-	-	-	-
64		20100414_Schoonaarde	0.13	0.09	-	-	-	-	0.25	0.20	-	-	-	-
65		20130527_Schoonaarde	0.18	0.15	-	-	-	-	0.32	0.28	-	-	-	-
66		20140703_Schoonaarde	0.19	0.16	-	-	-	-	0.42	0.33	-	-	-	-
67		20140415_Schellebelle	0.16	0.15	-	-	-	-	0.47	0.38	-	-	-	-
		AVERAGE	0.17	0.15	-	-	-	-	0.45	0.42	-	-	-	-
OVERALL			0.15	0.15	-	-	-	-	0.45	0.46	-	-	-	-

Discussion

In general the 4 detailed models of Boudewijn-Kallo, Zandvliet, Terneuzen and Wintam do not show better predictive abilities on velocities, compared with either NEVLA or SCALDIS. The possible reasons are listed as below:

- Wind forcing and salinity are not included in the 4 detailed model domains, although the wind driven and density driven currents in these domains are usually considered less important. Future sensitivity analysis are recommended to verify the impact of such forcing on velocities.
- All of the 4 detailed models are run with 2D mode while the currents are essentially a 3D process, although the 3D effect of currents are usually considered less important for these domains. Future systematic studies are recommended to verify the importance of number of vertical layers on velocity predictions.
- The 4 detailed models are nested from NEVLA model. During nesting only the flow perpendicular to the boundary sections are passed to the detailed model while the flow parallel to the boundary sections are ignored. So in nesting, information gets lost at the boundary.

The accuracy on velocity predictions gained from refined grid cell resolution are balanced out by the drawbacks mentioned above.

DEPARTMENT **MOBILITY & PUBLIC WORKS**
Flanders hydraulics Research

Berchemlei 115, 2140 Antwerp
T +32 (0)3 224 60 35
F +32 (0)3 224 60 36
waterbouwkundiglabo@vlaanderen.be
www.flandershydraulicsresearch.be